October 2021

ON SPATIOTEMPORAL CONNECTIVITY DYNAMICS: PERSPECTIVES FROM A NATURALLY FRAGMENTED METAPOPULATION

Joseph Drake
University of Massachusetts Amherst

ON SPATIOTEMPORAL CONNECTIVITY DYNAMICS: PERSPECTIVES FROM A NATURALLY FRAGMENTED METAPOPULATION

A Dissertation Presented

by

Joseph Carleton Balcerak Drake

Submitted to the Graduate School of the
University of Massachusetts Amherst in partial fulfillment
of the requirements for the degree of

DOCTOR OF PHILOSOPHY

September 2021

Organismic and Evolutionary Biology

ON SPATIOTEMPORAL CONNECTIVITY DYNAMICS: PERSPECTIVES FROM A NATURALLY FRAGMENTED METAPOPULATION

A Dissertation Presented

by

JOSEPH CARLETON BALCERAK DRAKE

Approved as to style and content by:

_____
Dr. Christopher Sutherland, Chair

_____
Dr. Xavier Lambin, Member

_____
Dr. Toni-Lyn Morelli, Member

_____
Dr, Lisa Komoroske, Member

_____
Dr. Craig Albertson,
Organismic and Evolutionary Biology

DEDICATION

This work is dedicated to my family. To my father and mother who worked hard to make sure I could succeed. You always let me play in the creeks and mud and explore the world. To my brother, you are the best mi hermano. And to my wife, Sarah, for loving me and supporting me through this ridiculous journey. I could not have done it without you.

And to the countless who have come before and will come after: thank you. To (and for) those untranslatable, I sound my barbaric yawp over the roofs of the world.

ACKNOWLEDGMENTS

This work has been made possible by many people and institutions too numerous to name here. I would like to thank the UMass Graduate School, Department of Environmental Conservation, and the Organismic and Evolutionary Biology Interdepartmental Program for supporting me through my journey here at UMass. Through the generous support of this community, I was able to achieve this degree.

I did not know how little I did not know when I first started, as befits an academic journey. I cannot express the appreciation that I have for my mentors, particularly my advisor Chris, for helping me see the blank spots on the map. And more importantly for helping me fill them in. Chris, you have helped me grow as a scientist beyond what I thought I could have, thank you for helping me slay those statistical monsters.

To those whom I worked with across the pond, I greatly appreciated your taking in this weird American for 3 summers. I would like to thank Dr. Allan McDevitt & Lab for collaborating on the work that produced chapter 4, your combined expertise made the publication possible. As well, I appreciated the warmth of those in Aberdeen (considering how little there was in Northern Scotland's weather) and your willingness to teach me and have me as a guest. To Emma, Richard, Laura, and all the other volers and volettes (as Xavier would say), thank you for the company and great field seasons. Xavier, thank you for the academic support, the civilized perspective, and the langoustines.

I would also like to thank the Sutherland, Komoroske, Morelli, and Grant lab groups for letting me sit in and be a member of the community at various times while I have been here at UMass. The academic and emotional support was crucial to my success. Thank you all so much. Dr. Toni Lyn Morelli provided fantastic perspective and

advice. Dr. Ben Padilla was a gift to have while in the trenches. Tim Duclos helped remind me to get outside and embrace New England. Thank you, Donovan, Jill, Patty, Gates, Kadambari, Nigel and so many more I can't possible fit in this space. You all were a part of my success.

I would also like to thank Dr. Kerry Griffis-Kyle and Dr. Nancy McIntyre for their help on my journey here. Without their support and mentorship, I would never have been able to make it here, let alone out of the desert in the first place. To my friends back home who have probably thought that they need to file a missing persons case, I appreciate your patience. And to my family: a most humble thank you. You made this struggle unmeasurably easier. Thank you for your support. Mom, Dad, Rob, and my wife Sarah, you are literally the best. Love you and thank you for keeping from drifting too deep into terra incognito.

ABSTRACT

ON SPATIOTEMPORAL CONNECTIVITY DYNAMICS: PERSPECTIVES FROM A NATURALLY FRAGMENTED METAPOPULATION

SEPTEMBER 2021

JOSEPH CARLETON BALCERAK DRAKE,

B.A., INDIANA UNIVERSITY - BLOOMINGTON

M.S., TEXAS TECH UNIVERSITY

Ph.D., UNIVERSITY OF MASSACHUSETTS AMHERST

Directed by: Dr. Christopher Sutherland

Connectivity has quickly become a central tenet of ecological research, frequently evoked for conservation research and management activities. However, the concept of connectivity has proliferated into many forms for many different perspectives. I was motivated to understand and identify core components of connectivity. Such an approach would help provide a clear roadmap for better applying connectivity in both basic and applied research settings while simultaneously making such applications easier to compare between studies. Generally said, population distributions, demography, landscape, and dispersal all contribute to connectivity in a meaningful way. While great progress has been made in modeling connectivity for many species, few if any, have been able to incorporate all the core components when describing their connectedness in the environment. However, one component seemed to stand out as being underappreciated: the role of population dynamics in the application of landscape connectivity. While reviewing the literature, I began to acquire an appreciation for how common modeling approaches assumptions to be made about these core components of connectivity.

Through computer simulations, I investigated the consequences of these assumptions to understand under which conditions each assumption was valid. In order to determine whether these theoretical simulation-based results applied in practice, I evaluated these assumptions empirically using a model system, the naturally fragmented mammalian metapopulation system in Assynt, Scotland, UK. The ability to uncover connectivity's influence is only as good as our ability to detect our study species, and thus I conclude the dissertation with the verification of emerging technological advances to measuring biodiversity and occupancy in the landscape.

I start my dissertation with a synthesis of connectivity research from across a wide spectrum of ecological subfields. A general consensus is that connectivity contains a structural component relating to the distribution and configuration of habitat in the landscape, and a functional component, that relates to the way the landscape impacts animal movement and dispersal. I discovered a third component that is often implicitly referenced, but often overlooked: the fundamental role of demography or spatiotemporal distribution of species in connectivity research. Overlooking such variation can lead to modeling assumptions that can bias estimates of connectivity. To demonstrate this, in Chapter 1, I conducted a series of simulations reflecting common assumptions about demographic contributions to connectivity. I found that the use of common proxies (occupancy and abundancy) indeed result in biased characterizations of connectivity. Extending the existing metapopulation modeling framework (stochastic patch occupancy modelling), I demonstrate that it is a powerful approach to addressing common assumption about connectivity. More generally however, I suggest that the demographically-weighted connectivity yields a conceptual framework for explicitly

linking population dynamics and the emergent patterns of connectivity that have value beyond classical metapopulation systems (Drake et al. 2021).

In Chapter 1 I argue connectivity is a dynamic property of landscapes, influenced by population distributions, distribution of habitat, and dispersal behavior. In Chapter 2, I sought to explore demographically-weighted connectivity and the implications of the common assumption that connectivity is a static component of the landscape. Using a spatially-explicit, stochastic patch occupancy model, I explored competing hypothesis about the dynamic nature of connectivity. Using data collected in a large scale, long-term study of water voles (*Arvicola Amphibius*), a system that has emerged as a model metapopulation system, I iteratively relaxed assumptions related to demographic-weighting and spatiotemporal dynamism in connectivity. This naturally fragmented spatially structured population provided empirical evidence that demographic-weighting and temporal variability substantially alter inferred connectivity. Further I verified that such assumptions impact the outcome of an important and commonly used conservation metric, metapopulation capacity, a description of the ability of landscape to allow a metapopulation to persist. Specifically, I demonstrated that static representations of connectivity, that do not consider demographic contributions, induced large amounts of error surrounding the point estimate of metapopulation capacity compared to our more general model. As well, models that accounted for spatiotemporal dynamism and demographic-weighting provided smaller and more precise estimates of metapopulation capacity, but with inter-annual variation than traditional static metrics. These results indicate that it is important to consider how connectivity assumptions may impact results

when using metrics such as metapopulation capacity to guide conservation planning (Drake et al. *In Review*).

In chapter 3, I demonstrate that the characteristics of the inter-patch landscape, though which dispersal must occur in order for spatially structured populations to persist, matters when characterizing connectivity. Landscape influences on connectivity have been increasing acknowledged, but the modeling of such impacts has been hampered by a distinct lack of movement data for most species. Thus, expert opinion has long been relied upon to define how dispersal is influenced by particular landscape features, and thus on connectivity. Using a recently developed cost distance extension of the stochastic patch occupancy model applied to the 20 year metapopulation time-series, I was able to estimate landscape cost and better understand how such landscape resistance alters predictions of landscape connectivity. I demonstrate that the interpatch matrix does matter to understanding connectivity, and that such information may be gathered using simple detection histories when more detailed movement data is unavailable.

My final data chapter highlights the utility of an exciting and emerging biodiversity monitoring tools, camera traps and environmental DNA (eDNA). Specifically, I introduced a new monitoring scheme to the Assynt, UK study area using camera-traps. By comparing camera traps and eDNA monitoring methods to the traditional latrine-based occupancy surveys currently used, I provide a formal comparison of the detection efficiency of these methods for a range of species. Using eDNA metabarcoding, we generated species detections from water and sediment samples from patches where camera traps were placed and where standard latrine surveys were conducted a large proportion of the expected mammalian community were detected. We

compared the efficacy of detection of water voles, field voles (*Microtus agrestis*), and red deer (*Cervus elaphus*), showing that water-based eDNA metabarcoding provided comparable results to traditional methods. These results help to verify an emerging technique that could potentially revolutionize non-invasive surveying methods and that could complement existing strategies. This method could help produce long-term 'distribution maps' of mammalian diversity at the landscape level, providing much needed help for conservation of endangered species and monitoring for invasive species. These methods could also help provide early detection or verification of connectivity for range-shifting species, reintroduced species, conservation corridors, or invasive species (Sales et al. 2020b).

My objective in this body of work was to make a meaningful contribution to the application of connectivity in ecology. Providing a synthesis of historical literature and recent advances across sub-disciplines, I identified the core components of connectivity and provided a framework to advance connectivity research called demographically-weighted connectivity. I applied this framework to demonstrate its impact in recovering model parameters in a real system and demonstrated how common connectivity assumptions impact the ability to recover important connectivity model parameters and what occurs when applied to conservation metrics. I have also demonstrated that demographic information, such as the dynamic spatiotemporal distribution of populations can be used to produce arguably more ecologically realistic estimates of connectivity. Thus, this work helps provide evidence to the demographic nature of connectivity and how our modeling assumptions may impact the efficacy of conservation plans and management actions. Moreover, this work provide support for advances in both

measuring and understanding occupancy and connectivity, both important to consider in a time of shifting conservation needs.

TABLE OF CONTENTS

Page

LIST OF TABLES

Table Page

LIST OF FIGURES

Figure Page

CHAPTER 1

THE VALUE OF CONSIDERING DEMOGRAPHIC CONTRIBUTIONS TO CONNECTIVITY – A REVIEW[1]

Abstract

Connectivity is a central concept in ecology, wildlife management and conservation science. Understanding the role of connectivity in determining species persistence is increasingly important in the face of escalating anthropogenic impacts on climate and habitat. These connectivity augmenting processes can severely impact species distributions and community and ecosystem functioning.

One general definition of connectivity is an emergent process arising from a set of spatial interdependencies between individuals or populations, and increasingly realistic representations of connectivity are being sought. Generally, connectivity consists of a structural component, relating to the distribution of suitable and unsuitable habitat, and a functional component, relating to movement behavior, yet the interaction of both components often better describes ecological processes. Additionally, although implied by 'movement', demographic measures such as the occurrence or abundance of organisms are regularly overlooked when quantifying connectivity. Integrating demographic contributions based on the knowledge of species distribution patterns is critical to understanding the dynamics of spatially structured populations.

Demographically-informed connectivity draws from fundamental concepts in metapopulation ecology while maintaining important conceptual developments from landscape ecology, and the methodological development of spatially-explicit hierarchical statistical models that have the potential to overcome modeling and data challenges.

Together, this offers a promising framework for developing ecologically realistic connectivity metrics.

This review synthesizes existing approaches for quantifying connectivity and advocates for demographically-informed connectivity as a general framework for addressing current problems across ecological fields reliant on connectivity-driven processes such as population ecology, conservation biology, and landscape ecology. Using supporting simulations to highlight the consequences of commonly made assumptions that overlook important demographic contributions, we show that even small amounts of demographic information can greatly improve model performance. Ultimately, we argue demographic measures are central to extending the concept of connectivity and resolves long-standing challenges associated with accurately quantifying the influence of connectivity on fundamental ecological processes.

Introduction

This The ability to accurately measure connectivity is crucial for managing habitat loss and fragmentation (Rayfield et al. 2011, Wasserman et al. 2012, Haddad et al. 2015, 2016) in order to preserve genetic diversity and promote population persistence (Hilty et al. 2020). Connectivity, conceptually, is the strength of links among locations mediated by effective dispersal (Calabrese and Fagan 2004) and how the environment facilitates or hinders those links (Taylor et al. 1993). Therefore connectivity is a property of a landscape that emerges for the set of spatial dependencies that arise between individuals and populations within a particular landscape (or seascape, etc…, Kool et al. 2013). Beyond this general definition, however, the ability to effectively quantify how,

when, and to what extent, connectivity contributes to ecological processes has been beset by semantic uncertainties (Kool et al. 2013) and debate (Tischendorf and Fahrig 2000, 2001, Moilanen and Hanski 2001).

Such uncertainty and debate is fueled, in part, by a diversity of ecological sub-disciplines and conservation applications that draw upon the concept and seek to quantify connectivity through a continually increasing array of models and metrics (Kindlmann and Burel 2008, Rayfield et al. 2011, Fletcher et al. 2016). Population dynamics (Clinchy et al. 2002), disease networks (Margosian et al. 2009), forestry planning (Banks et al. 2005), wildlife management (Horváth et al. 2019), conservation reserve design (Blowes and Connolly 2012, Gupta et al. 2019), spatial conservation planning (Daigle et al. 2020), invasive species mitigation (Drake et al. 2017a), landscape genetics (Marrotte et al. 2017), and more, all invoke the concept of connectivity, but often in different contexts and spatiotemporal scales. While we acknowledge that such context-dependency makes it unrealistic to find a single connectivity metric that would satisfy all applications, idiosyncratic uses of connectivity have proliferated into a loosely related set of tools. Therefore, we find it pertinent to synthesize the properties of connectivity to understand how common assumptions in various modeling approaches influence estimates of connectivity.

Connectivity is traditionally considered to be a function of two core components: a structural component, relating to the distribution of suitable and unsuitable habitat (Calabrese and Fagan 2004), and a functional component, relating to the influence of the landscape matrix on dispersal success (Kindlmann and Burel 2008, Rayfield et al. 2011). Comprehensive quantification of connectivity (i.e., the probability of an organism

successfully leaving point A and arriving at point B including what goes on in between), should ideally consider both structural and functional components. The consideration of both the available habitat and the movement behavior can be described as 'potential' connectivity (Calabrese and Fagan 2004) and can be applied to identify potential corridors or pinch points (Ziółkowska et al. 2012), and other useful conservation planning indices such as the probability of connectivity (Saura and Pascual-Hortal 2007). However, this approach is arguably incomplete because the underlying distributions of populations are often not incorporated (Moilanen and Nieminen 2002). Indeed, spatially explicit information about the distribution (e.g., occupancy), size (e.g., abundance), or demography (e.g., survival) of a population or set of populations is crucial for understanding how and why both structural and functional components of connectivity influence ecological dynamics across time and space. Changes in any one of these components can contribute to shifts in the emergent connectivity and the resulting ecological processes in important, yet hitherto unexplored, ways. For example, landscapes and populations change through space and time, and at different spatial and temporal scales, and the judicious inclusion of information about the dynamics of both in connectivity modeling is likely to provide greater insight about their relative contribution to the spatiotemporal dynamics of spatially structured populations.

Through our synthesis, we have identified a third component that is garnering increasing recognition when describing connectivity, i.e., landscape connectivity is the combination of structural, functional, and demographic components (Figure 1). Connectivity is a representation of movement processes, through the lens of *dispersal*, by individuals among focal habitats (Matthysen 2012, Baguette et al. 2013). These patches

contain varying qualities of habitat and exist in the *landscape* where movement between them responds to the intervening matrix. Incorporating a *demographic* weighting to established components based on the spatiotemporal distribution of the populations producing dispersers allows for a dynamic and demographically-informed view of connectivity, which we refer to as demographically-weighted connectivity (Figure 1).

Specifically, we advocate demographically-weighted connectivity as a dynamic framework synthesized from contributions across ecological and conservation literature for understanding the role of connectivity-driven processes that cuts across discrepancies among sub-disciplines about connectivity-driven processes. Further, using simulation, we explore key demographic assumptions (representing increasing amounts of biological realism found in connectivity studies) to demonstrate the value of incorporating demographic components of connectivity and the consequences for ignoring it. This simulation highlights the importance to estimating key parameters that control the scale of colonization and dispersal and their probabilities. Such a focused approach on connectivity and its core components should allow for increased integration across sub-disciplines and to help progress the search for general ecological processes (Rapacciuolo and Blois 2019). We reassert that individual decisions and population dynamics are not only a product of connectivity but also an important determinant of connectivity.

.

Demographic connectivity: synthesizing core contributions

Demographically-informed connectivity draws from fundamental concepts in metapopulation ecology (Hanski 1994, Hanski and Ovaskainen 2000, Ovaskainen and Hanski 2001) while maintaining important conceptual developments from landscape

ecology (Turner 2005), and the methodological development of spatially-explicit hierarchical statistical models that have the potential to overcome modeling and data challenges (Box 1). Ecological connectivity has traditionally been approached from either a structural or functional perspective (Taylor et al. 1993, 2010). This false dichotomy masks a complex gradient of ecological assumptions about connectivity. Instead, we argue that, in addition, connectivity metrics should consider demographic weighting, when applicable, across this gradient. Although movement is implied to qualitatively achieve measures of functional connectivity, demographic measures (e.g., occupancy, abundance; see below) have historically rarely been considered in investigations of connectivity (Prugh et al. 2008), but an increasing awareness for their need is developing (Fletcher et al. 2019). Next, taking recent developments and historic contributions from the literature, we develop the justification and importance of considering demographic contributions for a more holistic connectivity by discussing each component of connectivity in turn.

Dispersal

Dispersal, the movement of individuals and propagules that may have consequences for gene flow across space (Ronce 2007), links populations, making it essential to connectivity and, as a result, local colonization-extinction dynamics and the maintenance of gene flow and genetic diversity (Bowler and Benton 2005, Crooks and Sanjayan 2006, Baguette et al. 2013). However, lack of empirical dispersal knowledge is often cited as a serious impediment to research (Driscoll et al. 2014), particularly in applications of connectivity (Zeller et al. 2012). For example, when available, sample sizes are often small and lack power, and pooling likely masks important sex-, age-, and

stage-specific variation (Elliot et al. 2014a). Yet, it is the inclusion of information about dispersal that makes connectivity metrics functional. This is true whether considering fluid dispersed propagules (Munoz 2004), plants (Auffret et al. 2017), small flying insects (Jangjoo et al. 2016), anadromous fish (Bradbury et al. 2014), or large predatory mammals (Zeller et al. 2018). The constraints that impact dispersal for any given species will impact both the potential or actual connectivity that emerges from the landscape structure (Vasudev et al. 2015). Understanding dispersal is therefore key to accurately characterizing the intersection of, and mechanistic link between, landscape structure and population connectivity.

Unfortunately, this presents a limited perspective of an assumed measure of functional connectivity that often ignores the underlying population distribution. This is evident in applications of landscape resistance mapping. For example, when predicting functional connectivity for bullfrogs, *Lithobates catesbeianus*, in the Sonoran Desert, Drake et al. (2017b) produced resistance estimates to illustrate landscape-scale shifts in potentially connected habitat, regardless of occupancy state. Such demographically-naïve approaches are widely applied and, while useful, represent hypotheses of connectivity that are prone to biases (Zeller et al. 2012) resulting from a mischaracterization of the underlying distribution and behavior of individuals, i.e., of potential dispersers (Riotte-Lambert and Laroche 2021). Indeed, including information on known occurrences, and hence a refined representation of dispersal sources, can generate altogether different characterizations of landscape connectivity and of management priorities (Cushman et al. 2013, Drake et al. 2017a). Overlooking the underlying distribution of potential dispersers is likely to overstate state-specific dispersal of a landscape and introduces biases in the

characterization of connectivity which will be more strongly felt in more heterogeneous, spatially structured populations (Box 2).

Dispersal has three stages: emigration, transfer, and immigration, each a multi-faceted context-dependent process. Despite the importance of each stage and the fact that each plays out at, and is influenced by, factors at characteristic spatial and temporal scales (Clobert et al. 2012), functional connectivity approaches have often viewed dispersal solely through the lens of the transfer stage (Diniz et al. 2020). Data at each stage can be limited, but data on the transfer stage are often scarcest (Cozzi et al. 2018); assumptions outnumber data in model representation of this movement. Such scarcity begets the use of proxies, such as functional connectivity, for these largely latent processes.

In fact, recognizing what controls emigration and immigration may provide insight and may be as, if not more, important for estimating connectivity (Vasudev and Fletcher 2016). Variation in emigration rates has been linked to inbreeding avoidance and kin competition (Lambin et al. 2001, Bowler and Benton 2005), area-dependence (Wang and Altermatt 2019), and habitat quality (Hui et al. 2012). Likewise, immigration may depend on conspecific attraction (Matthysen 2005) and perception of site habitat quality (Betts et al. 2008), rather than solely the distance traveled from natal patches (Telfer et al. 2001). The balancing of dispersal costs and benefits is multi-causal and there is potential for a dynamic feedback loop whereby each of these demographic processes can be influenced by, and contribute to, variation in local- and landscape-level connectivity. Thus, factors such as the distribution and abundance of a population and dispersal

behavior introduce a spatiotemporal dynamism to the concept of connectivity that has been often overlooked (Drake et al. *In Review*).

Where information on the processes influencing dispersal's transfer stage is limited, patterns gleaned from observed emigration and immigration may provide a reasonable alternative source of dispersal data. Occupancy-based statistical methods can be used to interpret patterns of colonization and extinction (Hanski and Ovaskainen 2003, Ovaskainen and Hanski 2004) and have been commonly used to infer the scale and rate of dispersal (Sutherland et al. 2012, Driscoll et al. 2014). Analytical advances have gone a long way towards the integration of even simple demographic data such as occupancy or abundance to increase the mechanistic understanding of connectivity and its contribution to ecological processes, including predictions of how landscape features influence movement (Vasudev et al. 2015; Box 1). Moreover, advances in data collection have shown that a variety of sampling methods, including determining presence and absence of species through non-invasive methods such as hair snares (Dixon et al. 2006), scat samples (Long et al. 2007), and even environmental DNA (Sales et al. 2020b), can increase our ability to examine the impact of connectivity more accurately through the dispersal process for single species and for entire communities (Baguette et al. 2013, Rapacciuolo and Blois 2019). The rapid advances in sampling technology and analytical methods have revolutionized ecological monitoring and modeling such that landscape-scale inference about species occurrence and abundance distributions is commonplace. Considering how valuable this information can be to refining measures of connectivity, we advocate for an integration of landscape-scale estimates of population state variables into connectivity research (Sutherland et al. 2015, Morin et al. 2017, Meyer et al. 2020).

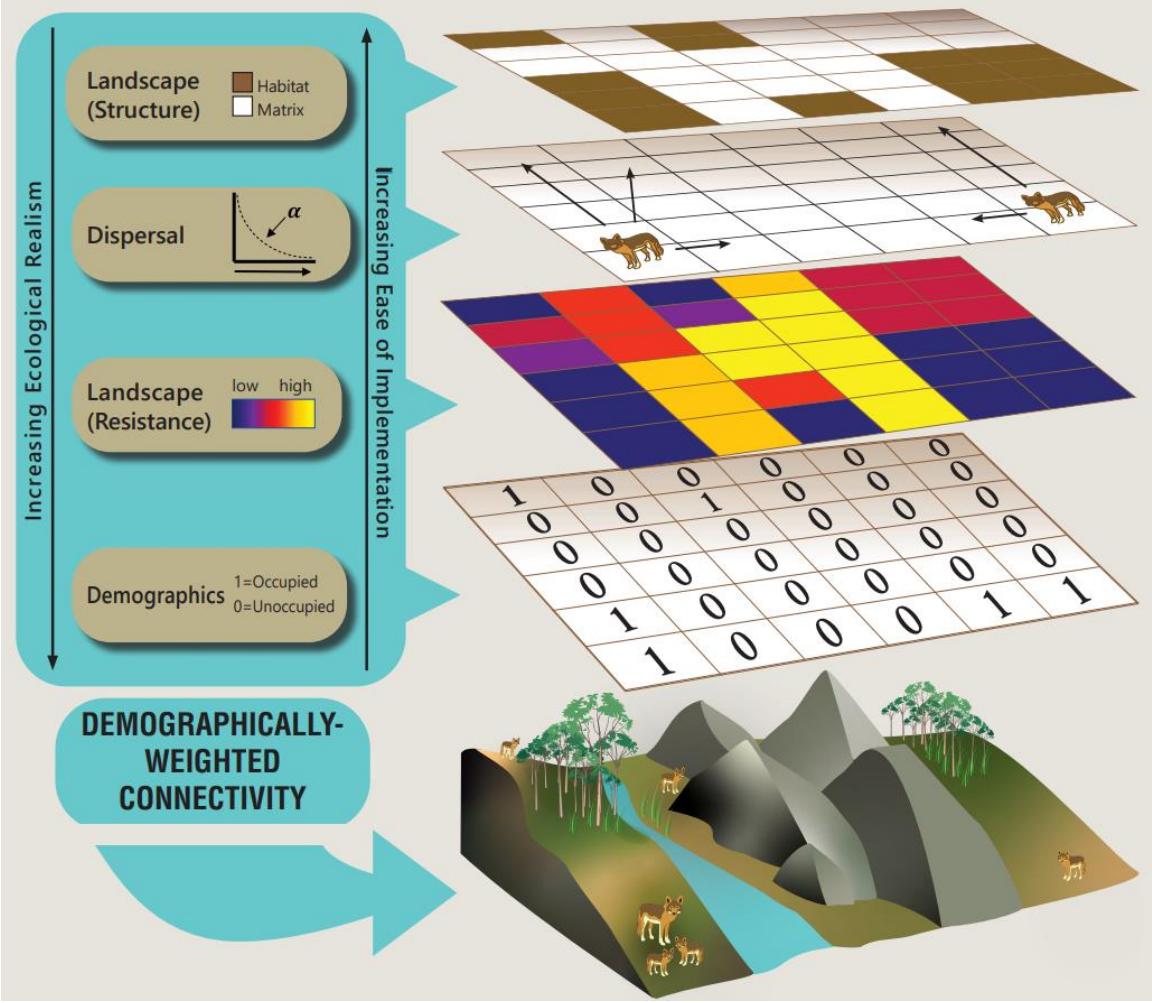

Figure 1. Demographically-weighted connectivity considers three core components of connectivity: landscape (structure and resistance), the dispersal process, and population demographic information. Landscape connectivity has often been seen as a static process among habitat patches on the landscape. Connectivity not only influences population dynamics but is influenced by them. Connectivity in the landscape shifts across space and time coincident with the spatiotemporal distribution of organisms. While some habitat may be within effective dispersal range (α) of an organism (Box 2), others may be functionally isolated due to a landscape that is resistant to successful dispersal. Even when such habitat is within the dispersal capability of another parcel of habitat, only when populations of organisms are there, and capable of dispersing, would habitat be functionally connected. The data used to weight connectivity may take the form of simple occurrence data (as shown here), but also abundance, number or breeders, fecundity, or any other demographic representation that is hypothesized to relate to the dispersal process and impact connectivity. Demographically-weighted connectivity thus provides an extended conceptual representation of landscape connectivity that considers, explicitly, the population dynamics and demographics which can influence connectivity and the ecological processes dependent upon it. Image designed by Tina Sotis based on research by Drake et al. (2021).

Landscape

For spatially structured populations, the landscape is often divided thematically into the habitat patch and the inter-patch matrix (but see Dilts et al. 2016). This paradigm is applicable across a wide assortment of environments, not solely in terrestrial ones (Baguette et al. 2013, Boulanger et al. 2020). The focal patch or patch network is often defined by breeding habitat (Compton et al. 2007) or stepping-stones of suitable habitat too small for long-term occupancy (Saura et al. 2014); these patches are surrounded by unsuitable inter-patch matrix typically not permanently occupied by focal species. The amount and relative position of patches defines the landscape structure but rarely reflects the realized distribution of populations or whether they are functionally connected via the intervening matrix. It is worth noting that the patch-matrix landscape model represents one (a binary) end of a spectrum, while continuously occupied landscapes (e.g., gradients of habitat suitability) represents the other end. All landscapes exist along this gradient, depending on the degree of landscape heterogeneity. Therefore, while demographically-weighted connectivity may seem to stem from a patch-centric view, these ideas are not limited to the binary matrix perspective.

Structural representations of landscape connectivity that focus solely on spatial structure of the patch network and overlook the underlying spatial distribution of individuals can generate biased representations of inter-patch connections (Lookingbill et al. 2010, Martensen et al. 2017). The simplifying assumptions of structural models can be useful when demographic data, such as the occupancy, is limited or absent (Urban and Keitt 2001), but may under-estimate connectivity when the distinction between patch and matrix is not clear (Wiens 2001). This is particularly true for continuously-distributed

organisms that use a wide variety of habitat (Dilts et al. 2016) or when a single patch dominates the network and ecological processes (Cavanaugh et al. 2014).

It is well established that the matrix matters (Ricketts 2001, Brady et al. 2009, Ruffell et al. 2017), and that overlooking properties of the intervening matrix poses challenges to estimating connectivity (Calabrese and Fagan 2004). For example, barriers to movement limit the colonization potential and reduce the neighborhood's disperser pool, thus limiting patch-specific contributions to network connectivity and ultimately limiting gene flow (Kimmig et al. 2020). So, while functionally isolated patches that are not occupied or are occupied and produce no emigrants are assumed to contribute to network connectivity under the structural paradigm, in reality, they make no contribution to actual connectivity. The consequences of not acknowledging such "zombie patches" is the equivalent of introducing false positive errors which could lead to bias in key model components and erroneous estimates of connectivity (Box 2). Further, considering occupancy dynamics for functional connectivity better reflects both the dispersal pool, through the inclusion of occupancy states and the dispersal process, through colonization-extinction dynamics (Sutherland et al. 2014, Chandler et al. 2015a). Thus, in the same way demographic data provides mechanistic interpretations of structural connectivity, it can also offer a mechanistic interpretation of functional connectivity.

Functional connectivity seeks to introduce biological realism by invoking increasingly realistic movement rules. Often this is through the use of landscape resistances that introduces variable strengths of spatial dependencies beyond Euclidean distance based measures (Zeller et al. 2012, Graves et al. 2014, Diniz et al. 2020). Resulting resistance surfaces are often modelled via cost-distance methods (Adriaensen et

al. 2003) or circuit theory applications (McRae 2006, McRae et al. 2008), that seek to quantify the interaction between movement and landscape structure. Thus, the objective of functional connectivity metrics is to identify inter-patch corridors with lower resistance to movement than the rest of the matrix (Beier and Noss 2008). As applied, many existing approaches to connectivity modeling represent hypotheses of naïve function that assume populations, and hence dispersers, are uniformly distributed through the landscape. In reality these dispersers are more likely to exhibit spatial heterogeneity (Zeller et al. 2018). This raises concerns about how well existing approaches represent the dispersal process, and the value of the resulting resistance surfaces in applied settings (Beier and Noss 2008, Laliberté and St-Laurent 2020). Noteworthy exceptions include the rarely applied weighting schemes available in the application of circuit theory (McRae et al. 2008, Dickson et al. 2019) and the development of a unified framework for connectivity that can integrate species distribution information (Fletcher et al. 2019).

While conceptually appealing, resistance models are challenging to parameterize due to the lack of information at the transfer stage, and if mis-specified, can be poor predictors of connectivity (Janin et al. 2009, Keeley et al. 2017), especially when parameterized using expert opinion (Koen et al. 2012, Zeller et al. 2012). Empirical estimates can be derived from techniques such as GPS telemetry, mark-recapture, or genetic data (Epps et al. 2007, Graves et al. 2014, Sutherland et al. 2015), or indirectly from observed locations of focal organisms. For example, Zeller et al. (2018) found that movement corridors were best recovered using resistance surfaces estimated by cost-distance pathways informed by GPS data, but also suggesting that circuit-theory based

algorithms be used to infer dispersal if opportunistic presence-only data is the data available.

Another emerging interest is the existence of short- and long-term habitat shifts in response to disturbances, wildfire, climate change, and fragmentation (Bishop-Taylor et al. 2018, Littlefield et al. 2019). Accounting for temporal variation in habitat structure and its influence on connectivity by considering long-term and ephemeral changes in landscapes (Ruiz et al. 2014a, Zeigler and Fagan 2014, Drake et al. 2017b, Bishop-Taylor et al. 2018) are likely to become increasingly important as more species undergo climate-induced range reductions (Littlefield et al. 2017) and loss of habitat and the subsequent increasing landscape resistance and reducing structural and functional connectivity (Dilts et al. 2016). In fact, like spatiotemporal (meta)population dynamics, shifts in the extent, structure, and quality of habitat is an important contributor to spatiotemporal variation in connectivity (i.e., connectivity dynamics, Zeller et al. 2020). In a study of fragmented Brazilian Atlantic Forest patches, Martensen et al. (2017) showed that temporal changes in patch size resulted in up to 150% increase in connectivity between patches compared to static snapshots of habitat availability. It is worth noting that the authors did not account for underlying occupancy dynamics which are predicted to be linked to patch size (Hanski 1998). In general, both functional and structural measures of connectivity do not have spatial or temporal dynamics built into their conceptual interpretations. Spatial habitat variability over ecological time scales is not equal to short-term changes in populations within that habitat, which, we argue, renders the domain incomplete because, a patch is not a population. Integrating aspects of the underlying population state directly resolves this concern.

Demographic Weighting

Ideally, weighting connectivity measures via locale-specific demographic contributions would not be necessary if all movements could be observed completely which we suggest is unlikely in practice. Thus, information on spatiotemporal changes in the distribution or size of a population, which provides a measure of dispersers and their contribution to ecological processes, should be used to inform connectivity. Integrating spatiotemporal heterogeneity in population size and hence in the production of dispersers, which we refer to as demographically-weighting, directly and explicitly introduces spatiotemporal dynamism into connectivity modeling (Sutherland et al. 2014, Drake et al. *In Review*). Such dynamism is crucial to identify the 'actual connectivity' between extant populations amongst occupied habitat (Calabrese and Fagan 2004). Examples of relevant and now commonly estimated demographic data useful for weighing the contribution of patches to connectivity are occupancy, a local state variable that describes the distribution of populations and whether they contribute to colonization-extinction dynamics (Chandler et al. 2015a, Howell et al. 2018), and population size, the number of potential dispersing life stages in occupied patches (Sutherland et al. 2014). Alternatives to occupancy and abundance may include the number of reproductively active individuals (Robertson et al. 2019), fecundity (Castorani et al. 2015, 2017), the number of successful reproducers (Robertson et al. 2018), stage-structure (Sutherland et al. 2012), conspecific condition (Clobert et al. 2009a, Cote and Clobert 2010), dispersal syndrome of individuals (Jones et al. 2015, Edelsparre et al. 2018, Fobert et al. 2019), individual condition (Shima and Swearer 2009, Marshall et al. 2010), and individual behavioral expression (Cote and Clobert 2007, Brown et al. 2017). Each has in common the fact that

they have the potential to vary spatially and therefore influence the number of potential dispersers, and hence connectivity.

These examples build upon earlier approaches to spatially realistic modeling in landscape ecology and metapopulation ecology. Hanski (1994) introduced a realistic metapopulation model that accounted for simple occupancy states in the measure of connectivity between patches. This model also used a Euclidean distance but suggested that any meaningful biological distance could be included (Box 1). This model also accounted for variation in habitat amount or quality (Hanski 1994), but was focused on within-patch metrics. Conservation practitioners often focused on identifying corridors through interpatch matrix informed by coarse population distributions to identify source locations and potential bottlenecks (Larkin et al. 2004). More recently, researchers have integrated species distribution models with information on dispersal to advance the realism of landscape connectivity, particularly useful for exploring predictions of range shift abilities in accordance with shifting habitats due to climate change (Ofori et al. 2017). These methods have, however, historically conflated the impact of landscape on movement and the mortality of dispersing individuals when quantifying resistance and connectivity (Zeller et al. 2012). Fletcher et al. (2019) used spatially absorbing Markov chains to disentangle these processes and improve least-cost path and circuit theory modeling, allowing multiscale temporal predictions as well as quantification of demographic parameters related to connectivity. Identifying such divergent causal mechanisms (avoidance vs. mortality) to influence ecological processes may be important for understanding how demography impacts spatiotemporal heterogeneity in connectivity and *vice versa*.

Spatiotemporal heterogeneity is an inherent characteristic of any spatially structured population, and where such heterogeneity is prevalent, the assumption that all populations contribute equally to connectivity is difficult to justify (Prugh et al. 2008, Box 2). This concern is regularly alleviated using theoretically justified proxies of population size such as patch size, and while surrogates likely capture longer term average population sizes, they fail to capture temporal stochasticity resulting from local population dynamics or whether the species is even present. In this regard, such proxies may result in misrepresentations of connectivity, potentially similar to those in structural measures. For instance, while simple patch occupancy may be enough to increase the accuracy of dispersal estimates, Clinchy et al. (2002) found that occurrence data masked population declines such that the population dynamic processes of pika could not be inferred without more detailed demographic data. Ultimately, connectivity measures that do not consider the spatial distribution of dispersers, may be overly simplistic for many ecological questions or management goals (Lambin et al. 2004).

Box 1: The current state of demographic connectivity modeling, a spatially realistic metapopulation perspective

Spatially realistic metapopulation theory (SMT) has the potential to act as a unifying force in ecological research (Hanski and Gilpin 1991, Hanski and Ovaskainen 2003), providing a strong conceptual basis and analytical framework for the conservation of fragmented species. Its implementation through the stochastic patch occupancy framework (Moilanen 1999) has allowed the exploration of connectivity's influence on (meta)population dynamics through the lens of dispersal. It has historically been difficult to implement (Baguette 2004, Sutherland et al. 2014), but recent advances have increased the popularity and utility of SMT.

Connectivity in SPOMs is often modelled as a function of dispersal from occupied patches in the spatially explicit patch network (Hanski 1994) and often relies on

an assumption of abundance scaling with patch size. This approach is often criticized, because when this assumption does not hold, it can cause erroneous inference, performing poorly as a connectivity predictor (Prugh 2009). While this model has classically relied on such assumptions, occupancy models that are used to estimate dispersal and infer connectivity would benefit from more direct inclusion of demographic data (Clinchy et al. 2002). This can be achieved with the flexibility of Bayesian hierarchical modeling (Risk et al. 2011, Sutherland et al. 2014, Howell et al. 2020a).

Bayesian hierarchical modeling has allowed for the accounting for imperfect detection (Royle and Kery 2007, Guillera-Arroita 2017, MacKenzie et al. 2018) and estimation of missing data (O'Hara et al. 2002, Risk et al. 2011, Sutherland et al. 2014), making traditionally error-prone data easier to analyze. Although the need to incorporate more detailed demographic data is not always needed (Chandler et al. 2015a), the inclusion of population size and structure can lead to more accurate representations of connectivity and population dynamics structure (Pellet et al. 2007, Sutherland et al. 2012). Weighting of model components can inherently increase acknowledgement of spatiotemporal heterogeneity of spatially structured populations (Thomas and Kunin 1999), allowing the combination of temporal dynamism and demographic weighting to produce more dynamic representations of connectivity (Drake et al. *In Review*).

Inclusion of other core components of demographic connectivity has been facilitated by the conditional flexibility of hierarchical modeling (Royle and Dorazio 2009). First, the internal state of patch dynamics, often overlooked by classical SPOMs (Holt 1992), can be estimated through the use of sub-models (e.g. Sutherland et al. 2014), thus directly addressing the population size/structure to patch area relationship directly (Bender et al. 1998). Second, recent advances by Howell et al. (Howell et al. 2018) has allowed the generalization of SMT to allow landscape resistance to be included in the model. This addresses a perennial criticism of the metapopulation framework in general (With 2004), allowing more mechanistic understanding of the dispersal process and acknowledging non-Euclidean movement to be estimated, reducing the reliance on expert opinion. As well, the inclusion of non-Euclidean dispersal and demographics address both system-scale and local issues of population dynamics (Howell et al. 2020a). This integration of landscape and metapopulation ecological fields has been long anticipated

(Hanski and Gilpin 1991) but rarely achieved (Moilanen and Hanski 1998, With 2004, Howell et al. 2018).

Demographic connectivity: synthesizing core contributions

Demographic Proxies

The use of patch size as a surrogate for population size is common in ecology, especially in landscape-scale investigations. This is largely due to the time-, labor-, and cost-intensive nature of gathering demographic data at spatial and temporal scales that are representative of landscape-scale or population-level processes. However, the relationship between patch size and abundance are not always linear (Deza and Anderson 2010) or even positive (Hovel and Lipcius 2001), and the strength of the relationship can be taxon- (Pellet et al. 2007) or stage-specific (Sutherland et al. 2012). Indeed, there is accumulating evidence suggesting that, when measuring connectivity, area-abundance assumptions do not hold and that demographic information representing real-time heterogeneity in abundance is preferred (Moilanen and Nieminen 2002, Prugh 2009).

In addition to the spatial misrepresentation of local abundances, area approximations that use a single measure of patch size implicitly assume a degree of temporal invariance with the potential to mask local dynamics (Sutherland et al. 2012). In this case, large patches will dominate, and potentially bias, inferences about network dynamics regardless of their internal state (Cavanaugh et al. 2014). Moreover, density-dependent factors (e.g., dispersal, local population dynamics) are completely overlooked, despite their importance in determining both local and regional (meta)population dynamics (Eriksson et al. 2014, Spanowicz and Jaeger 2019). Attempts at addressing the deficiencies of the static measures, such as incorporating time-varying measures of

habitat quality (e.g. Clinchy et al. 2002), are also likely to mischaracterize the response of either local population size or potential emigrants and overlook important thresholds (Harman et al. 2020).

Notwithstanding, population size is itself a proxy for the number of dispersers, which drives connectivity between patches. Dispersal rates can be sex-specific (Trochet et al. 2016) and/or stage-structured (Sutherland et al. 2014, Tucker et al. 2017). Further, different demographic life stages within the same habitat patch, may experience the landscape differently during the transfer stage of dispersal, and per-capita contribution to connectivity varies accordingly (Baguette et al. 2013). For example, in African lions, *Panthera leo*, differences in levels of risk aversion result in substantially different estimates of sex- and age-specific landscape resistance (Elliot et al. 2014b). Increases in mortality risk to dispersing individuals, whether due to human-wildlife conflict, predation, or exposure, can be masked in resistance surfaces (Fletcher et al. 2019), especially if demographic data is ignored when smaller and younger individuals experience increased mortality risk (Sibly et al. 1997). Such attention to demographic details also helps decipher effective dispersal which leads to successful habitat colonization and reproduction, a potentially crucial aspect to correctly interpret conservation objectives and ecological questions (Greenwood and Harvey 1982, Vasudev and Fletcher 2016) A failure to consider demographic determinants of connectivity has the potential, therefore, to lead to unsound management decisions (Elliot et al. 2014b).

Using common proxies for demography in connectivity can lead to bias (Box 2), but demographic data is hard and/or expensive to collect. Our simulation demonstrates what may occur if you fail to account for demographic variation or other additional

(un)known sources of bias/variation. Rather than forgoing connectivity research due to this, there is potential for an application of Bayesian hierarchical modeling (Box 1) to help account for this bias using a random effects parameterization. For example, Fletcher *et al*. (2011), used random effects to help account for variation in dispersal. Such an approach may help increase the robustness of connectivity models (Drake et al. *In Review*) to bias but are unfortunately phenomenological and may be less powerful than including demographic data directly.

Ultimately, connectivity is a dynamic property of an embedded population-landscape system. Populations vary in space and time and are often structured such that contributions to ecological dynamics are not equal among individuals. This is no different for connectivity, and as such, direct measures of the functional component of the local population in space and time are critically important because they represent fundamental spatiotemporal contributions to emergent landscape connectivity.

Eco-Evolutionary and Management Implications

Sources of Error and Structural Weaknesses Missing information about the functional state of a patch can arise in several ways, each with specific implications for inference about occupancy, dispersal, and hence, connectivity. One main source of error is the false negative error associated with imperfect detection: the assumption that a patch is not occupied after failing to detect a species at a site when it is actually present (Mackenzie et al. 2002, MacKenzie et al. 2003, Guillera-Arroita and Lahoz-Monfort 2012). Missing a patch completely, or assuming it isn't occupied (note that both overlook contributions to connectivity), overestimates dispersal rates and colonization in metapopulations and hence biases estimates of connectivity (Moilanen 2002). Imperfect

detection also skews resistance estimates of landscape features (Graves et al. 2014) and masks important demographic information resulting in biased estimates of dispersal and inferred connectivity when these observational errors are left unaccounted in models (MacKenzie et al. 2018). False positives can also occur, and while they are another important source of bias (Moilanen 2002, Miller et al. 2011), they are assumed to be less common (MacKenzie et al. 2018).

Interestingly, however, unweighted measures of connectivity, of which many are, systematically introduce false positives by failing to acknowledge the underlying spatiotemporal distribution of the population. Under the classical description of structural connectivity, where all viable patches are assumed to be hosting populations, landscape connectivity is overstated due to the inclusion of contributions from unoccupied parts of the landscape. Even when weighting schemes are incorporated similar errors can occur. For example, the estimated mean dispersal distance for the water vole, *Arvicola amphibius*, when assuming data perfectly represented patch states compared to when errors were explicitly acknowledged was 12.4 km and 2.10 km, respectively (Sutherland et al. 2012, 2014). The latter is more reflective of estimated dispersal confirmed by mark-recapture, telemetry, and genetic analyses (Stoddart 1970a, Telfer et al. 2003a, Aars et al. 2006, Fisher et al. 2009). More generally, contributions to connectivity are biased if area does not correlate to occupancy state or abundance (Box 2), or when occupancy states do not distinguish between functional states such as breeding and non-breeding populations (Sutherland et al. 2013). Sources of errors and biases in the underlying patch state such as erroneously missing or considering the functional importance of a patch, or misrepresentations of the functional component, erodes the connectivity signal resulting

in, at best, estimates of connectivity and associated dynamics with high uncertainty, or at worst, biased estimates of connectivity (Prugh 2009). Recent advances in how data are collected and analyzed have naturally facilitated the integration of demographic data and methods for addressing imperfect detection upon which the concept of demographically informed connectivity has been synthesized (Sutherland et al. 2015, Morin et al. 2017, Meyer et al. 2020, Box 1).

Box 2: Illustration of bias emerging from common connectivity modeling assumptions

We conducted a simulation (code available in Supplemental Materials Appendix 1) of spatially-explicit patch occupancy dynamics in a homogenous matrix to determine how commonly applied assumptions about demographics influence the ability to recover parameter estimates that influence connectivity. Using a metapopulation as an archetypal spatially structured system and the well-established stochastic patch occupancy model (Ovaskainen and Hanski 2004) as pedagogical demonstration, we iteratively relax spatiotemporal invariance and realism of demographic contributions.

We initialized the metapopulation simulation with each patch having an occupancy probability of ψ. These colonization-extinction rates are Markovian, i.e., they are conditional on the occupancy states, z, in the previous year for any given patch i:

$$\psi_{i,t} = (1 - z_{i,t-1})C_{i,t-1} + z_{i,t-1}(1 - \varepsilon_{i,t-1}),$$

where ε is the probability of extinction (ε =0.4) and C is the colonization probability. For every occupied patch, we generated local population size (N_i) by simulation a random Poisson variable according to an expected area~abundance relationship. This allowed for a stochastic variation in spatiotemporal abundances:

$$N_i \sim Pois(\exp(\beta_0 + \beta_1)) * z_{it}$$

where β_0 is the intercept ($\beta_0 = -1$) and β_1 is the slope parameter relating area to abundance, and the multiplication by z_{it}, the occupancy state, ensures only occupied sites have non-zero abundances. Patch areas were generated from a $U(1,3)$ distribution.

Transition rates themselves are a function of the number of individuals in a patch, i.e. they have a demographic basis:

$$C_{i,t} = 1 - \exp(-\gamma * S_{i,t}),$$

γ is the per capita effective dispersal rate and $S_{i,t}$ is the measure of connectivity:

$$S_{it}^{*} = \sum_{j \neq i} X_{it} * \exp(-\alpha d_{ij}),$$

where the exponentiated term $-\alpha d_{ij}$ is what makes this representation of connectivity spatially explicit, being a decreasing function from increasing interpatch distances, d_{ij}, scaled by the parameter α. Also, X_{it} represents a series of increasingly realistic demographic weightings (see below).

We explore sensitivities by considering variation in time series length (t=5, 10), patch network size (sizes=30, 100), and area~abundance relationship (γ=0.2, 0.03). In addition to this area~abundance relationship scenario, we generated abundances to have the same overall mean and variance but without the area~abundance relationship (this we refer to as 'disrupting' the relationship). We explored additional combinations of parameters including additional values, which are reported in Appendix 2, although the results and scenarios used here are representative of general model performance.

Varying both total abundance and heterogeneity of populations sizes allowed us to consider how different population structures in the landscape impact model recovery of parameter estimates. Varying the disperser scaling factor γ and the slope to estimate abundance allowed us to examine scenarios reflecting diverse metapopulations; from low population sizes with relatively low variance (ranging from approximately 1 to 11 mean = 2.72) such as those found in carnivores (e.g. Benson et al. 2016) to the those with high abundance and variance (ranging approximately from 1 to 154, mean=20.09).

The patch area-disperser abundance relationship has been a core incidence function model assumption (Hanski 1994) that has recently received increased scrutiny (Ozgul et al. 2009). This disruption of the area-abundance relationship may reflect biologically realistic scenarios where this relationship may not exist (Prugh et al. 2008) and provide insight into bias introduced into modeling populations that do not conform to this assumption (e.g. Hovel and Lipcius 2001).

We consider 5 formulations of the data-generating model that represents increasingly unrealistic assumptions about connectivity. First, we fit the data generating model (N_{it}) described above that included abundance effects on connectivity. Second, we approximate abundance with occupancy-weighted patch sizes ($A_i z_{it}$). Third, we

approximate abundance with occupancy state only (z_{it}), ignoring any potential information contained in the size of the patch. Fourth, we approximate abundance with unweighted patch size (A_i), ignoring the occupancy state. Finally, we fit a model that assumes all patch contribute to connectivity equally by ignoring patch size and demographic contributions (U).

These calculations were carried out in R (R Team 2019), using the NIMBLE package (de Valpine et al. 2017); each model combination was run 500 times, each run iterated 30,000 times with 10,000 burn-in and a single chain. We wish to note that these simulations were computationally intensive, requiring multiple processor cores to work over several days or weeks depending on the settings applied. Extended description of the model can be found in Appendix 2.

Influence of Demography for Parameter Recovery

Here we focus specifically on the ability to recover the parameter α, the spatial scale parameter of the dispersal kernel that represents the spatial scale of connectivity. Dispersal kernels are central to representing spatial population processes (Nathan et al. 2012). We use a negative exponential version (but other forms may be used; Appendix 1) of the incidence function model (Hanski 1994). This form relates the dispersal process to connectivity through the scaling parameter α, representative of the mean dispersal distance (Moilanen and Nieminen 2002). To determine the impact of increasing demographic assumptions on modelling connectivity, we calculated the mean estimator bias of the median connectivity parameter α for each of the 120 possible outcomes.

Unsurprisingly, the data-generating model, N_{it}, performed well and was unbiased in each scenario (mean bias <0.05; Supplementary Material Appendix 2). Estimates of α were more biased in high abundance scenarios than in low abundance scenarios. The amount of bias propagation i.e., increasing bias for longer time series and more patches, was inversely proportional to the amount of demographic information included (inset Figure 1). In fact, model z, which only used occupancy weighting, was the only model to reduce bias as data increased by year and patch number, and was able to have an acceptable amount of bias (from 5 year, 30 patches = 0.06 to 10 years, 100 patches = 0.024) even where the area-abundance relationship was disrupted in the low abundance variant; the high abundance variant of models weighted with z also reduced bias as

spatial and temporal data increased. This may be due to the ability of occupancy data to capture the dispersal process through temporal patterns of colonization-extinction across the landscape.

When the area-abundance relationship held, , model $A_i z_{it}$ exhibited negligible bias, whereas, when this relationship was disrupted, only low abundance variants in smaller patch networks with fewer years of data maintained reasonable bias in the estimator. As the amount of patch data increased both spatially and temporally, so did the bias. Of note is that the uninformed model U generally performed worse than model $A_i$when the area-abundance relationship held, but, unsurprisingly when this was disrupted, area weighting for connectivity models resulted in the greatest bias recorded (10 years, 100 patches = 0.262), performing less consistently than an unweighted metric (10 years, 100 patches = 0.192).

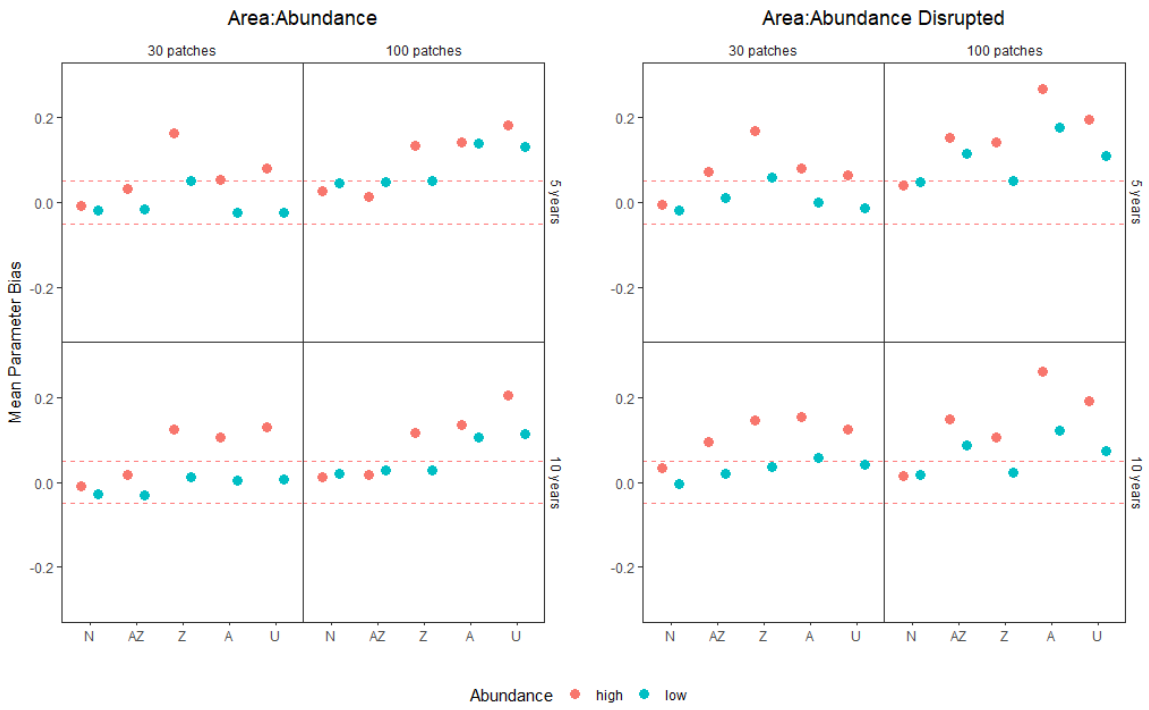

This exploration of several key assumptions found in connectivity studies show that disregarding demographic information can bias recovered parameter estimates and reduce model consistency. Further, this trend appears to couple with corresponding parameter coverage performance with decreasing demographic data lending to decreased coverage (Supplemental Material Appendix 2). Information such as disperser abundance

and structure of the populations in relation to the patch network can each have impacts individually or compounding to recover accurate connectivity assessments. As connectivity models become less general, results indicate that overestimation of parameter α (inset Figure 1), i.e. the overestimation of species ability to disperse, and hence a bias to connectivity, could lead to misguided conservation decisions. The results of this simulation suggest that although increased demographic fidelity allows for less biased parameter estimates, the choice to include *any* demographic information (e.g. occupancy) may be more important than neglecting the state variable in favor of area-based approximations or a demographically uninformed model. We prescribe care to be taken when invoking an area-based assumption for connectivity unless system or species-specific patch size to abundance relationships have been empirically confirmed.

This simulation also shows how powerful the SPOM framework can be at integrating demographic connectivity for describing ecological processes (Box 1) as well as the importance of demographic connectivity itself in recovering accurate parameter estimations. While this simulation framework provides a useful perspective on parameter recovery, we use it as a pedagogical tool. If applied towards hypotheses in real world systems, it also provides a useful testing framework to extend to other models and methods pertaining to heterogeneity in connectivity on the landscape. Model selection methods such as information criterion may also be applied to explore the intersection of model parsimony and mechanistic explanations of animal behavior and landscape connectivity. Also, the model is further generalizable through the inclusion of other biologically informative distances, such as least cost paths, as pointed out by Hanski (1994) and implemented by Howell et al. (2018). As well, imperfect detection is likely to be complicating factor for real data and this model could be extended to account for such observational error (e.g. Sutherland et al. 2014, Chandler et al. 2015). This simulation shows a reflection of the current state of connectivity modeling and the implications these common assumptions can have on inference. There is room for improvement and many of the works referenced throughout this manuscript show that it is a possible and worthwhile pursuit.

The Temporal Scales of Demographically-weighted Connectivity

Long-term planning for promoting the persistence of species is often the end-goal for management actions, yet conservation planning is often based on relatively short time scales (e.g., annually) and therefore requires demonstration of success at corresponding scales. Demographically-weighted connectivity is most likely to be important at this scale of generations and 10's of generations, i.e. at the scale of (meta)population dynamics which is driven by dispersal and colonization-extinction dynamics. For example, when considering species invasions or reintroductions, where small beachheads of organisms can lead to system-wide occupancy (Howell et al. 2020a), this framework may be especially useful as an addition to others, as the acknowledgement of demographic states or population distributions may be crucial to understanding colonization, persistence, and quickly shifting distribution of organisms though time in such systems.

Spatiotemporally shifting populations, when considered in connectivity analyses, can help account for the impact of intermittent or cyclic environmental disturbances and population dynamics (Lambin et al. 2001, Howell et al. 2020b, Zeller et al. 2020). This may come through shifts in organismal ranges, potentially due to spatiotemporally correlated extinctions and colonization events shifting the whole system's configuration. Such a scenario shifts the numbers and distribution of dispersers, and resulting genetic diversity, across time and space. For example, current genetic spatial structure may be the result of past demographic structure and dispersal patterns (Driscoll and Hardy 2005), reflecting a connectivity that no longer exists on the landscape. This may result from a temporal lag in observed genetic structure due to loss of connectivity compared to the

observed structure when the connectivity is facilitated by the removal of barriers to dispersal (Landguth et al. 2010, Driscoll et al. 2014). As well, demographic insights to connectivity, such as density dependent dispersal can be useful in determining the ability for species to track long-term climate change driven range shifts (Best et al. 2007). Determining the eco-evolutionary consequences to such shifts will be critical in the wake of large scale disturbances and environmental change (Dytham et al. 2014); demographically-weighted connectivity metrics can help identify key population processes and critical habitat, as well as reduce bias in estimates of dispersal and population dynamics (Sutherland et al. 2014).

Conservation actions often aim to achieve long-term persistence of species, habitats, or communities, even when constrained by the need for short term results. While we have focused on demographic-connectivity metrics, other metrics of 'potential' connectivity may still be appropriate to conservation planning; particularly those metrics that emerge at the landscape scale from finer pair-wise metrics. This approach to connectivity may incorporate behavioral data (such as mean dispersal), but may not consider the demographic state (e.g. occupancy or distribution) of a species across the available habitat. One such example is metapopulation capacity (Hanski and Ovaskainen 2000), which has been used to explore the ability of a specific spatial aggregation of habitat to allow long-term persistence of a species. Such measures are likely to provide insights into landscapes and habitat patches contributions to long-term population viability (Visconti and Elkin 2009). Such tools are capable of identifying land for reserve designs (e.g. Strimas-Mackey and Brodie 2018) but often still rely on connectivity

measures and proxies to determine population dynamics and persistence (Cabeza and Moilanen 2001).

The idea that demographics matter to connectivity, even at short time scales, and that the distribution of populations impacts connectivity inference is well supported in our simulation study (Box 2, Appendix 2). We demonstrated that as demographic data was abstracted out of models to greater degrees, the amount of bias increased, both as the number of patches or years increased. Particularly, if the population to area relationship does not hold, bias can emerge quickly and appeared to continue to propagate (Box 2, Figure 1). Likewise, when connectivity was demographically-weighted, the distribution of dispersers was accounted for, resulting in negligible bias in parameter estimates (Box 2, Figure 1).

Eco-Evolutionary and Management Implications

Dispersal's central role in life history is under strong selection (Ronce 2007). This leads to changes in dispersal phenotypes tied to changes in the costs of dispersal and potentially shifting dispersal life stage, relative probability of effective dispersal success, and dispersal propensity (Legrand et al. 2017). Changes in dispersal phenotype will impact functional connectivity, *i.e.*, the response to landscape and demographics (Legrand et al. 2017). Eco-evolutionary feedbacks driven by changes to functional connectivity and response to the landscape and conspecifics would, in turn, impact dispersal (Fronhofer and Altermatt 2017). This feedback may increase dispersal, for example, through the adaptation to more efficient use of matrix allowing increased long-distance dispersal success (Bonte et al. 2012). If increased isolation increases dispersal costs, which in turn reduces colonization, this will likely decrease the magnitude of and

selection for dispersal syndromes, shifting populations to increased residency instead (Matthysen et al. 1995, Legrand et al. 2017). However, Hanski & Mononen (2011) identified that simply changing model parameter values alters this prediction, especially when model assumptions are not reflective of the species biology (e.g. breakdowns in patch area abundance assumptions). Indeed, connectivity assumptions of dispersal evolution – usually spatiotemporal invariance. As with Hanski & Mononen (2011), a re-parameterization of connectivity models explicitly considering demography, and associated demographically-weighted connectivity feedbacks, also have the potential to alter standing expectations about the evolution of dispersal, particularly in the face of continued habitat fragmentation and loss (Thomas 2000, Cote et al. 2017).

The contribution of habitat fragmentation and habitat loss, or specifically the associated reductions in connectivity and gene flow (Mills and Allendorf 1996), is a major conservation concern (Soulé 1987). Also the reduction in dispersal or connectivity between patches (Griffen and Drake 2008) can decrease potential for viable adaptations to future disturbances for the whole population (Kimura et al. 1963, Bonte et al. 2018). This limits the distribution of dispersal phenotypes and genetic diversity, ultimately reducing the effective population size (Palstra and Ruzzante 2008), again increasing potential inbreeding risks and genetic drift. A potential, catastrophic scenario is mutational meltdown, the accumulation of deleterious mutations, happening in an expedited fashion in highly fragmented and increasingly isolated populations, leading potentially to metapopulation collapse (Higgins and Lynch 2001). Static, structural, or other forms of connectivity that rely on area assumptions, would likely miss demographically driven shifts in connectivity, resulting in overestimated persistence

(Wang and Whitlock 2003). As well, the increase in realistic estimates of dispersal rates by inclusion of demographic data that address population processes (Sutherland et al. 2014) can help resolve problems of cryptic population genetic interactions that emerge at shorter time scales, but have long-term eco-evolutionary consequences for conservation (Lowe et al. 2017).

As climate change, invasions, fragmentation, and other threats force species to adapt or shift their range (Shine et al. 2011, Cote et al. 2017, Maher et al. 2017, Littlefield et al. 2019), the role of connectivity in shaping species' responses will be a function of the combined effects of genetic bottlenecks, local adaptation, colonization-extinction dynamics, and dispersal barriers (Parmesan 2006, Saura et al. 2014, Bonte et al. 2018, Senner et al. 2018, Bani et al. 2019). Now, more than ever, moving beyond unrealistic assumptions and unrepresentative surrogates, and parameterizing connectivity models with accurate information on the underlying processes that give rise to, and respond to, connectivity is paramount (Lowe et al. 2017). In turn, viewing realized connectivity as inherently reliant on demographic inputs will offer greater insight about the eco-evolutionary consequences of connectivity and the mechanisms controlling persistence of (meta)populations (Kinnison and Hairston 2007). Indeed, we suggest that demographically-informed connectivity provides a conceptual framework (Figure 1) along with associated modeling innovations to better quantify connectivity with wide ranging basic and applied implications.

Looking Forward

Our review suggests that while both structural (e.g. available habitat) and functional (i.e. dispersal ability) connectivity paradigms are important, demographic weighting is a comparably, if not more, important dimension of connectivity. Our simulations illustrate the consequences of assuming all patches contribute equally to connectivity (Box 2). The ability to accurately characterize connectivity dynamics increases when unrealistic assumptions about the underlying population are relaxed through demographic-weighting. The simulations also suggest that inferences about the impact of connectivity on both short- and long-term population dynamics (and by extension genetic diversity) are likely to be biased if demographic contributions are ignored. While connectivity is obviously model-, situational-, species-, landscape-, or demographically-dependent, the generalities we derive are important for guiding future research.

Empirical modelling (Box 1) and simulations (Box 2) clearly demonstrate the value of integrating demographic information to increase mechanistic descriptions of connectivity, yet studies such as these are still limited in number and further work is needed. For example, stage-structured dispersal, area-based population scaling assumptions, and accounting for individual heterogeneity in dispersal need to be considered in more studies to better understand spatiotemporal heterogeneity to dynamic connectivity across landscapes (Zeller et al. 2020). Managing populations fragmented by increasingly inhospitable matrix and its subsequent increase in resistance to connectivity will be necessary as anthropogenic landscape changes accelerate. Thus, the role of the disperser, the variation of dispersal behavior in response to landscape, the complex

interaction of ecological and evolutionary processes, and the demographic influences upon them, is central to mitigating the detrimental effects of habitat loss and isolation (Burgess et al. 2014, Poli et al. 2020). However, perhaps more important is to ensure that these processes are accurately represented in models that are used to make predictions about connectivity and support specific conservation actions.

We also believe that demographic landscape connectivity falls naturally within the larger toolbox of existing approaches for understanding eco-evolutionary processes. In fact, many of the most interesting ecological questions and pressing conservation concerns may only be tractable with complementary methods, such as demographic connectivity modeling and landscape genetic techniques (Wan et al. 2018, Cushman et al. 2018, Zeller et al. 2018, Peterman et al. 2019). Not only can demographically-weighted connectivity be used to improve understanding of individual species, but across taxa as well (Cushman and Landguth 2012). We predict that it can help identify multi-species generalities of connectivity for community-level inference (Brennan et al. 2020) and for uncovering connectivity trends for biodiversity in general (Hartfelder et al. 2020). Terrestrial ecologists may do well to look to marine systems for examples of demographically- or population-based connectivity in dynamic environments and *vice versa* (Cowen and Sponaugle 2009, Castorani et al. 2015, Zeller et al. 2020). Demographic connectivity can help refocus sub-disciplines of ecology and conservation sciences to integrate data and methods (e.g. Howell et al. 2018) across spatiotemporal scales to provide inference and insight into fundamental ecological processes controlling biodiversity assembly rules like selection and dispersal (Pinto and MacDougall 2010, Rapacciuolo and Blois 2019).

The IUCN recently issued guidelines for connectivity conservation (Hilty et al. 2020). We agree that a focus on connectivity as a concept, and the central role it plays in mitigating global biodiversity loss is *absolutely* essential. We do note, however, that the guidelines put forth by the IUCN make very little mention of the demographic basis of connectivity and view populations as being a result of connectivity rather than acknowledging that population dynamics and connectivity are explicitly linked and should be treated as such. Claims that less than 10% of protected lands are viably "connected" for biodiversity conservation (Ward et al. 2020) are concerning, but acknowledgment of the demographic nature of connectivity is required to reaffirm if such claims are optimistic or pessimistic.

Conclusion

The connectivity paradigm has too often been suggested to be solely the driver of population dynamics and not to be driven by them. This is a remnant of the "if we build it, they will come' mentality (Hilderbrand et al. 2005). Such *field-of-dreams* hypotheses may be born out as Shakespearean tragedy. In an age of expanding rates of extinction (e.g., McCallum 2007, Ceballos et al. 2015, Sánchez-Bayo and Wyckhuys 2019), in a not too distant future, the world may no longer have the necessary reservoirs of biodiversity to abide such thinking. Instead, we must continue to elucidate how populations are connected: the more populations, the more chance for connectivity and recolonization of conserved habitat. Our framework addresses this directly. If we are not careful, we may conserve Nature's Stage (Beier et al. 2015) so perfectly that it lay set for *The Tempest* (Shakespeare 1623), yet no survivors may yet cling to the fragments of our shipwreck whom may take their cue and enter stage-right.

Here we have presented a general conceptual synthesis of existing approaches for measuring and estimating connectivity through the integration of information about the landscape, dispersal, and, importantly, demographic contributions – demographically-weighted connectivity. It is our hope that this review will lead to further integration of demographic information into connectivity frameworks and will facilitate the crosstalk between sub-disciplines of ecology themselves. Indeed, demographically-informed connectivity helps us prevent Prospero's hubris, moving the quantification of connectivity's influence on ecological processes forward, instead of losing our way in the coming storm.

Notes

[1] This chapter has been published in the Ecography.

Drake, J., X. Lambin, and C. Sutherland. 2021. The value of considering demographic contributions to connectivity - a review. Ecography https://doi.org/10.1111/ecog.05552

CHAPTER 2

SPATIOTEMPORAL CONNECTIVITY DYNAMICS IN SPATIALLY STRUCTURED POPULATIONS

Abstract

Connectivity is a fundamental concept linking dispersal to the emergent dynamics and ultimate persistence of spatially structured populations. Functional measures of connectivity typically seek to integrate aspects of landscape structure and animal movement to describe ecologically meaningful connectedness at the landscape and population scale. Despite this focus on function, traditional measures of landscape connectivity assume it is a static property of the landscape, hence abstracting out the underlying spatiotemporal population dynamics. Connectivity is, arguably, a dynamic property of landscapes, and is inherently dynamically related to the spatial distribution of individuals and populations across the landscape. Static representations of connectivity potentially overlook this variation and therefore adopting a dynamic approach should offer improved insights about connectivity and associated ecological processes. Using a large scale, long-term time-series of occupancy data from a metapopulation of water voles (*Arvicola amphibius*), we tested competing hypotheses about how considering the dynamic nature of connectivity improves the ability of spatially-explicit occupancy models to recover population dynamics. Iteratively relaxing standing assumptions of connectivity metrics, these models ranged from spatially and temporally fixed connectivity metrics to the most complex model that allowed temporally-varying connectivity measures that incorporate spatiotemporally dynamic patch occupancy states. Our results provide empirical evidence that demographic-weighting using patch

occupancy dynamics and temporal variability in connectivity measures each are important for describing metapopulation dynamics. However, we found that the inclusion of both temporal dynamism and spatial demographic processes is preferred. We highlight the importance of understanding the implications of commonly held assumption in connectivity modeling. We also show how these assumptions can produce varying levels of metapopulation capacity with increasing amounts of noise, oft overlooked in this ecologically important and connectivity driven metric. Thus, we argue that the concept of connectivity and its potential applications would benefit from recognizing inherent spatiotemporal variation in connectivity that is explicitly linked to underlying ecological state variables.

Introduction

Dispersal is a key, but complex, ecological process that impacts local population dynamics and, through resulting connectivity, shapes the emergent dynamics and ultimate persistence of spatially structured populations (Bowler and Benton 2005, Clobert et al. 2009b). Dispersal is generally defined as the movement between natal and breeding patches (Clobert et al. 2012, Matthysen 2012), and connectivity is the aggregate strength of these linkages among habitat patches (Calabrese and Fagan 2004). As such, connectivity represents the set of spatial dependencies that arise between individuals in a landscape (Kool et al. 2013) and offers a lens through which to view a suite of complex processes, which themselves are challenging to observe directly (Clobert et al. 2009b).

Dispersal ensures that (re)colonization of vacant habitat in fragmented landscapes can occur (Hanski and Gilpin 1997). Reductions in effective dispersal, and hence connectivity, can lead to reductions in recolonization rates and an increased frequency of

local extinctions (Brown and Kodric-Brown 1977), thereby shortening the time to extinction, even of once-stable metapopulations (Sutherland et al. 2014, Carroll et al. 2020). Indeed, the impacts of climate change and the rapid and global scale of anthropogenic land conversion are predicted to disrupt connectivity such that many populations are expected to inhabit novel landscapes that are more fragmented than they once were (Casagrandi and Gatto 2002, Carroll et al. 2020). Thus, connectivity lies squarely at the center of contemporary conservation science (Elliot et al. 2014b), yet approaches to quantifying connectivity often lack the mechanistic basis required to make them informative of realized connectivity on the landscape. Although quantifying connectivity is laden with unrealistic assumptions (Moilanen and Nieminen 2002), the discussion on which of the available metrics offer the most in terms of practical value has yet to reach a consensus (Zeller et al. 2018).

To date, connectivity has generally been treated as a static feature of a system (Kool et al. 2013), despite being an emergent property of demographic processes, e.g., dispersal and the spatial distribution of dispersers, which are both spatially and temporally dynamic (Sutherland et al. 2012, 2014). Even recent calls for a greater appreciation for dynamic nature of connectivity (e.g., McIntyre et al. 2018) overlook this demographic component and instead focus on long-term changes in habitat due to environmental change (Bishop-Taylor et al. 2018) or climate change (Ruiz et al. 2014b, Drake et al. 2017b). There are two potential shortcomings of overlooking demographic contributions to connectivity. First, despite an implicit focus on movement, the treatment is generally time invariant, and hence simplistic, raising questions about the utility of inferred connectivity, particularly for future projections, and especially for non-

equilibrium populations. Second, many approaches for quantifying connectivity typically ignore the underlying spatial distribution, and heterogeneity therein, of the dispersing individuals, thus assuming spatially and temporally homogeneous contribution to connectivity across the system.

In contrast, connectivity dynamics are an explicit focus of spatially realistic metapopulation theory (SMT; Hanski 1999, Hanski and Ovaskainen 2003) where connectivity is treated as a landscape aggregate of weighted patch contributions, where the weighting scheme relates directly to the occupancy state of a patch (i.e. are dispersers present?), and the size of the population occupying the patch (i.e. how many potential dispersers are present?), both of which change in space and time. Given the proliferation of species distribution models (Ovaskainen et al. 2016, Acevedo et al. 2017), occupancy models (MacKenzie et al. 2018), and abundance models (Kery and Royle 2016) that offer a framework for spatially explicit predictions of ecological state variables at landscape scales, there is no reason weighting schemes applied in metapopulation models cannot be formally integrated into connectivity modeling in general (Sutherland et al. 2014, Morin et al. 2017, Meyer et al. 2020). Metapopulations therefore represent ideal systems in which to investigate the consequences of the restrictive assumptions of spatiotemporal invariance for inference about connectivity, a topic that has hitherto received little attention, despite its potential to fundamentally alter predictions about landscape connectivity.

Acknowledging that the definition of connectivity is tied closely to the specific scale and context in which it is required and the available data, the existence of a single unifying measure is unlikely. Instead, it is crucial to understand how specific assumptions

impact model outcomes and inference so they can be applied sensibly and responsibly. We seek to empirically address this knowledge gap through the analysis of data collected from a long-term, large-scale model mammalian metapopulation to evaluate how predictions of metapopulation dynamics and persistence are influenced by commonly held assumptions of connectivity. Bayesian analysis of stochastic patch occupancy models (SPOMs: Ovaskainen 2002, Ovaskainen and Hanski 2004), a flexible class of metapopulation models, lends itself naturally to the relaxation of the implicit assumptions often made in landscape ecology about spatiotemporal (in)variability of model parameters and patch occupancy states, and to formal comparison of model performance. We analyze a patch occupancy time series using, first, a spatiotemporally homogeneous metapopulation model, i.e., one that assumes all patches are occupied and that dispersal parameters are temporally invariant, and then iteratively relax the assumptions of spatial and temporal invariance analogous to increased realism in how demographic contributions to connectivity are characterized. Our approach seeks to quantify the relative contributions of spatial and temporal variability in these demographic contributions to connectivity dynamics, and in doing so attempts to advance the ideas of demographic connectivity, a concept that has been largely overlooked outside of metapopulation ecology.

Methods

Study System

We focus on a model mammalian metapopulation system in Assynt, northwest Scotland, UK. The species is the riparian specialist water vole, *Arvicola amphibius*, and the patch network is a river network consisting of 98 vegetated patches embedded in

approximately 140 km^2 area of unsuitable heather matrix. Around 10% of the total 860 km waterway network represents suitable habitat, patches are therefore highly fragmented (mean nearest neighbor distance of 0.5 km), and vary in size from 50 m to nearly 3 km (mean=0.847 km). Patches are connected by dispersal, they exhibit frequent turnover, and the metapopulation fluctuates around a long-term average of 55% occupancy, i.e., the system functions as a classic metapopulation (Sutherland et al. 2012, Sutherland 2013). Between 1999 to 2012, the water vole patches were surveyed between 1 and 4 times per year during the breeding season (July and August). Surveys involved fecal latrine searches as indicators of vole occupancy. In short, the data are year- and patch-specific binary detection histories representing imperfect observations of patch occupancy for a diffuse patch network that lends itself naturally to analysis using spatial occupancy models (see below). For further details on the study system and data collections, see Sutherland et al. (2012, 2013, 2014).

Spatial occupancy modeling framework

The 14-year 98-patch time-series of detection/non-detection data was analyzed using a Bayesian spatial occupancy model (Risk et al. 2011, Sutherland et al. 2014, Chandler et al. 2015a). Here, the latent patch occupancy state, z, is treated as a partially observed Bernoulli random variable, with site (i) and year (t) specific occupancy probability $\psi_{i,t}$. In the initial year, where no information about occupancy states or dynamics in the previous year are available, occupancy is modelled as:

$$z_{i,1} \sim \text{Bernoulli}(\psi_1), \quad [1]$$

where ψ_1 is the expected proportion of occupied sites in the initial year (1999). In subsequent years (i.e., $t > 1$), occupancy states are modeled as:

$$z_{i,t} \sim \text{Bernoulli}(\psi_{i,t}), \quad [2]$$

where occupancy probability is a Markovian process that depends on the occupancy state in the previous year and conditional colonization ($\gamma_{i,t}$, if $z_{i,t-1}$ = 0) and extinction ($\varepsilon_{i,t}$, if $z_{i,t-1}$= 1) probabilities:

$$\psi_{i,t} = (1 - z_{i,t-1})\gamma_{i,t} + z_{i,t-1}(1 - \varepsilon_{i,t-1}). \quad [3]$$

Assuming that patch size and population size are correlated, the probability of extinction, $\varepsilon_{i,t}$, is modelled as a function of patch size, here the length of the riparian habitat patch, using a logit linear model:

$$\text{logit}(\varepsilon_{i,t}) = \delta_0 + \delta_1 A_i, \quad [4]$$

where A_i is the time invariant length of a patch *i* and δ_0 and δ_1 are the regression parameters to be estimated.

Unoccupied sites are assumed to be (re)colonized with probability $\gamma_{i,t}$, which is modelled as an asymptotically increasing function of connectivity ($S_{i,t}$):

$$\gamma_{i,t} = 1 - \exp(-S_{i,t}), \quad [5]$$

where $S_{i,t}$ is a measure of connectivity. The general formulation of the connectivity term, which we adapt below, is given by:

$$S_{it}^{*} = \beta \sum_{j \neq i} A_i z_{i,t} \exp(-\alpha d_{i,j}), \quad [6]$$

where β is the per capita effective dispersal rate parameter, A_i is patch length and $z_{i,t}$ is the patch state which sets the contributions of empty patches to zero. The term $\exp(-\alpha d_{i,j})$ is a spatial function that declines with inter-patch distance, $d_{i,j}$, the spatial scale of the decline being determined by the scale parameter α. This function can be

thought of as a dispersal kernel and is the spatial weighting that defines the distance-dependent contribution of a patch to the connectivity of all other patches.

To evaluate how specific assumptions influence the estimates of model parameters and the corresponding inference about connectivity, we define four alternative formulations of equation 6. These formulations are focused on two aspects of the model and data that broadly represent analogies of commonly made assumptions. The first relates to the *structural connectivity* paradigm that defines connectivity as a property of the landscape rather than the populations residing within them (Urban and Keitt 2001), and the second relates the definition of 'function' in the *functional connectivity* paradigm which seeks to introduce aspects of species movement ecology (Adriaensen et al. 2003).

We represent the structural assumption by setting all patches in the network to be occupied ($z_{i,t} = z = 1$) which produces a measure of connectivity that is the aggregate of spatiotemporally homogenous contributions from every patch weighted by their size which is heterogeneous in space but temporally invariant. We then relax that assumption by adopting the classical metapopulation formulation of the model where patch contributions are weighted also by the occupancy state, which is spatiotemporally dynamic. The functional assumption is implied by the inclusion of the dispersal function that is also typically assumed to be temporally invariant. Contributions to connectivity are defined by the per-capita effective dispersal rate (β) and the scale parameter (α), so by setting those parameters to $\alpha_t = \alpha$ and $\beta_t = \beta$, respectively, we enforce temporal invariance. We then relax that assumption by modeling year specific dispersal parameters (i.e., α_t and β_t) as random deviates coming from a hyper distribution: $\theta_t = \theta + \epsilon_t$, where $\theta_t \sim \text{Normal}(0, \sigma_\theta^2)$ and $\theta = \{\alpha, \beta\}$. This iterative relaxation of connectivity modeling

assumptions reflects increasing realism of connectivity estimated from occupancy data with focus on demographic contributions. We refer to these as *unweighted with time-invariant dispersal* (UI), *demographically-weighted with time-invariant dispersal* (DI), *unweighted with time-varying dispersal* (UV), and *demographically-weighted with time-varying dispersal* (DV). Full connectivity model formulations and descriptions are provided in Table 3.

Finally, acknowledging that the data, $y_{i,j,t}$, denoting whether latrines were detected during the *j*th visit to patch *i* in year *t*, arise via an imperfect observation process, we assume the data are conditional on the estimated latent occupancy state z:

$$y_{i,j,t} \mid z_{i,t} \sim \text{Bernoulli}(z_{i,t}p_t), \quad [7]$$

treating year-specific detection probabilities as random effects (Sutherland et al. 2014):

$$\text{logit}(p_t) \sim \text{Normal}(\mu_p, \sigma_p), \quad [8]$$

Model comparison

We use a Gibbs variable selection approach (GVS: O'Hara and Sillanpaa 2009, Tenan et al. 2014) to quantify support for competing model structures. In the GVS approach, the indicator variables represent variables that define specific model structures, and the mass of the posterior distribution of the indicator variables correspond to support for hypothesized connectivity model formulations. We introduce two latent indicator variables, I^z and I^D that correspond to the weighting scheme (i.e., whether occupancy state weighting is included or not), and the random effect structure of the dispersal parameters, α_t and β_t, respectively. These enter the model as:

$$S_{it} = \begin{cases} \sum A_i \times \exp(-\alpha d_{ij}), & \text{if } I^z = 0 \\ \sum A_i \times z_i \times \exp(-\alpha d_{ij}), & \text{if } I^z = 1 \end{cases}, \quad [9]$$

for the occupancy weighting, and as $\beta_t = \beta + \epsilon_{\beta,t} \times \mathrm{I}^D$ and $\alpha_t = \alpha + \epsilon_{\alpha,t} \times \mathrm{I}^D$, which imposes temporal invariance on effective dispersal when $I^D = 0$. For both binary indicator variables, we used a $I \sim \mathrm{Bernoulli}(0.5)$ prior, assuming no prior information about support for either outcome, and hence posterior distributions that deviate from 0.5 suggest support or not for specific assumptions.

The above model comparison offers a means by which to assess statistical support for the four hypothesized forms of connectivity. However, we were also interested in evaluating the ecological significance of these assumptions and do so by calculating the metapopulation capacity under each of the models. Metapopulation capacity (MC) incorporates measures of patch area, connectivity, spatial network structure, and dispersal behavior to quantify the relative ability to support metapopulations in a spatially explicit metric (Hanski and Ovaskainen 2000, Schnell et al. 2013). Therefore, comparing MC can inform how dispersal behavior in a connectivity context supports long-term persistence a patch network. While generally used in analyses comparing scenarios of augmented networks, here, for a single network but with competing models, it can be instructive to evaluate how sensitive this important measure is to specific assumptions of temporally variable connectivity.

Table 3. Alternative formulations of the standard metapopulation connectivity function. Connectivity ($\boldsymbol{S}$) is modelled as a function of patch size ($\boldsymbol{A_i}$), a proxy for population size, and a distance-dependent spatial function $\boldsymbol{e^{(-\alpha d_{i,j})}}$. The occupancy column relates to the structural assumption about contributions to connectivity and the dispersal column relates to functional assumptions about the temporal nature of dispersal. The GVS column is a summary of the model support based on the posterior distribution of the indicator variable used in the Gibbs Variable Selection.

Definition	**Occupancy**	**Dispersal**[†]	**Equation**	**GVS**
Unweighted with time-invariant dispersal (UI)	$z_{i,t} \equiv 1$	α and β	$S_{i,t}^{UI} = \beta \sum_{j \neq i} A_i e^{(-\alpha d_{i,j})}$	0.0014
Unweighted with time-varying dispersal (UV)	$z_{i,t} \equiv 1$	$\alpha_t$and β_t	$S_{i,t}^{UV} = \beta_t \sum_{j \neq i} A_i e^{(-\alpha_t d_{i,j})}$	0.0082
Demographically-weighted and time-invariant (DI)	$z_{i,t}$	α and β	$S_{it}^{DI} = \beta \sum_{j \neq i} A_i e^{(-\alpha d_{i,j})} z_i$	0.0927
Demographically-weighted and time-varying dispersal (DV)	$z_{i,t}$	α_t and β_t	$S_{it}^{DV} = \beta_t \sum_{j \neq i} A_i e^{(-\alpha_t d_{i,j})} z_i$	0.8977

[†] For models without temporally varying connectivity, the parameters β and α are static, whereas in models with temporally varying connectivity it is treated as a year-specific random effect where $\theta_t = \theta + \epsilon_t$, where $\theta_t \sim \text{Normal}(0, \sigma_\theta^2)$ and $\theta = \{\alpha, \beta\}$.

Each of the models were analyzed using MCMC, fitted in R 3.6.1 (R Core Team, 2019) using the R package NIMBLE (de Valpine et al. 2017), with 3 chains of 80,000 iterations, 30,000 discarded for burn-in. Model priors (see Appendix S1) were chosen to

be non-informative (Gelman 2006, Gelman et al. 2017). Prior sensitivity analysis, based on visual inspection of posteriors, suggested that inference was not sensitive to prior specification. Visual diagnostics of model chains as well as autocorrelation lag plots provided evidence of convergence (Plummer et al. 2006). Using parameter estimates from each connectivity model, we used the R package metacapa (Strimas-Mackey and Brodie 2018b) to calculate metapopulation capacities using the joint posterior distribution of parameters from the metapopulation model, thus we are able to report point estimates of MC with associated uncertainty. All visualizations were produced using the R package ggplot2 (Wickham 2016). Parameter estimates are presented as posterior means, unless otherwise noted, with 95% Credible Intervals [CI's].

Results

We found substantial support for the demographically-weighted with time-varying dispersal hypothesis (DV: $\text{pr}(I^Z + I^D = 2) = 0.90$, Table 3). Considering GVS-based support for each hypothesis was calculated separately, in relative terms, models containing demographic weighting carried slightly more combined model weight ($\text{pr}(I^z = 1) = 0.99$ and $\text{pr}(I^D = 1) = 0.91$, Table 3). Also, support for uninformed and invariant model was negligible (UI: $\text{pr}(I^Z + I^D = 0) < 0.01$, Table 3). Thus, we provide evidence of dynamic connectivity in spatially structured populations and the importance of considering spatiotemporal weighting related to both the underlying state-variable and the strength and scale of connectivity.

The support for the inclusion of the occupancy weighting is compelling and intuitive: connectivity measured as a function of occupied, rather than all, patches better predicts occupancy dynamics as it includes information about the spatial distribution of

potential dispersers. The support for temporal variability in the strength of connectivity is interesting (Figure 2) and deserves further discussion (see below). The dispersal kernel is defined by the scaling parameter, α, and the rate of effective dispersal, β. For the time invariant models, α was 0.275 [<0.001 – 0.744] and 0.387 [0.195 - 0.632] for the unweighted and weighted models, respectively (Appendix S2). Estimates of the average α (i.e., the mean of the random effect distribution) for the models that allowed for temporal variability via a random effect were 0.495 [0.170 – 1.12] and 0.528 [0.267 – 0.997], for unweighted and weighted respectively. Year-specific estimates ranged from 0.431 [0.084 – 0.916] to 0.793 [0.149 - 1.773] for the unweighted model and 0.436 [0.149-0.818] to 0.770 [0.243 - 2.368] for the weighted model (Appendix S2). Thus, estimates of the scale of dispersal is higher without weighting, and although average values are similar between temporally varying and invariant models, there exists substantial interannual variation. For β, estimates from the static models were 0.054 [0.006 – 0.175] and 0.103 [0.041 - 0.203] for the unweighted and weighted models, respectively, compared to corresponding random effects average estimates of 0.076 [0.021 – 0.247] and 0.124 [0.044 - 0.346] for the time-varying models. Yearly estimate of β ranged from 0.061 [0.009-0.208] to 0.267 [0.046-0.885] for the unweighted model and 0.085 [0.016-0.266] to 0.482 [0.100-1.508] for the weighted model (Appendix S2). For dispersal rate, estimates are lower without weighting, and again while average values are similar between temporally varying and invariant models, there exists substantial interannual variation. In general, the inclusion of either demographic weighting or temporally varying dispersal parameters (i.e. increased realism) produces shorter dispersal distances ($1/\alpha$) and higher per capita dispersal rates (β) (Appendix S2).The

temporally dynamic model parameters α_t and β_t, the width and height of the kernel, respectively, were negatively correlated (Figure 2a), and interestingly, the observed temporal variability in both α_t and β_t were not related to annual metapopulation size (number of occupied patches) in an obvious way (Figures 1b and 1c). Differences among patch occupancy estimates were negligible among models (Appendix S2).

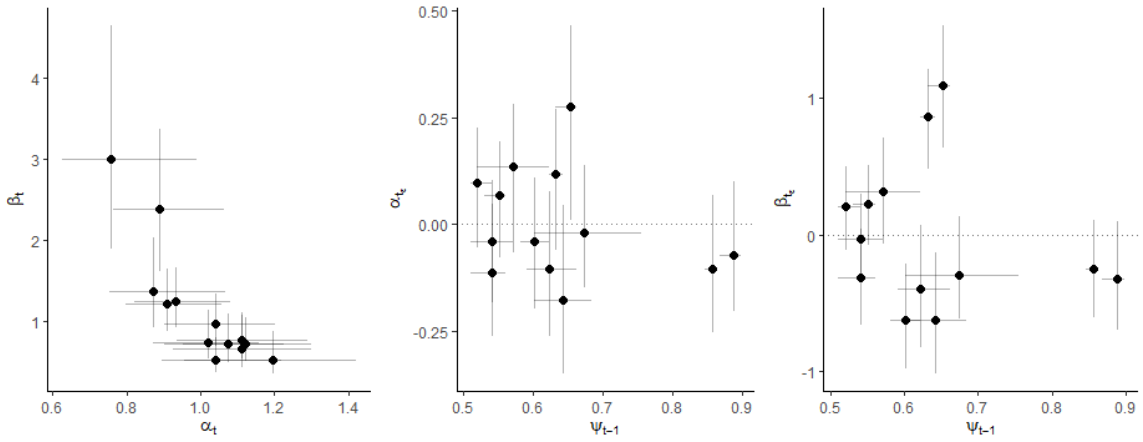

Figure 2. The random effect variance relationship of raw parameter estimates representing our connectivity process from the demographically-weighted, time-varying model (DV) to each other and estimated occupancy in the previous years. This represents the underlying raw parameter estimates variance around the mean of the random effect. *Left column*: The random effect variances, $\boldsymbol{\epsilon_t}$, for the rate of effective dispersal $\boldsymbol{\beta_t}$ and dispersal scaling parameters $\boldsymbol{\alpha_t}$. *Middle column*: random effects variance of $\boldsymbol{\alpha_t}$ and previous years occupancy estimates, $\boldsymbol{\psi_{t-1}}$. *Right column*: random effects variance of $\boldsymbol{\beta_t}$ and previous years occupancy estimates, $\boldsymbol{\psi_{t-1}}$. Error bars represent 50% CI for parameter values.

To understand how estimates of connectivity model parameters translate to characterizations of landscape connectivity, we calculated two year-specific measures of total connectivity for each of the four formulations using the model-specific connectivity function and, for convenience and relative comparisons across models, naïve occupancy values. First, we computed the *landscape-level* average colonization probability (i.e., from equation 5) which is the average colonization probability across each pixel of a raster defined as a rectangular polygon contained within a 2 km buffer around the patches

in the network (Appendix S3). Second, we calculated a *network-level* average colonization probability which is the average colonization probability across each patch in the network. Average landscape level colonization was lowest for the dynamic models (DV= 0.184 [0.175 – 0.201]; UV 0.212 [0.189 - 0.215], Figure 3a), while the static, unweighted model had the highest 14 year mean (UI= 0.308 [0.297 - 0.316], Figure 3a). Comparing the range of annual values, however, changes this trend with the dynamic, weighted model having the largest range of annual colonization means (DV range = 0.073 [0.066 - 0.080] to 0.499 [0.477 – 0.522], Figure 3a). However, inclusion of only demographic weighting allowed a temporal realism to emerged via demographic covariate weighting influence in the static, weighted model, but with a smaller range of values (DI: 14 year mean= 0.227 [0.216 – 0.239]; range = 0.136 [0.128 – 0.145] to 0.309 [0.294 – 0.323]). Network-level colonization estimates followed similar trends (see Appendix S3). In general, including either demographic weighting or temporally-varying dispersal kernels (i.e. increased realism) induces heterogeneity in the realized functional landscape connectivity, while static and invariant measures estimate greater connectivity on average.

Metapopulation capacity, the measure of relative potential of a landscape to maintain persisting metapopulations, was lowest when connectivity was assumed to be a fully dynamic property of the system regardless of the weighting structure used (Figure 3b). In contrast, the assumption about weighting structure did affect predictions of MC for the less supported temporally invariant models: assuming all patches are occupied results in a higher estimate of MC when compared to estimates from the weighted connectivity model (MC = 13.09 [4.01 – 68.95] and 9.88 [5.88 – 17.22], respectively).

Estimated MC using the model with most posterior support, demographic weighting with temporally-varying dispersal, was on average around half that of the static-structural model (DV: mean capacity = 6.63, range = 4.92 [1.13 - 14.88] to 8.86 [4.65 – 19.18]). For both dynamic models, MC was highest in 2006 (9.28 [3.87- 26.66] and 8.63 [4.39 – 21.07] for UV and DV, respectively), still lower than static metrics (Figure 3b). MC values for the demographically-weighted but time-invariant connectivity was intermediate relative to these extremes (static MC = 9.88 [5.88 – 17.22]).

Discussion

We present an empirical evaluation of two widespread assumptions used in the generation of connectivity metrics. In an attempt to understand how characterizations of connectivity propagate in terms of characterizing the dynamics of spatially structured populations, we advance discussions about the dynamic nature of connectivity. We show that spatiotemporal assumptions about effective dispersal rates and the underlying distributions of the potential pool of dispersers influence most aspects of statistical estimation and ecological inference using spatially explicit stochastic patch occupancy models. We confirm the theoretical assertion that it *is* important to consider connectivity dynamics as an inherent property of any spatially structured landscape, and critically, we highlight the fundamental, but often overlooked, role of demography as a major contributor to connectivity dynamics (Drake et al. 2021b).

We use four competing parameterizations of a stochastic patch occupancy model that represents statical analogies of commonly made assumptions in connectivity models. These included assumptions about spatial structure of the system, specifically the inclusion or not of a demographic weighting scheme that explicitly conditions

connectivity on the underlying patch occupancy states, and temporal variation in contributions to connectivity, i.e., in effective dispersal rates. We note also that the use of a Bayesian hierarchical model allows latent occupancy states to be estimated and thus included in the weighting while still accounting for imperfect detection (Royle and Kery 2007). These amount to a test of two important components of the quantification of connectivity: refined representations of where dispersers are, and of the dispersal process itself, both of which are inherently dynamic in space and time. We present these results in the context of a classic metapopulation, i.e., a highly structured patch network with high rates of dispersal-driven turnover, which is ideally suited to exploring the consequences of connectivity assumptions. As such, our conclusions, which are likely to hold to various degrees depending on where the system lies on the discrete-continuous continuum, offer generalities that contribute to a better understanding of the causes and consequences of dynamic connectivity.

Our iterative relaxation of assumptions represents a transition of increasing biological realism; here we specifically focus on how demographic contributions to connectivity are introduced. The degree of support for competing formulations of connectivity followed this realism gradient: the UI model (unweighted with time-invariant dispersal) receiving least support, and the DV model (demographically-weighted with time-varying dispersal) overwhelmingly supported, with models that included a relaxation of either the structural (Dx vs. Ux) or functional (xT vs xI) falling in between. In our case, relative support for the relaxation of specific assumptions suggests that demographic weighting was more important than allowing for temporally-varying dispersal (Table 3). This outcome is notable as the assumptions being relaxed in

this study represent those often violated, out of necessity or convenience, in many studies (Drake et al. 2021b). In particular, and for example, water voles experience frequent turnover events, limiting the pool of dispersers and introducing false positives in structural measures. The relative importance of specific contributions to connectivity may be inconsistent across systems, wherein depending on landscape heterogeneity and dispersal behavior, relative importance of demographics may shift. We emphasize that this does not limit the generality of our approach: the framework we have presented is able to quantify the relative contributions of these two demographic components to connectivity dynamics.

Implicitly assuming homogenous contributions to connectivity across the landscape does not consider the inherent spatial variation in the distribution of dispersing individuals. In fact, this is akin to a false positive observation process in occupancy models, the consequences of which have been described in detail recently (Royle and Link 2006, Miller et al. 2011). False positives could lead to mis-estimation of dispersal or colonization ability, extinction rates, and a reduction in patch turnover rates (Moilanen 2002, Sutherland 2013). For example, even relatively small rates of false positives, *i.e.* designating empty sites as occupied, results in biased inferences about occupancy estimates (Royle and Link 2006) and occupancy dynamics (Sutherland et al. 2013). Similarly, we find support for our demographically-weighted connectivity models that account for such assumptions that create false-positives (Table 3, Figure 3). The degree to which this assumption will affect inference is linked to the dependency of spatial dynamics (e.g. occupancy) on dispersal (Drake et al. 2021b), although we argue that such weighting is necessary in any dispersal dependent systems.

Connectivity metrics rarely consider temporal dynamics (but see Ruiz et al. 2014, Bishop-Taylor et al. 2018, Zeller et al. 2020). Our fully spatiotemporally dynamic formulation of a connectivity model allowed for multiple sources of temporal variability, both in the underlying occupancy states and the effective dispersal parameters. What results is substantial variation in effective dispersal (Figure 2), which in turn results in variation in estimates of both colonization potential (Figure 3a) and metapopulation capacity (Figure 3b). While individual variability can account for some variation in effective dispersal (Baguette et al. 2013), the spatiotemporal distribution of the disperser pool among habitat patches will likely contribute greatly to the observed variation in effective dispersal. Inclusion of such information into connectivity metrics will better describe observed colonization and occupancy, especially if those population dynamics are thought to be influenced through demographic processes such as the rescue-effect (Brown and Kodric-Brown 1977), Allee effects (Amarasekare 1998), or conspecific attraction (Morgan et al. 2019). As well, environmental shifts (such as climate change) may induce changes in dispersal probability or distances, but these shifts can play out at much different scales (often larger and longer) than demographic processes. Such long-term processes can influence the structural and functional connectivity between patch networks (Drake et al. 2017b, Bishop-Taylor et al. 2018). However, effective connectivity, connectivity weighted by the effective disperser pool, will be driven at shorter scales and by populations and by shifts in their dispersal. Local contributions to connectivity, and local connectivity measures, are thus dependent on the location in time and space of conspecifics, as well as the patches they reside in. We assessed the biological significance of overlooking these seemingly obvious processes (true

occupancy states and temporally varying dispersal rate parameters) when generating connectivity metrics; first by comparing systemwide summaries of colonization rates, and second by comparing resulting measures of metapopulation capacity.

Metapopulation capacity, although a relative metric, can be sensitive to the scale of dispersal (Blazquez-Cabrera et al. 2014, Strimas-Mackey and Brodie 2018a). Sensitivity analyses are important but uncommon when reporting the MC metric to understand a network's ability to support the metapopulation relative to dispersal capability. Also important, but rarely calculated, is the uncertainty around MC as a point estimate. Uncertainty around key parameters for MC, such as the dispersal rate and scale, propagate and therefore contribute to uncertainty in any derived metric, and MC is no exception. Using the full joint posterior distribution of model parameters, we Compared metapopulation capacities of the same network under different assumptions. This showed remarkable variation both in terms of point estimates and associated uncertainty. Connectivity dynamics, resulting either from demographic or temporal sources, produced lower estimates of MC and had lower average annual MC than their static counterparts. Demographically-weighting resulted in smaller CIs than their unweighted counterparts for both static and dynamic models. While models incorporating heterogeneity through either demography or dynamism allow for temporal variation to emerge in MC metrics, the static-unweighted model predicted higher MC with extreme uncertainty (Figure 3b). This lack of variation should not be interpreted as an 'averaged' MC; our results suggest that such structurally derived models may consistently misgauge MC with high uncertainty: MC more than halved in some years when considering fully dynamic connectivity relative to static metrics. We stress the need to account for uncertainty in

MC; even when accounting for both sources of dynamism, there is the potential for erroneous assessment of population persistence and network resilience as temporal heterogeneity in dispersal matters (Matter et al. 2020) and may be masked by model assumptions or the time series used (Ovaskainen and Hanski 2001, Schnell et al. 2013).

SPOMs, a tool developed to address questions of dynamics in systems assumed to be in long-term equilibrium or quasi-equilibrium (Hanski 2004), have been criticized for their reliance on snap shot data that are either short-term or small-scale or both (Baguette 2004). Such snap-shot dispersal estimates may not be accurate if estimated from short time-series or small spatial scale (Nathan et al. 2012), potentially over- or under-estimating dispersal rates depending on stochastic variations. Assuming connectivity is static also amounts to estimating long-term average effective dispersal rates, overlooking potentially important temporal heterogeneity that can be informative of both demographic and landscape processes impacting population dynamics. This important year-to-year variation not only emerges in model parameters, but also in related system-wide properties (Figure 3); although such variation may not pose a problem to certain conservation goals when connectivity or dispersal is not average in one direction, it may be devastating in the other. Thus, focusing on a single dispersal capability of a species or population, either from snapshot data, or assumed invariant processes, may not be adequate, and may mask short-term events that can significantly influence long-term connectivity trends.

Existing approaches to connectivity modelling have been describe as often being too naïve or conservative for management reality (Nathan et al. 2012, Diniz et al. 2020). One example of this is the fact that spatiotemporal variation in spatially structured

populations can be masked by restrictive model assumptions, precluding the discovery of important underlying variation driving population processes. Our aim here has been to increase awareness about the implications of commonly used modeling decisions on conclusions drawn about a wide range of processes of interest in (meta)population and landscape ecology (e.g. population synchrony, colonization-extinction dynamics, landscape connectivity), and in particular highlight the importance of considering demographic processes as an important component of connectivity dynamics (Drake et al. 2021b). Indeed, connectivity is dynamic, and we argue, via empirical demonstration, that appropriate modeling decisions that link the dynamic process of animal behavior to the underlying spatial structure of the landscape and the in-situ populations are essential for accurate characterization and management of connectivity.

Here we produce seldomly reported quantification of the uncertainty associated with estimates of MC, and the first to do so with full joint posterior distributions of model parameters. Interestingly, the homogeneous model that produces estimates of temporal averages of time varying parameters and makes unrealistic assumptions about the distribution of potential dispersers has extremely large degree of uncertainty that is practically useless from an applied perspective (Figure 3b). The addition of biological realism reduces uncertainty in resulting estimates of MC, although predictions appear more sensitive to the use of estimates from models that allow for temporal invariance than use realistic representations of the distribution of potential dispersers (Figure 3b).

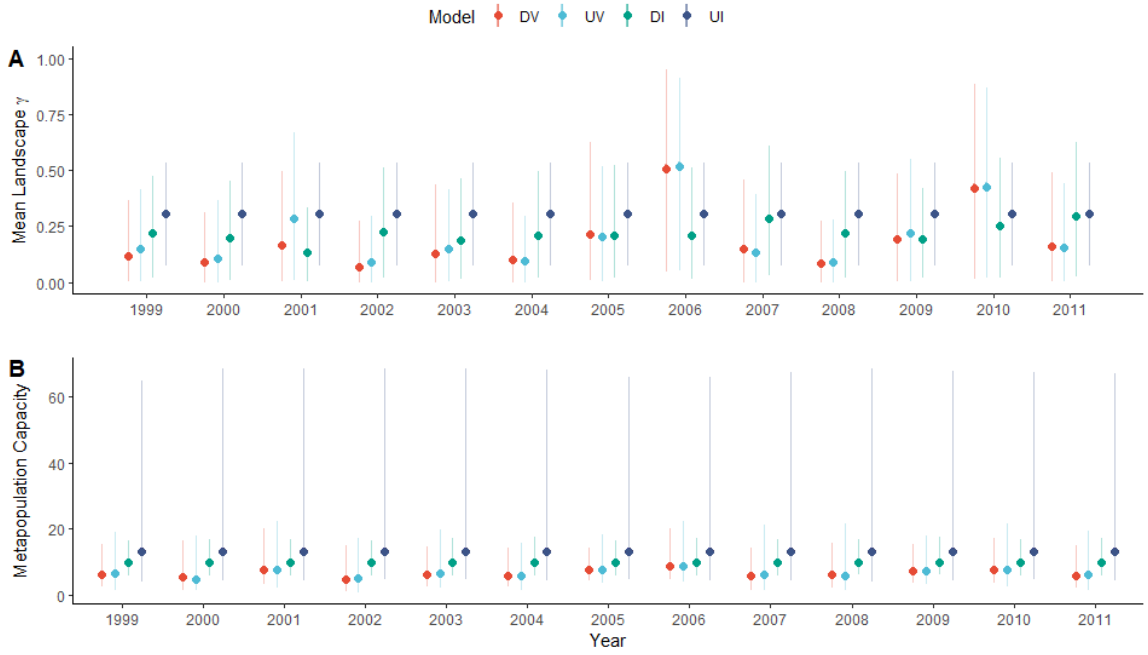

Figure 3. Descriptions of local and landscape level processes may depend on the model of connectivity used and its underlying assumptions such as if they are demographically-weighted and time-varying (DV), unweighted and time-varying (UV), demographically-weighted and time-invariant (DI) or unweighted and time-invariant (UI). 2a) Annual measures of total colonization probability under each of the four connectivity parameterizations of the stochastic patch occupancy model. The measures show the landscape level summary of individual landscape pixel colonization probabilities. Points represent the average across all pixels. The vertical lines represent the 95% interval spanning the 0.025 and 0.975 quantiles of the empirical distribution of landscape colonization probabilities, product of the realized connectivity between patches (See Appendix S3). 2b) Annual metapopulation capacity (Hanski & Ovaskainen, 2000) calculated using the joint posterior distribution of parameter estimates for each of the four connectivity parameterizations of the stochastic patch occupancy model. Points represent the posterior means MC and vertical lines are the 95% Bayesian credible intervals. These credible intervals provide insight into the level of noise surrounding the point estimates of metapopulation capacities which are almost exclusively ignored in the literature.

CHAPTER 3

WHEN DOES THE MATRIX MATTER? SPATIALLY STRUCTURED POPULATIONS AND THE ROLE OF THE MATRIX IN DISPERSAL BEHAVIOR AND METAPOPULATION DYNAMICS

Abstract

Connectivity is considered an essential component of the landscape, influencing ecological processes and is often the focus of conservation management. A functional perspective of connectivity can include the resistance to dispersal an organism experiences due to the structure of the landscape. Attempts to reduce the reliance on expert opinion derived resistance representations has seen the recent development of models to formally estimate the influence of landscape structure on dispersal from an increasing variety of data types. Recent statistical innovations and the existence of model metapopulation systems with long-term time-series of colonization-extinction dynamics offers a framework for directly investigating the interplay between landscape structure and dispersal, and ultimately emergent patterns of connectivity. Here I investigate the influence of landscape structure on dispersal and emergent metapopulation processes, including functional landscape connectivity, using a novel spatially-explicit metapopulation model that directly estimates landscape resistance. Using a 21-year time-series of occupancy data, I empirically demonstrate that landscape resistance impacts colonization for a classically functioning mammalian metapopulation. As per standing predictions, colonization was positively related to distance-based connectivity, but I found strong evidence that connectivity is best measured using cost distance rather than Euclidean distances. Colonization was impacted by increasing resistance with elevation,

related to increased topographically rugged landscape features in the study area, influencing the relative isolation and long-term occupancy of habitat patches. These results provide evidence to reconcile general ecological assumptions of Euclidean-based movements for spatially structured habitat specialists and the impact interpatch matrix has on dispersal behavior at different spatial scales. The spatial distribution of populations, habitat, and interpatch matrix can all impact connectivity, a spatiotemporally dynamic phenomenon. This model provides an example of the flexibility of metapopulation modeling to increase our understanding of the role of the landscape in dispersal and (meta)population dynamics.

Introduction

Connectivity is a complex ecological process that is vital to ensure genetic diversity and promote population persistence (Hilty et al. 2020), and has emerged as a concept central to contemporary conservation and the management of populations, in the face of global patterns of habitat loss and fragmentation (Crooks and Sanjayan 2006, Haddad et al. 2016). While it is generally accepted that connectivity is a function of dispersal, the movement of organisms or propagules that has consequences for gene flow across space (Ronce 2007), this is highly context dependent and generalities are elusive(Van Dyck and Baguette 2005). Description of connectivity are then only as good as our ability to characterize the underlying processes (Drake et al. 2021b). Thus, understanding connectivity and what governs or constrains it (Vasudev et al. 2015) is vital to understanding basic species biology and in applying ecological theory (Moilanen and Hanski 2001) to conservation and wildlife management.

While a knowledge of dispersal preferences and constraints would thus be useful for research and management (Russo et al. 2016), limited knowledge of dispersal for most organisms still hampers effective connectivity conservation and management (Driscoll et al. 2014, Komonen and Müller 2018). Some progress has been made to uncover the internal and external factors influencing dispersal (Bowler and Benton 2005, Le Galliard et al. 2012). However, dispersal is still often difficult to observe reliably (Ims and Yoccoz 1997) resulting in data on natural dispersal being rare (Fisher et al. 2009, Driscoll et al. 2014). To understand how determinants of dispersal scale up to the landscape level and impact connectivity, and thus (meta)population dynamics, approaches are often limited in scope or laden with unrealistic but necessary assumptions about the representation of dispersers and their behavior (Chapters 1 and 2).

According to expectations from landscape ecology, the structure of the interpatch matrix influences dispersal which is especially true for highly spatially structured populations where dispersal through the matrix is necessary to recolonize habitat patches, i.e., metapopulations. However, many structured populations use specialized long distance dispersal where theory suggests straight line movements are least costly (Van Dyck and Baguette 2005), and there is some evidence from experimental translocations to support this notion (Fisher et al. 2009). Yet, in heterogeneous landscapes where a gradient of habitat suitability exists, Euclidean measures of distance may be a poor descriptor of dispersal pathways (Zeller et al. 2012); classical connectivity measures based on Euclidean distances therefore may poorly approximate connectivity, particularly when the interpatch matrix is inhospitable (Ricketts 2001).

Such a series of seemingly conflicting responses to the potential resistance of landscape features may be a result of limitations of individual methodologies to capture the response (Van Dyck and Baguette 2005) or from the spatiotemporal scale of effect that the biological response may exert (Miguet et al. 2016). As well, we may ask, for spatially structured species, like habitat specialists, *when does the matrix matter*? Habitat specialists that exist in spatially structured landscapes may either remain habitat specialists through dispersal and non-dispersal modes, or such specialism may be relaxed during certain life-stages or opportunistically to facilitate dispersal (Elliot et al. 2014b). Thus, understanding when, or if, the matrix imposes strict limitations on movement during dispersal can increase our understanding of how species persist in fragmented landscapes (Vasudev et al. 2015) as well as how to best focus recovery efforts and facilitate management with limited resources (e.g. which life stage may better facilitate connectivity-based recovery efforts; are connectivity 'corridors' of specific habitat needed for a study species?).

Spatially explicit metapopulation models may provide a flexible solution to investigate such questions. They are couched in ecological theory (Hanski 1999) and have been important for analyzing population dynamics in naturally and anthropogenically fragmented systems (e.g. Sutherland et al. 2014). Models such as the Incidence Function Model (IFM) can be parameterized using easily obtainable detection/non-detection data (Hanski 1994, 1998, MacPherson and Bright 2011). By assuming extinction is inversely related to patch area and colonization is related to connectivity, dependent on habitat patch structure and dispersal of focal organisms, these models can provide inference into (meta)population dynamics.

While Hanski (1994) suggested that non-Euclidean or cost distances may be incorporated into IFMs and stochastic patch occupancy models (SPOMs) in general, this was rarely achieved and could be simplistic, such as potential costs along straight line paths (Moilanen and Hanski 1998). Also the inclusion of cost-weighted distances into connectivity models rely on resistance surfaces, but frequently, the use of expert opinion is relied upon to choose cost values instead of estimating them directly from data that may not be available (Spear et al. 2010, Zeller et al. 2012).

Recent developments in SPOMs by Howell et al. (2018) have helped to resolve these issues by directly estimating cost values for landcover features from detection/non-detection data. This relaxation of the assumption of a homogeneous matrix and straight line dispersal may reduce bias in connectivity parameter estimates (Revilla et al. 2004) while simultaneously allowing increased mechanistic understanding of dispersal ecology, connectivity, and population dynamics. Importantly, these methods allow for direct testing of specific hypotheses about how a landscape feature may differentially contribute to landscape patterns of connectivity (or its inverse, isolation). Such measures of the (in)hospitability of the matrix is important as population persistence can be tied to the quality of matrix (Casagrandi and Gatto 1999, Vandermeer and Carvajal 2001) and the relative patch isolation induced by such features may influence the strength patches exert on population dynamics.

Here I develop a spatially-realistic metapopulation model that draws from recent modelling advancements to infer landscape influence on dispersal. Using a stochastic patch occupancy model that invokes both metapopulation and landscape ecological paradigms (Howell et al. 2018), I formally estimate the effects of landscape structure on

resulting measures of connectivity and resulting colonization-extinction dynamics in a naturally occurring metapopulation system (Sutherland 2013).This model system provides an opportunity to test a long standing assumption on the role (or rather, lack thereof) the interpatch matrix has in shaping dispersal behavior in long-distance, directed dispersal movement expected in spatially structure habitat specialists (Van Dyck and Baguette 2005). Using this framework, I estimated landscape resistances, least-cost distances, and non-Euclidean connectivity directly from long-term occupancy trends, forgoing the need for expert opinion or genetic-based resistance surfaces. Such 'ecological distances' (*sensu* Royle et al. 2013) help to describe complex, and often unobservable, dispersal behavior and the intervening landscapes influence to connectivity helping to increase our general understanding of dispersal (Van Moorter et al. 2021).

Methods

Study system and data

Water voles (*Arvicola amphibius*) occur across much of Europe, but within the United Kingdom are threatened by invasive mink and riparian habitat loss (Rushton et al. 2000, Strachan 2004, Brzeziński et al. 2018). As a habitat specialist, it has a surprisingly long dispersal capability, upwards of four times larger than would be expected based on allometric relationships of mammalian dispersal (Sutherland et al. 2000). Mean dispersal has been estimated between 1.9 km and 3.5 km but mark-recapture methods have shown individuals successfully traveling greater than 20 km (Lambin et al. 2012, Sutherland et al. 2014). Located in northwest Scotland, the Assynt region is currently still believed to lie outside of the mink invasion front, and supports a naturally fragmented water vole metapopulation (Lambin et al. 2004, Aars et al. 2006, Sutherland et al. 2012). This

metapopulation patch network contains 112 vegetated patches located on a large river network (860 km) situated within a 140 km^2 area. Thus, suitable habitat represents a fragmented patch network that makes up less than 10% of the total 860 km waterway, with mean nearest neighbor distance of 0.5 km and the mean patch length varies from 50 m to almost 3 km in length (mean=0.847 km). Patches are surrounded predominately by unsuitable heather or bog and mire matrix and are situated in a rugged landscape that ranges in elevation from sea-level to 850 m (Appendix F), encapsulating landcover types that range from coastal to mires to montane habitats. As such, this system acts as an example of a classic metapopulation (Moilanen and Hanski 1998) where patches exhibit frequent turnover. i.e., colonization-extinction dynamics, but metapopulation occupancy fluctuates around a historical long-term average occupancy rate of approximately 56% (Drake et al. 2021a).

From 1999 to 2019, repeated fecal latrine surveys were conducted at each patches during the breeding season (July and August). Water voles deposit latrines as territory marking in prominent locations (e.g., riverbanks, runs) and are easy to see and are easily recognizable, and are therefore ideal for determining the presence of water voles. Up to 4 surveys were conducted at each site in each year (mode = 3, range: 0,4) resulting in detection histories that record whether evidence of water voles (at least one latrine) was observed. Note that latrines are not observed perfectly, and multiple visits generate binary detection/non-detection data where a 1 is evidence of occupancy, whereas, because of imperfect detection, 0's are not indicative of absences. These data can be incorporated into analyses using hierarchical models that use repeated visits to account for such

imperfect detection (see statistical methods below). For further details on surveys and the study system refer to Sutherland et al. (2012) and Sutherland (2013).

Landscape Covariates and hypotheses

In Assynt, the riparian network is embedded within a landscape that is best described as uniformly heather dominated, which is unsuitable breeding habitat for water voles, with patchily distributed riparian grassy flushes that represent suitable breeding habitat. We assume, therefore, that this apparent binary habitat matrix is homogeneous in terms of its potential to facilitate or impede movement (Lambin et al. 2012). The major source of variation in the landscape is the topographical relief: elevation in the area ranges from sea level to 850 m, with slope values that range from 0° (flat ground) to 84° (almost vertical). Indeed, elevation has been demonstrated to impact water vole population genetic structure (Berthier et al. 2005) as well as reduce occupancy probability (Fedriani et al. 2002). I hypothesize, therefore, that resistance will be positively associated with elevation such that higher elevation areas are more resistant to movement (Vasudev et al. 2015).

Elevation data was extracted from BNG Ordnance Survey data (10m contours; Ordnance Survey 2017) for an area defined by a 5km buffer around patch location (5km being the upper limit of typical dispersal, Sutherland et al 2014). I aggregated the elevation layer to a 200m X 200m resolution raster using the mean of aggregated cells. This allowed for a reasonable reduction in computation time while still remaining fine enough to be biologically justifiable to provide information on matrix influence to dispersal among patches (Berthier et al. 2005, Fisher et al. 2009, Koen et al. 2010, Le

Galliard et al. 2012). This raster represents the cost covariate surface used in the modified metapopulation model (see statistical model).

Resistance-based Stochastic Patch Occupancy Model

To determine landscape resistance to dispersal, I analyzed the 21-year, 112 patch time series of detection/non-detection data. I used a Bayesian implementation of a spatial occupancy model (Sutherland et al. 2014, Chandler et al. 2015b, Drake et al. 2021a) that incorporates recent advances to relax Euclidean distance assumptions (Howell et al. 2018). Colonization, typically, is assumed to be a function Euclidean interpatch distances However, inference into the intervening landscape's influence on connectivity can me made directly from the presence/absence data using pattens of extinction and colonization events (see Howell et al 2018).

Our hierarchical model contains 1) a state model that describes first order Markovian colonization-extinction dynamics, and 2) an observation model that is conditional on the latent occupancy state (z). The model treats z as a partially observed Bernoulli random variable, with site (i) and year (t) specific occupancy probability $\psi_{i,t}$. In the initial year, data is assumed to be detected perfectly to initialize the model and in subsequent years (t >1), occupancy is modeled as:

$$z_{i,t} \sim \text{Bernoulli}(\psi_{i,t}), \text{ [1]}$$

where the occupancy probability depends on the occupancy state in the previous year and is equal to the colonization probability, $\gamma_{i,t}$, if unoccupied (i.e., $z_{i,t-1} = 0$) and the extinction probability, $\varepsilon_{i,t}$, if occupied (i.e., $z_{i,t-1} = 1$). A statistical rescue effect (Hanski 1999) can be included by adjusting extinction to include the potential for recolonization: $\varepsilon_{i,t-1}(1 - \gamma_{i,t-1})$. This first-order Markovian process is modelled as:

$$\psi_{i,t} = (1 - z_{i,t-1})\gamma_{i,t-1} + z_{i,t-1}[1 - \varepsilon_{i,t-1}(1 - \gamma_{i,t-1})]. \text{ [2]}$$

Following the assumption that patch size and population size are correlated, the probability of extinction $\varepsilon_{i,t}$ is modelled as a function of patch size, the length of riparian habitat patch. Using a logit linear model:

$$\text{logit}(\varepsilon_{i,t}) = \delta_0 + \delta_1 A_i, \text{ [3]}$$

where A_i is the time invariant length of patch i and δ_0 and δ_1 are the regression parameters to be estimated.

I model (re)colonization of unoccupied patches with probability $\gamma_{i,t-1}$, which is assumed to be caused by the contribution of immigration from an increasing function of connectivity (S) between all occupied patches from the previous year within the landscape (Hanski 1994, Moilanen 2004):

$$\gamma_{i,t-1} = 1 - \exp(-S_{i,j,t-1}). \text{ [4]}$$

Using a version of the standard metapopulation model connectivity term (S) and is a measure describing a distance dependent influence of occupied source patches:

$$S_{i,j,t-1} = \sum_{j \neq i} \beta * \exp\left(-\frac{d_{i,j}^2}{2\alpha^2}\right) z_{i,t-1}, \text{ [5]}$$

where β is the population-level per capita effective dispersal rate, $d_{i,j}$ represents interpatch distances, and α determines the scale of dispersal.

In the above formulation, $d_{i,j}$represents the Euclidean distance between patches (Sutherland et al. 2014, Chandler et al. 2015b) which can be considered a restrictive assumption when attempting to characterize animal movement from observational data (Royle et al. 2013, Sutherland et al. 2015). Recently, Howell et al. (2018) relaxed the Euclidean distance assumption and use estimated least cost path distances to explicitly

account for the effect of landscape covariates in the intervening matrix on dispersal. Specifically, they developed a method that estimates resistance coefficients (θ) from typical metapopulation data.

Using the covariate raster described above and for any given value of θ, cost-weighted distance ($d_{i,j}^{cost}$), the accumulation of costs moving between any two locations in the grid, can be calculated. This is calculated by multiplying the Euclidean distance for a transition to an adjacent pixel and the cost associated with that transition, as taking the sum of the path between the pair of patches.

$$d_{i,j}^{cost} = \sum_{l=1}^{L-1} \text{cost}(x_l, x_{l+1}) \, \|x_l - x_{l+1}\| \text{ , [6]}$$

where$x_l - x_{l+1}$ is the Euclidean distance between patches i and j. It is conditional on:

$$\text{cost}(x, x') = \frac{\exp(\theta_1 * c_1(x)) + \exp(\theta_1 * c_1(x'))}{2}, \text{ [7]}$$

which is a cost function for a single covariate.

The least cost path ($d_{i,j}^{LCP}$) is the path that minimizes the cost-weighted distance travelled between patches (Adriaensen et al. 2003) by moving through adjacent cells x and x' in the grid, i.e.,:

$$d_{i,j}^{LCP} = \min(d_{i,j}^{cost})$$

Finally, the latrine detection data ($y_{i,k,t}$) during k^{th} visit to patch i during year t, when $t > 1$, is modelled as an imperfect detection process which is conditional on the estimated latent occupancy state z:

$$y_{i,k,t} \mid z_{i,t} \sim \text{Bernoulli}(z_{i,t}, p_{i,k,t}), \text{ [8]}$$

where $p_{i,k,t}$ is the probability of detecting a species that is present at patch i, during year t, and visit k. I model the detection process as logit-linear function of the size of the patch:

$$logit(p_{i,k,t}) = b_0 + b_1 A_i, \text{ [9]}$$

where b_0 and b_1 are regression parameters to be estimated while A_{ikt} is the time invariant area of the patches record during each survey k. This could also be modeled as a random effects model. As well, for this occupancy model, I assume closure.

In addition to the resistance-based SPOM that included elevation as a resistance covariate I fit a Euclidean distance version of the same model (i.e., setting $\theta \equiv 0$). This comparison is used to discuss the consequences of assuming Euclidean dispersal when movement is influenced by landscape structure.

To improve tractability and reduce computation time by only considering patch locations and likely dispersal distances, I retained landscape covariate information within a 5 km buffer of patch locations to focus on areas likely to be pertinent for animal movement within the system and helps prevent edge effects in path calculations between patches.

I used a Bayesian framework and a modified version of the custom Metropolis-within-Gibbs sampler developed by Howell et al. (2018). The sampler is implemented in R 3.6.1 (R Core Team 2019) and the package *gdistance* is used for calculating cost distances (van Etten 2017). For each model, I ran three chains of 45,000 iterations and discarded the first 5,000 as burn in. Non-informative priors were used for all parameters (Gelman et al. 2003) and are described in Appendix F. Visual diagnostics of model chains and Potential Scale Reduction Factor scores <1.1 for each estimated parameter

(Appendix G) provided evidence of convergence (Gelman et al. 2003). Models were compared using deviance criterion and by comparing effects sizes and 95% credible intervals which are reported in brackets, e.g. [0.025,0.975] (Hobbs and Hooten 2015, Hooten et al. 2015). R code and data is available in Appendix H.

Results

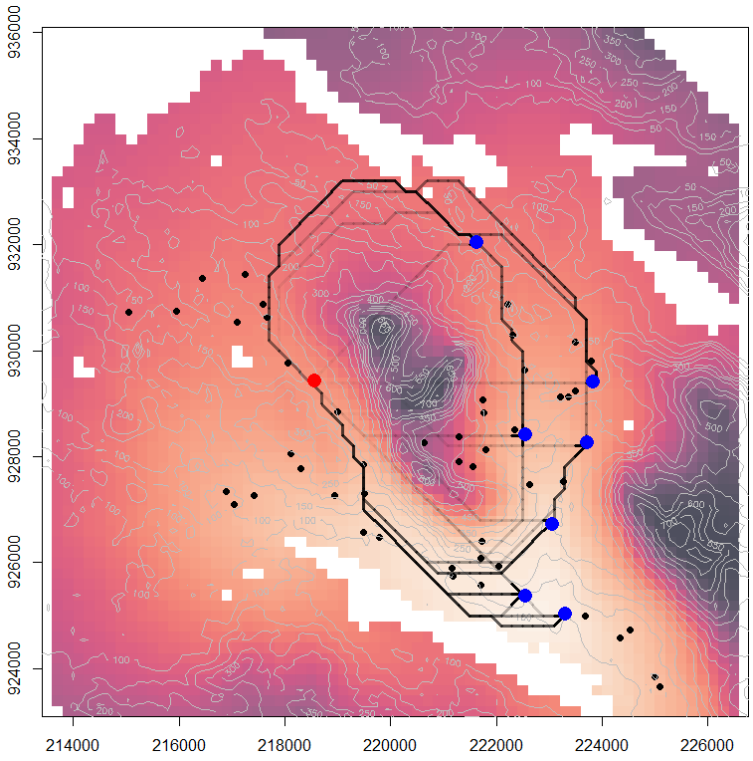

Figure 4. Least cost paths between potential source (blue circles) patches and a receiving patch (red circle) among patches (black circles) in the Assynt landscape. These paths are drawn from the posterior distribution of potential least-cost pathways in the estimated cost surface based off the resistance covariate for elevation. Higher cost areas are darker colors and elevation (m) is visualized in the contours and the transparency of the paths relate to the relative colonization probability, and when a path is drawn multiple times, the line darkens even though it the probability of colonization declines as cost distance increases. For example, paths that try to cross over Quinag, the high relief mountain situated in the middle of the image, quickly lose colonization probability compared to those that follow lower elevation paths.

The results provide evidence of landscape structure inducing resistance to dispersal, impacting connectivity and colonization. Landscape resistance increased with elevation (mean α = 0.87, 95% CI [0.67-1.06], Table 4). The influence that elevation has on connectivity can be seen in least-cost path visualizations (Figure 4) where the

effective distances between patches separated by areas of high elevation are longer because of the estimated impedance of movement by higher elevation. In other words, Euclidean and ecological distance are similar when low elevation areas separated patches (Figure 6D) but diverge when patches are separated by higher elevation areas (Figure 6A).

Landscape structure impacted connectivity among patches in the landscape. Least-cost paths were generally longer than straight-line Euclidean distances between patches (Figure 4), and the spatial scale of dispersal, α, and mean posterior estimates for ecological distance-based dispersal rate, β, were also impacted by the landscape structure (mean α =2.58 [2.08-3.21]; β = 0.044 [0.032-0.058]). Consistent with previous research on this system, extinction probability was impacted by the size of the patch (Table 4). The detection probability was found to be impacted by the size of the patch in which observations were taking place during each survey (Table 4; Figure 3A). Failure to account for such imperfect detection more importantly would have biased colonization and extinction estimates and produced negatively biased occupancy estimates as seen in the naïve counts (Figure 3D).

Deviance estimates suggest that the resistance-based model (2808.28 [2698.4 – 2926.38]) performed better relative to the Euclidean-based model (2819.89 [2708.11 – 2940.09]), but 95% CI did overlap. The inclusion of a resistance model appeared to have very little influence on estimated detection parameters, and only a small impact to the inferred extinction relationship at the smallest patches (Figure 5B). Likewise, spatiotemporal occupancy dynamics did not appear to be greatly impacted by the inclusion of landscape structure compared to accounting for imperfect detection for each

model respectively (Figure 3A & 3D; Appendix J). Resistance based time-series average occupancy was 64.25% (annual range: 45.29% to 89.23%) while the Euclidean-based model average occupancy was 64.06 (annual range: 45.1% to 89.24%).

Whereas inclusion of a resistance-based model impacted connectivity model parameters. Mean posterior estimates for the ecological distance model α was less than the mean estimate for Euclidean based model (Table 4). Also, the dispersal rate was larger for resistance-based model relative to the Euclidean-based model (Table 4).

Table 4. Posterior estimate means, standard deviations and 95% credible intervals (CI) for detection and occupancy model parameters and metapopulation dynamics for both resistance-based and Euclidean-based spatially explicit stochastic patch occupancy models.

Model	Parameter	Description	Mean	2.5% CI	97.5% CI
Resistance-based	$\boldsymbol{\alpha}$	Dispersal scale parameter	2.583	2.081	3.206
	$\boldsymbol{\beta}$	baseline colonization probability	0.044	0.032	0.058
	$\boldsymbol{\delta_0}$	intercept of extinction logit-linear model	0.031	-0.323	0.433
	$\boldsymbol{\delta_1}$	slope of extinction logit-linear model	-0.643	-0.912	-0.404
	$\boldsymbol{b_0}$	Detection model logit-linear intercept	1.044	0.931	1.157
	$\boldsymbol{b_1}$	Detection model logit-linear slope	0.354	0.238	0.475
	$\boldsymbol{\theta_1}$	linear effect of elevation on landscape resistance	0.866	0.673	1.057
	Deviance	deviance	2808.3	2698.4	2926.4
Euclidean-based	$\boldsymbol{\alpha}$		6.249	4.611	8.821
	$\boldsymbol{\beta}$		0.024	0.017	0.031
	$\boldsymbol{\delta_0}$		-0.199	-0.519	0.153
	$\boldsymbol{\delta_1}$		-0.613	-0.869	-0.391
	$\boldsymbol{b_0}$		1.036	0.924	1.15
	$\boldsymbol{b_1}$		0.354	0.235	0.477
	Deviance		2819.9	2708.1	2940.1

Spatiotemporal occupancy dynamics did not appear to be greatly impacted by the inclusion of landscape structure (Figure 5A & 5D; Appendix J). While non-Euclidean

cost-distances increase realism for dispersal behavior in relation to colonization, accounting for detection probability impacted estimated occupancy. The detection probability was found to be impacted by the size of the patch in which observations were taking place during each survey (Table 4; Figure 5A). Failure to account for such imperfect detection would have biased colonization and extinction estimates. Accounting for imperfect detection also increased the proportion of time a patch was estimated to be occupied compared to naïve counts (Figure 5D). As well, model performance appraised by deviance suggests that the resistance-based model (2808.28 [2698.4 – 2926.38]) performed better relative to the Euclidean-based model (2819.89 [2708.11 – 2940.09]), but 95% CI did overlap.

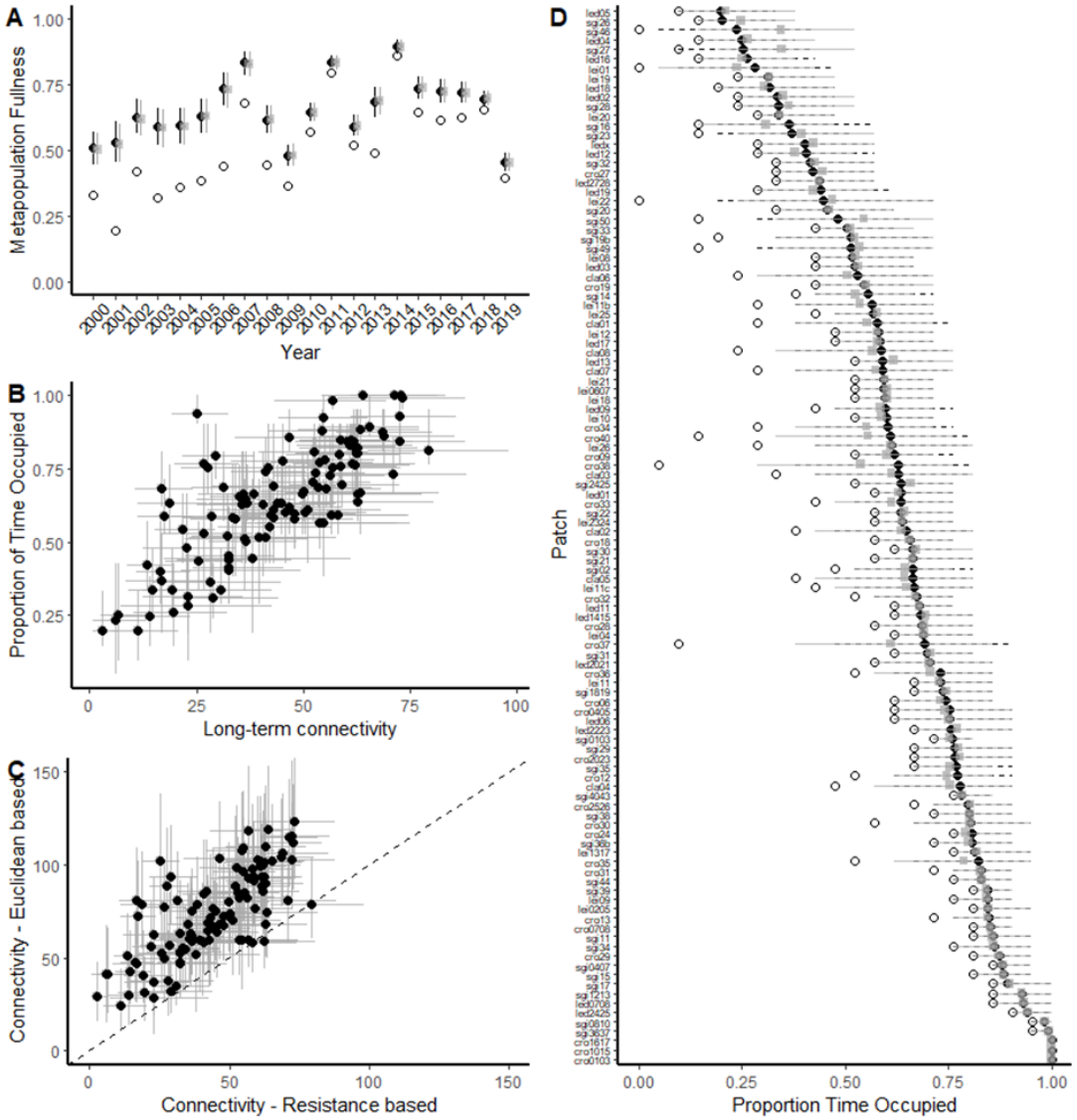

Figure 5. Accounting for imperfect detection in both resistance-informed SPOM (black circles with 95% CI) and Euclidean-based SPOM (grey square with 95% CI) increases the estimated occupancy of the Assynt Metapopulation compared to naïve observations of detected occupancy (open circles). (B) The Resistance-based model's long-term connectivity (connectivity-weighted by time-series average occupancy) of individual patches is correlated with the proportion of time occupied (C) The correlation between each patches mean connectivity value (black circles with 95% CI) between Euclidean-based and resistance informed SPOMs. Euclidean models almost always estimate higher connectivity for each patch to contribute to proportion of time occupied during the 21-year time series. (D) The Proportion of time each patch was occupied during the 21-year time series of our survey. Naïve counts (open circles) are always lower except for the largest patches in the network, of some which never where completely unoccupied during each year. Accounting for imperfect detection increases the estimated proportion of time occupied during our survey period for both resistance-informed SPOMs (black circles with 95% CI) and Euclidean-based SPOMs (grey square with 95% CI). The time occupied is correlated negatively with increased relative isolation from surround patches.

Discussion

Here I have presented clear evidence that landscape structure impacts realized connectivity and the dispersal of water voles in Assynt. This model metapopulation system provides insight on how the landscape structure and the matrix can influence assumed Euclidean dispersal behavior in habitat specialists. Our results also suggest a plastic dispersal strategy exists for a habitat specialist when populations are spatially structured. For the water vole, this emerges as overland dispersal which resemble Euclidean assumptions in the absence of resistant landscape features. This plastic dispersal strategy allows for reduced exposure to typically inhospitable matrix when dispersing between preferred habitat. However, these results do also clarify a standing assumption on the role of the matrix in directed dispersal movements: the interpatch matrix can influence dispersal behavior, thus invalidating Euclidean connectivity assumptions.

This model estimated the impact elevation has in governing spatiotemporal dynamics of a spatially structured metapopulation. While some studies have identified the role of large topographic features in shaping genetic structure (eg. Berthier et al. 2005), there has been no consensus on the influence of intervening matrix to dispersal and colonization in the water vole. These riparian specialists were assumed to disperse along water ways to reduce exposure to non-selected habitat; however, genetic evidence had suggested that more generalist dispersal behavior may be occurring overland, disregarding interpatch matrix costs (Telfer et al. 2001). As well, in the closely related southern water vole (*A. sapidus*), no landscape features proved a barrier to dispersal based on estimated genetic distances (Centeno-Cuadros et al. 2011). In contrast to those results, Berthier et al. (2005) found topographic features such as cliffs and valleys

disrupted gene flow of the fossorial water vole (*A. terrestris*), but smaller features, such as more specific landcover types, did not appear to induce genetic discontinuities beyond those found by isolation by distance. Contrary to the dispersal behavior described above, water voles are rarely observed more than a few meters from preferred habitat such as riparian banksides (Lawton et al. 1991) and daily movements are often constrained to their home range sizes, well below 100m (Stoddart 1970b). Our result support the idea of plastic dispersal strategies in water voles in contrast to their habitat specialism (Aars et al. 2006).

The results also suggest that water voles avoid higher elevation features during dispersal. This can impact colonization rates between patches that are relatively close as the crow flies (Figures 4 & 6). In Assynt, higher elevation locations are often rugged, difficult to traverse, and can resemble alpine habitats or be composed of bare rock. Such open habitat may be avoided in addition to the topographic relief. Even if the path is longer, lower elevation routes may be preferred, being less resistant to dispersal as the vole trundles. For example, a steep topographic feature called Quinog (Figure 4) induces high costs to movement and estimated individual least cost paths circumvent it. This can also be seen in the resistance surface for individual patches (Figure 5C) or the entire landscape (Figure 5D). Rising to over 800m, this mountain severely restricts colonization between major networks of patches in Assynt, UK. However, such large features may not dominate the colonization patterns within clustered subnetworks of patches, thus not contradicting previous results that may miss such patterns. Determining which method more accurately describes the dispersal process likely depends on the type of dispersal (Van Dyck & Baguette 2005), the scale of the question (i.e. spatial: landscape vs

subnetwork; temporal: intra-annual vs interannual vs multi-generational) and the precision or grain of data available (e.g. occupancy vs. telemetry; Miguet et al. 2016).

To explore beyond the importance of landscape resistance impact to inter-annual dispersal events, I calculated the connectivity of each patch weighted by its time-series average occupancy (Figure 5D). Taking a random draw of the posterior distribution of connectivity parameter estimates, I calculated the mean connectivity contribution using of each patch in the network for both resistance-based and Euclidean-based connectivity models. For almost every patch, Euclidean-based connectivity provided higher estimates of connectivity relative to the resistance-based model (Figure 5C). Euclidean-based estimates also have wider 95% CI for long-term connectivity estimates. Weighted by the long-term average occupancy of each patch (which had similar estimates across models; Figure 5D), this suggests a potential for bias in Euclidean-based connectivity estimates, and the resulting inflation of colonization potential relative to resistance-based connectivity estimates.

Stochastic patch occupancy models have historically been criticized for neglecting to consider the interpatch matrix when estimating connectivity (With 2004). While some habitat may exist in a homogeneous matrix, patches are often situated in a complex mosaic of heterogeneous land cover types. These land cover types may differ in their relative resistance to dispersal movements either through increased costs (Ricketts 2001) or mortality risks (Fletcher et al. 2019). Elevation is often correlated with vegetation communities and may act as a proxy for these features at larger scales helping to explain overall landscape influence on connectivity.

This model could also be extended to explore multiple landscape structures. For example, detailed spatial information on the distribution of habitat or vegetation types may provide insight into the relative contribution to resistance each feature has on resistance. The landscape is generally not experienced as individual components, but rather as a whole (Peterman and Pope 2020). The SPOM now provides an excellent framework to incorporate increasingly detailed landscape ecological perspectives to explorations of metapopulation dynamics (Howell et al. 2018).

Connectivity is also a spatiotemporally dynamic phenomenon and the spatiotemporal distribution of habitat could impact inferences in colonization-extinction dynamics (Chapter 2; Bertassello et al. 2021), shifting the effective connectivity between patches either through long-term shifts (Bishop-Taylor et al. 2017) or through punctuated moments of ephemeral connectivity windows (Zeigler and Fagan 2014). This is likely not a problem in Assynt, inter-patch matrix remains relatively static with few changes since surveys began in the time series (personal communication, X. Lambin). Recent satellite imagery of the Assynt area also shows <0.7% landcover assignment changes between recorded years (Space Intelligence 2021).

So, does the matrix matter? For the water vole, that depends. While genetic analyses (Telfer et al. 2003b, Aars et al. 2006) and translocation experiments (Fisher et al. 2009) suggest that the interpatch matrix may be disregarded by dispersing water voles at some scales, our results indicate that the interpatch matrix exerts influence on colonization-extinction dynamics at interannual potentially larger time scales and at the metapopulation and patch spatial scale. Models that include landscape resistance show a smaller estimated mean dispersal scale and higher dispersal rate with no overlap in 95%

CI with Euclidean-based model estimates (Table 4). Not including the isolating effect of landscape resistance between patches caused overestimation of the scale of dispersal (Figure 5C), leading to potentially biased model predictions (Moilanen 2002).

In sum, the matrix does matter to dispersers, but not all patches are separated by high resistance (here, high relief) features. Such low elevation areas may have connectivity that does not diverge from Euclidean-based modeling assumptions (Figures 6A & 6B). Comparatively, due to increased chance of encountering high relief features as distance increases, long distance dispersal will more likely be impeded than movements within closely clustered networks (Figure 6). In such closely clustered networks, plastic dispersal strategies may benefit individuals that disregard some generally highly impermeable boundaries during non-dispersal periods by limiting their exposure to inhospitable conditions (Van Dyck and Baguette 2005, Legrand et al. 2017). These movements would differ from typical foraging or exploratory movements, where the matrix exerts a stronger influence to movement. However, certain structures in the matrix (such as topographic relief) may induce such high costs to dispersing individuals, they will be avoided in favor of less resistant paths. Such features shape emergent landscape connectivity and reduce the utility of Euclidean dispersal assumptions in explaining colonization-extinction dynamics. Such insights are key to resolve limitations to our understanding of dispersal in arvicoline rodents (Le Galliard et al. 2012), and increase our understanding of dispersal's role as ecological process in general (Driscoll et al. 2014).

While estimates for resistance covariates and connectivity parameters do show that colonization processes matter in a spatially explicit context (Table 4, Figures 4 &

5C), other parameters showed less differences between model estimates. Mean occupancy estimates and 95% CI were similar between resistance and Euclidean distance-based models (Figure 5A). As well, while mean extinction estimates diverged at lower patch sizes between models, 95% CI widely overlapped. The similarity in estimates of occupancy between resistance and Euclidean-based models suggests that SPOMs may be able to phenomenologically describe occupancy trends without a mechanistic explanation when data on the landscape structure is absent. This resilience to Euclidean connectivity assumptions should be further tested. Predictions based on a phenomenological approach are likely to be biased and caution should be used to inform management decisions based on such assumptions.

Landscape resistance may mediate the potential emergence of source-sink dynamics in the Assynt system. The probability an individual successfully encounters and settles in a potential sink once it has left a source should influence the strength of sources and sinks on metapopulation dynamics (Pulliam 1988). Landscape resistance could increase the functional isolation of potentially low-quality patches that Euclidean-based connectivity would suggest are highly connected. This may reduce proximity to source locations and reduce the contribution to overall dynamics (Heinrichs et al. 2016). Water voles, with limited perceptual ranges, but relatively long dispersal capabilities are also able to reduce reliance on proximate, if poor quality patches, increasing occupancy at higher quality patches across Assynt. This should reduce the effect of source sink patterns on the severity of dynamics (Heinrichs et al. 2016). Such understanding of the way landscape structure can impact colonization-extinction dynamics and thus in defining the strength of source- sink dynamics within metapopulations is crucial for making

appropriate management decisions for habitat and species (Dunning et al. 1992, Elliot et al. 2014b, Barthold et al. 2016, Heinrichs et al. 2016).

Connectivity estimates that include functional responses to the landscape are essential for applied conservation (Hilty et al. 2020). Expert opinion derived resistance surfaces can be useful hypothesis of connectivity, but a growing need to evaluate these from data are needed to validate theoretical predictions of connectivity (Ricketts 2001, Zeller et al. 2020). In the UK, recolonization of habitat by water voles after mink eradication may be impeded by topographic features, slowing expected recovery efforts. Also, extending models like the one presented here to include increasingly detailed demographic-weighting could help increase the mechanistic descriptions of spatiotemporally dynamic connectivity (Sutherland et al. 2014, Howell et al. 2018, Zeller et al. 2020). While I incorporated a weighting based on the distribution of occupied habitat, better accounting for the distribution and demography of dispersers could better describe the magnitude of resistance of individual landscape features to dispersal, the process that ultimately governs realized connectivity (Driscoll et al. 2014, Drake et al. 2021b). Increasing our understanding of the landscape's influence on connectivity, and ultimately persistence of species in the landscape, will require mechanistic explanations of the influence landscape structure has on ecological processes.

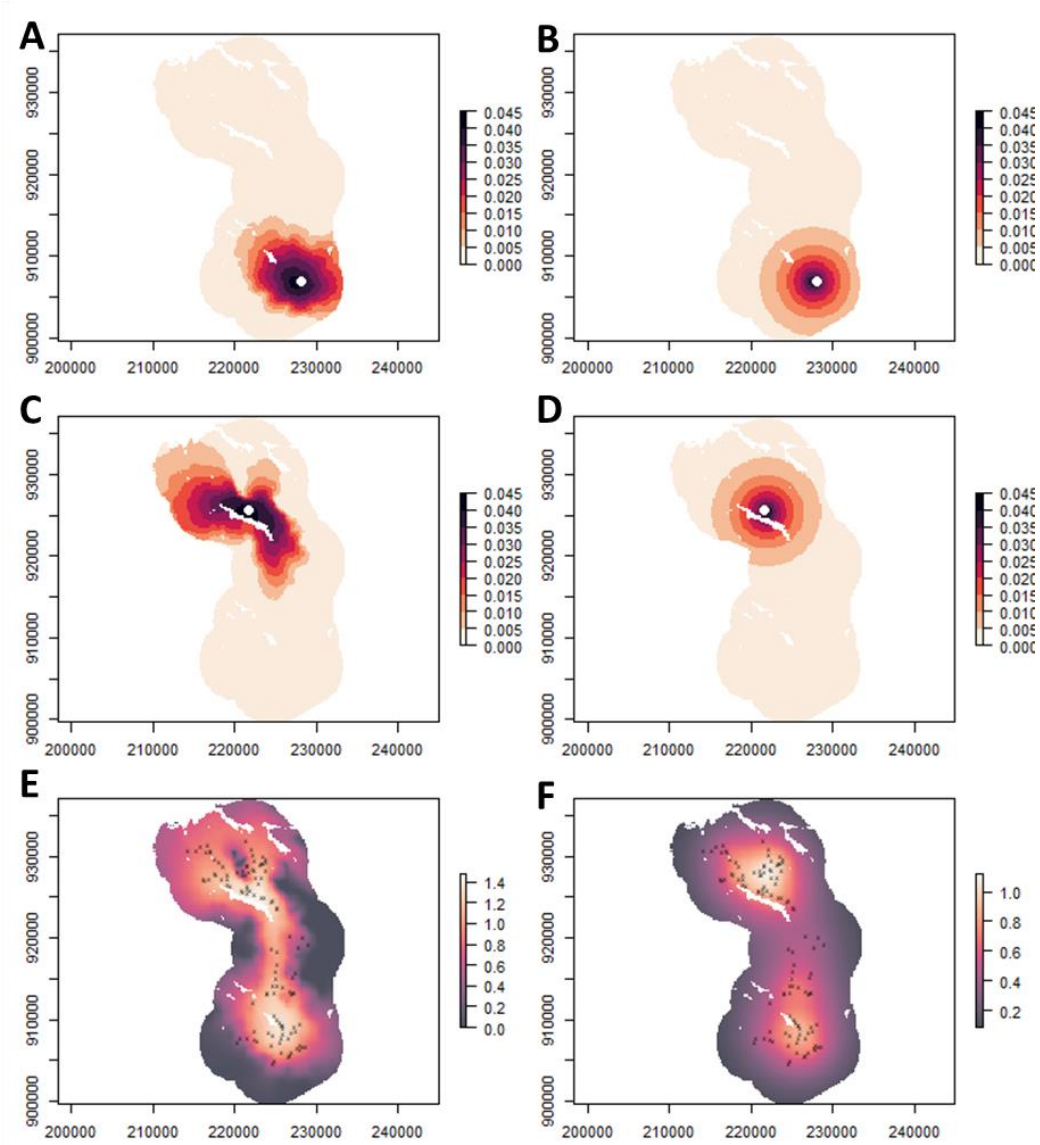

Figure 6. Non-Euclidean connectivity surfaces estimated from long-term occupancy trends compared to Euclidean connectivity assumptions in Assynt, UK for a mammalian metapopulation. (A) The landscape resistance informed connectivity surface for a patch located in a relatively lowland, low topographic relief area. (B) The Euclidean based connectivity surface for the same habitat patch as panel A. (C) The landscape resistance informed connectivity for a patch located near high topographic relief landscape structure. (D) The same habitat patch as in panel C yet using Euclidean connectivity assumptions. Notice that the Euclidean-based surface assumes the same connectivity probability in all directions, missing the reduction in connectivity when the model is generalized to include landscape structure. (E) The full potential connectivity of the landscape when considering elevation induced resistance. (F). The Euclidean-based connectivity surface both over- and under- estimates connectivity depending on the location in the landscape.

CHAPTER 4

FISHING FOR MAMMALS: LANDSCAPE-LEVEL MONITORING OF TERRESTRIAL AND SEMI-AQUATIC COMMUNITIES USING EDNA FROM RIVERINE SYSTEMS[1]

Abstract

Environmental DNA (eDNA) metabarcoding has revolutionized biomonitoring in both marine and freshwater ecosystems. However, for semi-aquatic and terrestrial animals, the application of this technique remains relatively untested. We[2] first assess the efficiency of eDNA metabarcoding in detecting semi-aquatic and terrestrial mammals in natural lotic ecosystems in the UK by comparing sequence data recovered from water and sediment samples to the mammalian communities expected from historical data. Secondly, using occupancy modelling we compared the detection efficiency of eDNA metabarcoding to multiple conventional non-invasive survey methods (latrine surveys and camera trapping). eDNA metabarcoding detected a large proportion of the expected mammalian community within each area. Common species in the areas were detected at the majority of sites. Several key species of conservation concern in the UK were detected by eDNA sampling in areas where authenticated records do not currently exist, but potential false positives were also identified. Water-based eDNA metabarcoding provided comparable results to conventional survey methods in per unit of survey effort for three species (water vole, field vole and red deer) using occupancy models. The comparison between survey 'effort' to reach a detection probability of ≥.95 revealed that 3–6 water replicates would be equivalent to 3–5 latrine surveys and 5–30 weeks of single camera deployment, depending on the species. eDNA metabarcoding can be used to

generate an initial ‘distribution map’ of mammalian diversity at the landscape level. If conducted during times of peak abundance, carefully chosen sampling points along multiple river courses provide a reliable snapshot of the species that are present in a catchment area. In order to fully capture solitary, rare and invasive species, we would currently recommend the use of eDNA metabarcoding alongside other non-invasive surveying methods (i.e. camera traps) to maximize monitoring efforts.

Introduction

Environmental DNA (eDNA) metabarcoding (the simultaneous identification of multiple taxa using DNA extracted from an environmental sample, e.g. water, soil, based on short amplicon sequences) has revolutionized the way we approach biodiversity monitoring in both marine and freshwater ecosystems (Valentini et al. 2016, Deiner et al. 2017). Successful applications include tracking biological invasions, detecting rare and endangered species and describing entire communities (Holman et al. 2019). Most eDNA metabarcoding applications on vertebrates to date have focused on monitoring fishes and amphibians (Hänfling et al. 2016, Valentini et al. 2016). What has become apparent from studies in lentic systems (ponds and lakes) is that semi-aquatic and terrestrial mammals can also be detected (Hänfling et al. 2016, Harper et al. 2019). As a result, there has been an increasing focus on the use of both vertebrate (Harper et al. 2019) and mammal-specific primer sets (Ushio et al. 2017, Leempoel et al. 2020, Sales et al. 2020a) for detecting mammalian communities using eDNA metabarcoding.

Mammals include some of the most imperiled taxa, with over one-fifth of species considered to be threatened or declining (Visconti et al. 2011). Monitoring of mammalian biodiversity is therefore essential. Given that any optimal survey approach is likely to be

species-specific, very few species can be detected at all times when they are present. This imperfect detection (even greater for elusive and rare species) can lead to biased estimates of occurrence and hinder species conservation (Mackenzie et al. 2002). For mammals, repeated surveys using several monitoring methods are usually applied. These include indirect observations such as latrines, faeces, hair or tracks, or direct observations such as live-trapping or camera trapping surveys over short time intervals such that closure/invariance can be assumed and detectability estimated (Nichols et al. 2008). Each of these methods has associated efficiency, cost and required expertise trade-offs, which become more challenging as the spatial and temporal scales increase.

Environmental DNA sampling yields species-specific presence/absence data that are likely to be most valuable for inferring species distributions using well-established analytical tools such as occupancy models (Mackenzie et al. 2002). These models resolve concerns around imperfect detection of difficult to observe species. When coupled with location-specific detection histories, these can be used to infer true occurrence states, factors that influence occupancy rates, colonization-extinction probabilities and estimates of detection probability (MacKenzie et al. 2018). The use of eDNA sampling to generate species-specific detection data has unsurprisingly increased in recent years, and in many cases has outperformed or at least matched conventional survey methods (Lugg et al. 2018, Tingley et al. 2019). Although comparisons between eDNA analysis and conventional surveys for multi-species detection are numerous (see table S1 in Lugg et al. 2018), studies focusing on detection probability estimates for multiple species identified by metabarcoding are rare (Valentini et al. 2016, Abrams et al. 2019).

The aim of this study was to assess the efficiency of eDNA metabarcoding for detecting semi-aquatic and terrestrial mammals in natural lotic systems in the UK. We conducted eDNA sampling in rivers and streams in two areas (Assynt, Scotland and Peak District National Park, England). Together these locations have the majority of UK semi-aquatic and terrestrial mammalian species present (Appendix K). Our objectives were twofold: first, we sought to establish whether eDNA metabarcoding is a viable technique for monitoring semi-aquatic and terrestrial mammals by comparing it to the mammalian communities expected from historical data, a group for which eDNA sampling has rarely been evaluated in a natural setting. Secondly, we evaluate the detection efficiency of water- and sediment-based eDNA sampling in one of these areas (Assynt) for multiple species compared to multiple conventional non-invasive survey methods (latrine surveys and camera trapping).

Materials and Methods

Latrine surveys

Assynt, a heather-dominated upland landscape in the far northwest of the Scottish Highlands, UK (Figure 7a), is the location of an ongoing 20-year metapopulation study of water voles *Arvicola amphibius* led by the University of Aberdeen (Appendix K). Here, we mainly focus only on data collected in 2017. The metapopulation is characterized by 116 discrete linear riparian habitat patches (ranging from 90 m to nearly 2.5 km) distributed sparsely (4% of waterway network) throughout the 140 km^2 study area (Sutherland et al. 2014). Water voles use prominently placed latrines for territory marking (Appendix K). Using latrine surveys, a reliable method of detection (Sutherland et al. 2014), water vole occupancy status was determined by the detection of latrines that

are used for territory marking (Sutherland et al. 2013). During the breeding season (July and August), latrine surveys were conducted twice at each site. In addition to water vole latrines, field vole *Microtus agrestis* pellets are also easily identifiable, and so field vole detections were also recorded along waterways as a formal part of the latrine survey protocol. Live-trapping was then carried out at patches deemed to be occupied by water voles according to latrine surveys to determine their abundances (this was used to determine which sites were sampled for eDNA; Figure 7a).

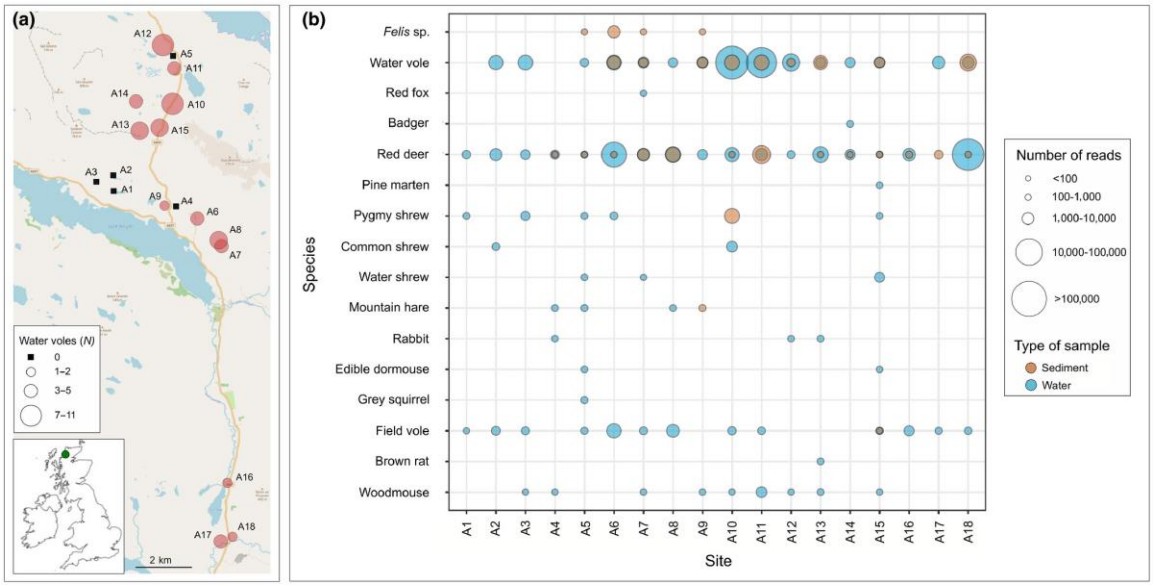

Figure 7 (a) Environmental DNA (eDNA) sampling sites in Assynt, Scotland; the size of sites corresponds to abundance categories based on summer live-trapping. (b) A bubble graph representing presence/absence and categorical values of the number of reads retained (after bioinformatic filtering) for eDNA (water in blue and sediment in orange) from each wild mammal identified in each site in Assynt (A1–A18)

Camera trap data

Camera traps were deployed at the beginning of July and thus overlapped temporally with the latrine survey in Assynt. Data were collected from cameras deployed at seven of these patches. Within each of these patches, cameras were deployed at the midpoint of the areas where active signs (latrines, grass clipping, burrows) were detected,

and if no signs were detected, at the midpoint of historical water vole activity (J. Drake, C. Sutherland and X. Lambin, pers. comm.). These will also capture images of any species present in the area that come within close proximity of the camera (Appendix K).

Cameras were deployed approximately 1 m above-ground on iron ‘u-posts’ to avoid flooding, prevent knock-down by wind/wildlife and optimize both depth of field and image clarity. Cameras (Bushnell HD Trophy Cam) were set at normal detection sensitivity (to reduce false-triggers from grass/shadows), low night time LED intensity (to prevent image white out in near depth of field), three shot burst (to increase chance of capturing small, fast moving bodies) and 15-min intervals between bursts (to increase temporal independence of captures and decrease memory burden). The area each camera photographed was approximately 1–2 m^2. Animals were identified on images and information was stored as metadata tags using the R (R Core Team 2017) package camtrapR following the procedures described in Niedballa, Courtiol, and Sollmann (2016). Independence between detections was based on 60-min intervals between species-specific detections.

eDNA Sampling

A total of 18 potential water vole patches were selected for eDNA sampling in Assynt from 25 to 27 October 2017. The time lag between the latrine/live-trapping and eDNA surveys was because of two main reasons: (a) legitimate concerns around cross-site DNA contamination during latrine/live-trapping where researchers moved on a daily basis between sites as well as regularly handled and processed live animals (for decontamination procedures see Supporting Information) and (b) the selection of eDNA sampling sites was based on the latrine surveys and abundance data provided by live-

trapping so could only occur after this was completed by August 6th. Water and sediment samples were collected from patches where water voles were determined to be absent (five sites; A1–A5); with 1–2 individuals present (three sites; A9, A16 and 18); 3–5 individuals (five sites; A6, A8, A11, A14 and A17); and 7–11 individuals (five sites; A7, A10, A12, A13 and A15; Figure 7a). Each of these streams/rivers differed in their characteristics (in terms of width, depth and flow) and a representation of the sites is depicted in Appendix K. Three water (two litres each) and three sediment (~25 ml) replicates were taken at each patch (further details of sample collection are provided in Appendix K).

In addition to Assynt, eDNA sampling was also conducted on a smaller scale in the Peak District National Park, England (Appendix K) to incorporate additional mammals that are not known to be present in Assynt (Appendix K). Here, the occurrence of water vole was identified by the presence of latrines in two sites (P1 and P2) at the time of eDNA sampling, whilst no latrines were identified at one site (P3). At site P1, an otter *Lutra lutra* spraint was identified at the time of eDNA sampling (Appendix K). These three sites were sampled in March 2018 using the same methodology as in Assynt but were taken in close proximity (<50 cm) to water vole latrines where present (Appendix K).

eDNA laboratory methods

DNA was extracted from the sediment samples using the DNeasy PowerMax Soil kit and from the water samples using the DNeasy PowerWater Kit (both QIAGEN Ltd.) following the manufacturer's instructions in a dedicated eDNA laboratory in the University of Salford. In order to avoid the risk of contamination during this step, DNA

extraction was conducted in increasing order of expected abundance of water voles in the eDNA samples (all field blanks were extracted first, followed by the sites with supposedly zero water vole abundance, up to the highest densities last). Along with field blanks (Assynt = 8, Peak District = 2), six lab extraction blanks were included (one at the end of each daily block of extractions). A decontamination stage using a Phileas 25 Airborne Disinfection Unit (Devea SAS) was undertaken before processing samples from different locations. Additional information regarding decontamination measures and negative controls can be found in the Supporting Information.

A complete description of PCR conditions, library preparation and bioinformatic analyses is provided in Appendix K. Briefly, eDNA was amplified using the MiMammal 12S primer set (MiMammal-U-F, 5′-GGGTTGGTAAATTTCGTGCCAGC-3′; MiMammal-U-R, 5′-CATAGTGGGGTATCTAATCCCAGTTTG-3′)(Ushio et al. 2017) targeting a ~170 bp amplicon from a variable region of the 12S rRNA mitochondrial gene. A total of 147 samples, including field collection blanks (10) and laboratory negative controls (12, including six DNA extraction blanks and six PCR negative controls), were sequenced in two multiplexed Illumina MiSeq runs. To minimize bias in individual reactions, PCRs were replicated three times for each sample and subsequently pooled. Illumina libraries were built using a NextFlex PCR-free library preparation kit according to the manufacturer's protocols (Bioo Scientific) and pooled in equimolar concentrations along with 1% PhiX (v3, Illumina). The libraries were run at a final molarity of 9 pM on an Illumina MiSeq platform using the 2×150 bp v2 chemistry.

Bioinformatic analysis was conducted using OBITools metabarcoding package (Boyer et al. 2016) and the taxonomic assignment was conducted using ecotag against a

custom reference database (see Appendix K). To exclude MOTUs/reads putatively belonging to sequencing errors or contamination, the final dataset included only MOTUs that could be identified to species level (>98%), and MOTUs containing <10 reads and with a similarity to a sequence in the reference database lower than 98% were discarded (Cilleros et al. 2019). The maximum number of reads detected in the controls for each MOTU in each sequencing run was removed from all samples (Appendix K). For water voles, field voles and red deer (the most abundant wild mammals in terms of sequence reads in our dataset), this equated to a sequence frequency threshold of ≤0.17%, within the bounds of previous studies on removing sequences to account for contamination and tag jumping (Schnell et al. 2015, Hänfling et al. 2016, Cilleros et al. 2019).

Occupancy/detection analysis in Assynt

The data collection from the different survey types described above (water-based eDNA, sediment-based eDNA, latrine and camera traps) produced the following site-specific detection/non-detection data:

1. Latrine: two latrine surveys at 116 patches.
2. w-eDNA: three water-based eDNA samples at 18 of the 116 patches surveyed.
3. s-eDNA: three sediment-based eDNA samples at 18 of the 116 patches surveyed.
4. Camera: six 1-week occasions of camera trapping data at seven of the 18 patches surveyed by both Latrine and eDNA (w-eDNA + s-eDNA) surveys.

We chose to focus on three species that were detected by at least three of the four methods: water voles, field voles and red deer *Cervus elaphus*. Water voles and field voles were recorded using all four survey methods and had detection histories for 14 surveying events ((Latrine × 2) + (w-eDNA × 3) + (s-eDNA × 3) + (Camera × 6)). Red

deer were not recorded during latrine surveys and had detection histories for 12 surveying events ((w-eDNA × 3) + (s-eDNA × 3) + (Camera × 6)). To demonstrate the relative efficacy of the four surveying methods, we restricted the analyses to the 18 sites where both latrine surveys were conducted and eDNA samples were taken, seven of which had associated camera trapping data. Although each surveying method differs in terms of effort and effective area surveyed, each is a viable surveying method that is readily applied in practice. A unit of survey effort here is defined as one latrine survey, one w-eDNA replicate, one s-eDNA replicate or 1 week of camera trapping. So, while the specific units of effort are not directly comparable, the relative detection efficacy per surveying method-specific unit of effort is of interest and will provide important context for designing future monitoring studies and understanding the relative merits of each surveying method. Analysing the data using occupancy models allowing for method-specific detectability enables such a comparison in per unit effort efficacy between eDNA metabarcoding and multiple conventional survey methods.

A single season occupancy model (Mackenzie et al. 2002) was applied to the ensemble data where detection histories were constructed using each of the surveying events as sampling occasions (MacKenzie et al. 2018). The core assumption here is that the underlying occupancy state (i.e. occupied or empty) is constant over the sampling period, and therefore, every sampling occasion is a potentially imperfect observation of the true occupancy status. Because occasions represent method-specific surveying events, we used ‘surveying method’ as an occasion-specific covariate on detection (Latrine, w-eDNA, s-eDNA and Camera). Our primary objective was to quantify and compare method-specific detectability, so we did not consider any other competing models. For

comparing the methods, we compute accumulation curves as (Mackenzie and Royle 2005):

$$p^*_{smk} = 1 - (1 - \hat{p}_{sm})^k$$

Where p^*_{smk} is the cumulative probability of detecting species *s*, when species *s* is present, using method *m* after *k* surveying events based on the estimated surveying method-specific detection probability for each species ($\hat{p}_{sm}$). We vary *k* from 1 to a large number and find the value of *k* that results $p^*_{smk} \geq 95$. We conducted the same analysis separately for water voles, field voles and red deer. Analysis was conducted in R (R Core Team 2017) using the package unmarked (Fiske and Chandler 2011).

Results

Mammal detection via eDNA metabarcoding

The two sequencing runs generated 23,276,596 raw sequence reads and a total of 15,463,404 sequences remained following trimming, merging and length filtering. After bioinformatic analysis, the final 'filtered' dataset contained 23 mammals (Appendix K). For mammals, ~12 million reads were retained after applying all quality filtering steps (Appendix K). Reads from humans, cattle *Bos taurus*, pig *Sus scrofa*, horse *Equus ferus*, sheep *Ovis aries* and dog *Canis lupus familiaris*, were not considered further as the focus of this study was on wild mammals (Appendix K). *Felis* was included because of the potential of it being wildcat *Felis silvestris* or domestic cat *F. catus*/wildcat hybrids. A final dataset comprising ~5.9 million reads was used for the downstream analyses (Appendix K).

In Assynt, the wild species identified were the red deer (18/18 sites); water vole (15/18); field vole (13/18); wood mouse *Apodemus sylvaticus*—9/18; pygmy shrew *Sorex*

minutus—4/18; wild/domestic cat *Felis* spp.—4/18; mountain hare *Lepus timidus*—4/18; rabbit *Oryctolagus cuniculus*—3/18; water shrew *Neomys fodiens*—3/18; common shrew *Sorex araneus*—2/18; edible dormouse *Glis glis*—2/18; grey squirrel *Sciurus carolinensis*—1/18; pine marten *Martes martes*—1/18; brown rat *Rattus norvegicus*—1/18; red fox *Vulpes vulpes*—1/18 and badger *Meles meles*—1/18 (Figure 7b). All of these species are distributed around/within Assynt Appendix K), with the exception of the edible dormouse and the grey squirrel. These are unequivocally absent from the region. The edible dormouse is only present in southern England and the grey squirrel is not distributed that far north in Scotland (Mathews et al. 2018).

Of the wild mammals in the Peak District, the water vole, field vole, wood mouse and otter were found in two sites (P1 and P2). The red deer, pygmy shrew, common shrew, water shrew, red squirrel *Sciurus vulgaris*, grey squirrel, pine marten and badger were each found at a single site (Appendix K). Only rabbit was found in site P3. All species identified are currently distributed within the Park (Appendix K), except the red squirrel and pine marten. The pine marten, which is critically endangered in England, has only two reliable records that have been confirmed in the Park since 2000 and the red squirrel has not been present for over 18 years (Alston et al. 2012).

Overall, water samples yielded better results than sediment samples regarding species detection and read count for both areas sampled (Figure 7b; Appendix K). In Assynt, only the wild/domestic cat was exclusively detected in sediment samples (four sites), whereas water samples recovered eDNA for ten additional species not found in the sediment samples. The red deer, water vole, field vole, mountain hare and pygmy shrew

were also found in sediment samples in Assynt (Figure 7b), and water vole and wood mouse in the Peak District sediment samples (Appendix K).

Occupancy Analysis

Of the 18 sites where both latrine and eDNA surveys were conducted, water voles were detected at 13 and field voles were detected at 11. A total of seven wild mammals were recorded at the seven sites with a camera trap from 10 July to 25 October 2017 (Appendix K). There were several incidences where a shrew could not be identified to species level using camera traps. For camera traps, water voles were recorded at all sites, red deer at five out of seven, field voles and weasels at three sites, water shrews and otters at two and a red fox at a single site.

For the 18 sites in Assynt, estimated site occupancy (with 95% confidence intervals) from the combined surveying methods was 0.91 (0.63–0.98) for water voles and 0.88 (0.57–0.98) for field voles. Red deer were observed at every patch by at least one of the methods, and therefore occupancy was 1 (Table 5). For all three species, per sample detection probability was higher for eDNA taken from water than for eDNA taken from sediment (Table 5; Figure 8). The surveying method-specific efficacy pattern was similar for water voles and field voles (Table 5; Figure 8): latrine surveys had the highest probability of detecting the species (0.77 and 0.52 respectively), followed by eDNA from water (0.57 and 0.40 respectively), then camera trapping (0.50 and 0.20 respectively) and finally eDNA from sediment (0.27 and 0.02 respectively). Detection probability was higher for water voles than field voles using all four methods (Table 5; Figure 8). No effort was made to record red deer presence during latrine surveys. Like the water voles and field voles, red deer detection was higher using eDNA from water (0.67,

CI: 0.53–0.78) compared to eDNA from sediment (0.10, CI: 0.04–0.21). Unlike the voles, which were more detectable by cameras than sediment eDNA, red deer detection on cameras was similar to sediment eDNA (0.10, CI: 0.04–0.24).

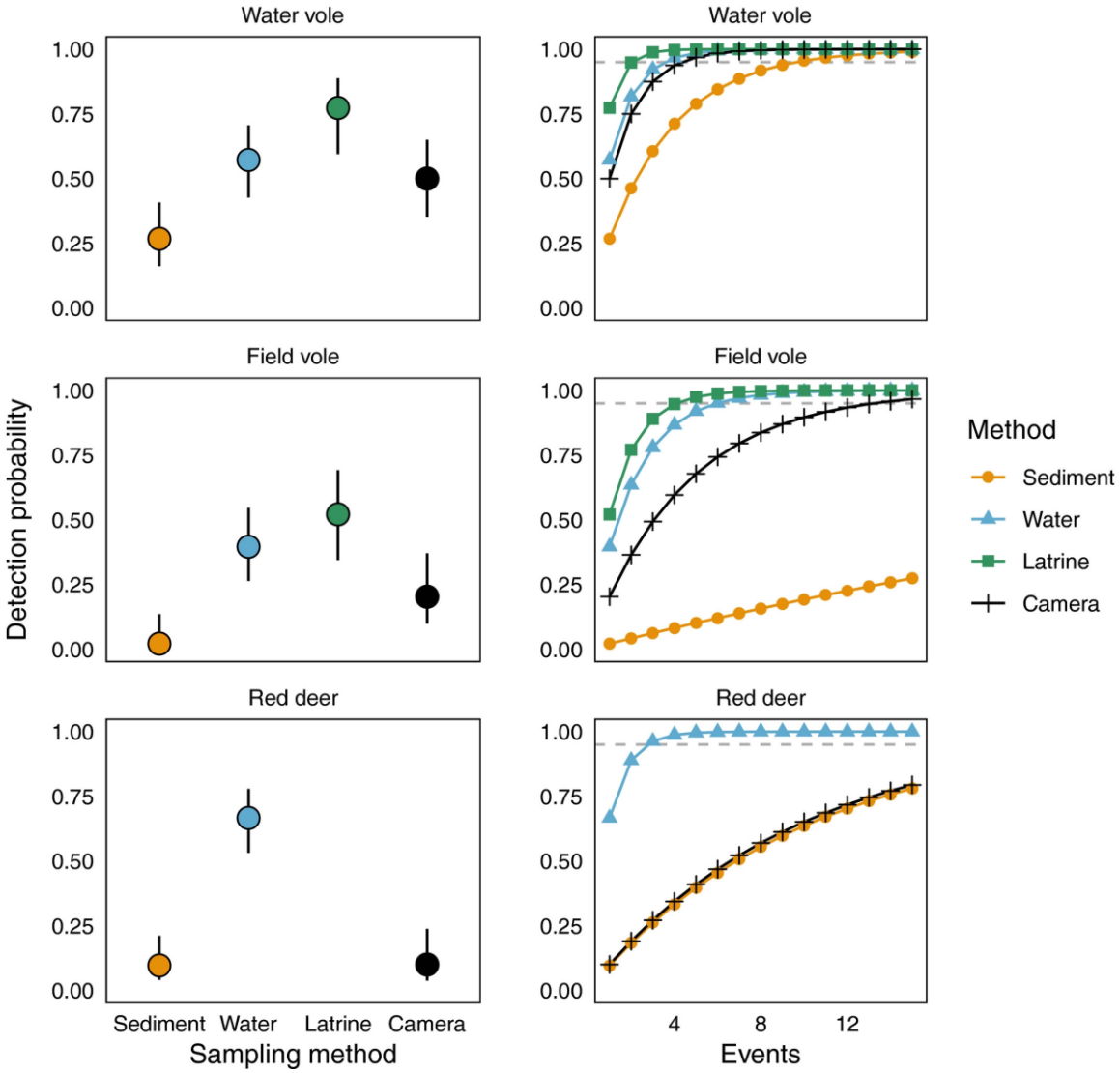

Figure 8. Figures on the left show estimated detection probabilities of each survey method for each of three focal species; the vertical lines are 95% confidence intervals. Figures on the right show the method- and species-specific cumulative detection probability with increasing number of sampling events; the horizontal dashed line shows a probability of .95 for reference.

The patterns described above detail surveying event-specific detectability. We also computed the cumulative detection probability for each method and each species

($\hat{p}_{sm}$). The cumulative detection curves over 15 surveying events are shown in Figure 2. The number of surveying events, *k*, required to achieve $p^*_{psm} \geq 0.95$ for water voles was three surveys, four samples, 10 samples and 5 weeks, for latrines, water eDNA, sediment eDNA and cameras respectively. The number of surveying events, *k*, required to achieve $p^*_{psm} \geq 0.95$ for field voles was five surveys, six samples, 141 samples and 14 weeks, for latrines, water eDNA, sediment eDNA and cameras respectively. The number of surveying events, *k*, required to achieve $p^*_{psm} \geq 0.95$ for red deer was three samples, 30 samples and 29 weeks, for water eDNA, sediment eDNA and cameras respectively (see also Figure 8).

Table 5. (Table 1 in pub) Estimated site occupancies and detection probabilities, with associated 95% confidence intervals in brackets, obtained for water-based eDNA (w-eDNA), sediment-based eDNA (s-eDNA) and conventional survey methods (Latrine and Camera) in Assynt, Scotland.

Species	**Occupancy**	**Detection Probability**			
		Latrine[†]	**w-eDNA**	**s-eDNA**	**Camera**
Water Vole	0.91 (0.63–0.98)	0.77 (0.59–0.89)	0.57 (0.43–0.71)	0.27 (0.16–0.41)	0.50 (0.35–0.65)
Field Vole	0.89 (0.57–0.98)	0.52 (0.34–0.69)	0.40 (0.26–0.55)	0.02 (0.00–0.14)	0.20 (0.10–0.37)
Red Deer	1.00 (1.00–1.00)	-	0.67 (0.53–0.78)	0.10 (0.04–0.21)	0.10 (0.09–0.24)

Discussion

Despite the increasing potential of eDNA metabarcoding as a biomonitoring tool (Deiner et al. 2017), its application has largely been focused on strictly aquatic or semi-aquatic animals, thus restricting management and conservation efforts of the wider ecosystem (Williams et al. 2018). Here, we demonstrate the ability of eDNA

metabarcoding to provide a valuable 'terrestrial dividend' for mammals from freshwater lotic ecosystems, with a large proportion of the expected species from the wider landscape being detected in each of the two study locations. In particular, we have demonstrated that water-based eDNA sampling offers a promising and complementary tool to conventional survey methods for the detection of whole mammalian communities.

Detection of mammalian communities using eDNA metabarcoding

Of the species known to be common in both Assynt and the Peak District, eDNA metabarcoding readily detected the water vole, field vole and red deer at the majority of sites surveyed (Figure 77b; Appendix K). Pygmy, common and water shrews, wood mice and mountain hares were also detected by eDNA metabarcoding at multiple sites in Assynt (Figure 7b). A higher eDNA detection rate is expected for aquatic and semi-aquatic mammals compared to terrestrial mammals in aquatic environments due to the spatial and temporal stochasticity of opportunities for terrestrial mammals to be in contact with the water (Ushio et al. 2017). The semi-aquatic water vole was generally detected by eDNA metabarcoding where we expected to find it and at relatively high read numbers (Figure 7b; Appendix K). This is in line with previous studies in lentic systems (Harper et al. 2019). However, the red deer was the only terrestrial species detected by eDNA sampling at all sites in Assynt, and the terrestrial field vole at over 70% of surveyed sites.

In addition to lifestyle (semi-aquatic or terrestrial), the number of individuals of each species (i.e. group-living) may be important for eDNA detection (Williams et al. 2018). As a counter example to this, otters and weasels were notably absent in the eDNA samples in Assynt despite being captured by camera traps (Appendix K). Otters were present in the water eDNA samples at two sites in the Peak District, albeit at a lower

number of reads in comparison to most of the other species detected (Appendix K). This mirrors previous studies where eDNA analysis has performed relatively poorly for otter detection in captivity and the wild (Thomsen et al. 2012, Harper et al. 2019). Carnivores were generally detected on fewer occasions (e.g. red foxes, badgers and pine martens; Figure 7b; Appendix K) or not at all (e.g. stoats and American mink in addition to those discussed above) in comparison to smaller mammals and red deer, and a similar pattern has been shown with North American carnivores in a recent study using eDNA from soil samples (Leempoel et al. 2020). For some of these species, species ecology/behaviour such as a relatively large home range and more solitary nature (e.g. red foxes) may go some way towards explaining a lack of, or few, eDNA records. Furthermore, as demonstrated by Ushio et al. (2017) poor efficiency for amplifying some mammal species might be associated to suboptimal experimental conditions (e.g. inadequate primer design, primer bias, DNA concentration, species masking and/or annealing temperatures).

Regarding the sampling medium for eDNA, we demonstrated that water is a more effective method for detection of mammal eDNA than sediment (Table5; Figure 7b; Appendix K). For one of our focal species, the water vole, 75% of sites which were deemed unoccupied by latrine surveys and those with ≤2 individuals (eight sites) in Assynt, returned a non-detection for sediment eDNA as opposed to 37.5% of sites for water (Figure 7; Appendix K). Distinct temporal inferences are provided by eDNA recovered from water and sediment samples. DNA bound to sediments can remain detectable for a longer period (i.e. up to hundreds of years) and provide historical data, whereas, eDNA retrieved from water samples provide more contemporary data due to a

faster degradation in the water column (Turner et al. 2015). It is worth investigating further if sediment eDNA could indicate the presence of a more 'established' population, where a certain threshold of individuals and long-term occupation (i.e. historical) is required for detection in sediment (Appendix K; Leempoel et al., 2020; Turner et al., 2015).

Importantly, sparse or single eDNA records should be carefully verified. The edible dormouse and grey squirrel sequences identified within the Assynt samples (Figure 7b) and red squirrel within the Peak District (Appendix K) highlight the caveats associated with this technique. If management decisions had relied on eDNA evidence alone, false positives for these species could lead to unnecessary resources being allocated for management/eradication programmes as the edible dormouse and grey squirrel are classified as invasive species within Great Britain. These potentially arose due to sample carryover from a previous sequencing run on the same instrument (a known issue with Illumina sequencing platforms; Nelson et al. 2014) which included those species for the reference database construction. Controlling for false positives is certainly a huge challenge in eDNA metabarcoding and the need to standardize and optimize thresholds for doing so is an ongoing debate (Ficetola et al. 2015, Harper et al. 2019).

Even with these concerns around false positives highlighted, two records are potentially noteworthy in a conservation context for UK mammals because of the relatively high read number associated with these records (Appendix K). The first of these is the *Felis* records in sediment samples in multiple sites in Assynt (Figure 7b). Even with a 'pure' *F. silvestris* as a reference sequence, it was not possible to distinguish

between the wild and domesticated species for this 12S fragment (data not shown). Despite ongoing conservation efforts, there may now be no 'pure' Scottish wildcats left in the wild in the UK but isolated populations (perhaps of hybrid origin) may exist in this region (Sainsbury et al. 2019). Given that these eDNA detections were all from sediment samples, it is possible that they may be historical rather than contemporary (see above). The other significant eDNA record was the pine marten in the Peak District. The pine marten *Martes martes* is known to occur in the Scottish Highlands but had disappeared from most of the UK and recently has been recovering from historical persecution, including a potential expansion of its range. Still, authentic records from northern England are scarce or lacking altogether (Alston et al. 2012, Sainsbury et al. 2019). However, a record of a recent roadkill exists from just outside the Park's boundary (BBC News 2018). The high number of reads recovered for the Peak District sample (4,293 reads vs. 25 in the Assynt sample) adds credence to this positive eDNA detection but further investigations are warranted into the potential presence of this species in the area.

Comparisons between surveying methods

Comparisons of species detection by traditional survey approaches and eDNA analysis are now numerous in the literature, and mainly focus on what is and what is not detected within and across different methods (Hänfling et al. 2016, Leempoel et al. 2020). Yet, there has been growing incorporation of occupancy modelling to estimate the probability of detecting the focal species, in comparison to one other survey method, either for a single species (Lugg et al. 2018, Tingley et al. 2019) or multiple species (Valentini et al. 2016, Abrams et al. 2019). Simultaneous multi-method comparisons for multiple species have been lacking and this study directly addresses this for the first time.

The probability of detecting the water vole and field vole was higher for the latrine surveys than eDNA sampling (both water and sediment) and camera traps (Table 5; Figure 8). However, when considering confidence intervals, there was considerable overlap between latrine, water-based eDNA metabarcoding and camera traps for both species, with only sediment-based eDNA metabarcoding yielding a low probability of detection (Table 5). Detection probabilities for water-based eDNA metabarcoding and camera traps were similar for water voles, with camera traps less likely to detect the field vole than water-based eDNA. For the red deer (for which no latrine survey was undertaken), water-based eDNA metabarcoding had a much higher probability of detection than either sediment-based eDNA metabarcoding or camera traps (which performed similarly; Table 5). Despite the increasing adoption of camera traps in providing non-invasive detections for mammals (Hofmeester et al. 2019), camera traps were outperformed by water-based eDNA metabarcoding for the three focal species in this component of the study. Here, camera traps were deployed so as to sample the habitat of the water vole (see Appendix K), which may explain lower detection for other terrestrial species in comparison to eDNA metabarcoding (see above). Studies focusing on a single species often report that eDNA analysis outperforms the conventional survey method in terms of detection probabilities (Lugg et al. 2018). For metabarcoding, there is clearly a need to carefully consider the potential for cross contamination between samples and how false positives (and negatives) could impact detection probabilities using occupancy modelling with eDNA data (Lahoz-Monfort et al. 2016, Brost et al. 2018). Among the recommendations made by Lahoz-Monfort et al. (2016) to account for these uncertainties, one was the simultaneous collection of data from more conventional

surveying methods. Here, we have demonstrated general congruence between surveying methods for the water vole (Appendix K) and using certain species to apply a multiple detection methods model would be appropriate in further studies (Lahoz-Monfort et al. 2016). Alternatively, using repeated sampling and known negative controls in occupancy models that fully incorporate false-positive errors could be applied in the absence of other surveying data (Brost et al. 2018). Overall, multi-species metabarcoding studies may trade-off a slightly lower (but comparable) detection probability than other survey methods for individual species (Figure 8) in favour of a better overall 'snapshot' of occupancy of the whole mammalian community (Ushio et al. 2017).

The comparison between survey 'effort' for the four methods to reach a probability of detection of ≥.95 is highly informative and provides a blueprint for future studies on mammal monitoring. Focusing on the water vole for example, three latrine surveys would be required. A total of four water-based and 10 sediment-based eDNA replicates or 5 weeks of camera trapping would be required to achieve the same result (Figure 2). This increases for the field vole in the same habitat, with five latrine surveys and six water-based eDNA replicates. Sediment-based eDNA metabarcoding would be impractical for this species and camera trapping would take 14 weeks. What is important here is the spatial component and the amount of effort involved in the field. Taking 4–6 water-based eDNA replicates from around one location within a patch could provide the same probability of detecting these small mammals with three latrine surveys. In many river catchments, there may be 100s to 1,000s of kilometres to survey that would represent suitable habitat, and only a fraction of that may be occupied by any given species. This is particularly relevant in the context of recovery of water vole populations

post-translocation or in situations where remnant populations are bouncing back after invasive American mink *Neovison vison* control has been instigated. On a local scale, finding signs of water voles through latrine surveys is not necessarily difficult, but monitoring the amount of potential habitat (especially lowland) for a species which has undergone such a massive decline nationally is a huge undertaking (Morgan et al. 2019).

The use of eDNA metabarcoding from freshwater systems to generate an initial, coarse and rapid 'distribution map' for vertebrate biodiversity (and at a relatively low cost) could transform biomonitoring at the landscape level. For group-living (i.e. deer) and small mammal species, carefully chosen sampling points (with at least five water-based replicates) along multiple river courses could provide a reliable indication of what species are present in the catchment area if conducted during times of peak abundance (i.e. Summer and Autumn). Then, on the basis of this, practitioners could choose to further investigate specific areas for confirmation of solitary, rare or invasive species (e.g. carnivores) with increased effort in terms of both the number of sampling sites and replicates taken. At present, we would recommend the use of eDNA metabarcoding alongside other non-invasive surveying methods (e.g. camera traps) when monitoring invasive species or species of conservation concern to maximize monitoring efforts (Abrams et al. 2019, Sales et al. 2020a).

It is clear that eDNA metabarcoding is a promising tool for monitoring semi-aquatic and terrestrial mammals in both lotic (this study) and lentic systems (Ushio et al. 2017, Harper et al. 2019). We detected a large proportion of the expected mammalian community (Appendix K). Water-based eDNA metabarcoding is comparable or outperforms other non-invasive survey methods for several species (Figure 8). However,

there remain challenges for the application of this technique over larger spatial and temporal scales. Technical issues of metabarcoding in laboratory and bioinformatic contexts have been dealt with elsewhere (Harper et al. 2019) but understanding the distribution of eDNA transport in the landscape and its entry into natural lotic systems is at an early stage (and incorporating such variables in occupancy modelling approaches). This clearly requires more detailed and systematic eDNA sampling than undertaken here, particularly in an interconnected river/stream network with organisms moving between aquatic and terrestrial environments. Leempoel et al. (2020) recently demonstrated the feasibility for detecting terrestrial mammal eDNA in soil samples but this study has shown that sampling a few key areas in freshwater ecosystems (e.g. larger rivers and lakes) within a catchment area could potentially provide data on a large proportion (if not all) of the mammalian species within it, even when some species are present at low densities (Deiner et al. 2017). In this regard, future studies might also investigate the value of citizen science, where trained volunteers can contribute to data collection at key sites, thus scaling up the reach of research whilst raising public awareness and the significance of mammalian conservation concerns (Parsons et al. 2018).

Notes

[1] This chapter was published in the Journal of Applied Ecology on March 10, 2020 in Volume 57, Issue 4, pp707-716.

[2] This chapter is a collaborative effort with the following authors: Naiara Guimarães* Sales, Maisie B. McKenzie*, Joseph Drake*, Lynsey R. Harper, Samuel S. Browett, Ilaria Coscia, Owen S. Wangensteen, Charles Baillie, Emma Bryce, Deborah A. Dawson, Erinma Ochu, Bernd Hänfling, Lori Lawson Handley, Stefano Mariani, Xavier Lambin, Christopher Sutherland, Allan D. McDevitt .

Authors contributions: A.D.M., X.L., C.S., O.S.W., I.C., S.M., N.G.S., S.S.B., E.O., B.H. and L.L.H. conceived the study; Monitoring and live-trapping of water voles was part of X.L., C.S., E.B. and J.D.'s ongoing work in Assynt; J.D. analysed the camera trap data; D.A.D. advised on primer set/data validation and provided information and data on mammals in the Peak District; A.D.M., N.G.S., S.S.B. and M.B.M. carried out the eDNA sampling; M.B.M., N.G.S., S.S.B., C.B. and A.D.M. performed the laboratory work; N.G.S., O.S.W., L.R.H., M.B.M., C.B. and A.D.M. carried out the bioinformatic analyses; N.G.S., A.D.M., I.C. and M.B.M. analysed the eDNA data; C.S. and J.D. conducted the occupancy modelling; A.D.M., N.G.S., C.S., J.D., M.B.M. and L.R.H. wrote the paper, with all authors contributing to editing and discussions.

*These authors contributed equally to this work.

The eDNA component of this project was funded by the British Ecological Society (grant no. SR17/1214) and a University of Salford Internal Research Award awarded to A.D.M. J.D. was supported by the University of Massachusetts Organismal and Evolutionary Biology Research Grant and Spring 2018 Graduate School Fieldwork Grant. We thank Kristy Deiner for enlightening conversations about these results. We are grateful to Jerry Herman and Andrew Kitchener for the tissue samples from National Museums Scotland. Christine Gregory, Douglas Ross and Sarah Proctor provided water vole and otter information for sampling in the Peak District and Sara Peixoto provided sequence assemblies. We thank the various landowners for permission to sample on their property. We thank Brittany Mosher and the anonymous reviewers for significantly improving the manuscript. The authors declare that no conflict of interest exists.

CHAPTER 5

CONCLUDING REMARKS

Connectivity has been increasingly invoked for conservation and management. Semantic and the complexity that has arisen from a proliferation of applications of the concept can lead to confusion and misapplication of tools to measure the phenomenon. In Chapter 1, I synthesized approaches and concepts of connectivity from a diverse spectrum of ecological subfields. While a single metric is unable to encapsulate the diversity of ways connectivity emerges, through my review I found that a series of core components reflected the processes that underlie the emergent phenomenon of connectivity in the landscape. Connectivity includes the distribution of habitat, the structure of the landscape, the behavior response to this landscape, and importantly, but seemingly underappreciated, the spatiotemporal dynamics of the distribution of potential of dispersers. The contribution this last component plays is large, and to emphasize this contribution to ecological processes, I put forth a conceptual framework entitled *demographically-weighted connectivity*. This framework includes the identified core components while purposefully not excluding any pre-existing perspective of connectivity. Rather, I view connectivity on a spectrum of increasingly realistic representations where the decision to include any given facet of connectivity is driven by the research questions and logistical and data limitations. Understanding how models perform as this realism is abstracted out is key to making informed connectivity-based management decisions.

I conducted a simulation study to better understand how common connectivity assumptions impact the resulting inference. Bias increased as reality was abstracted out

using common connectivity modeling assumptions. A key takeaway is to consider that inclusion of any demographic data, including the presence or absence of populations in the landscape may reduce bias in parameter estimates of connectivity models as it captures at least some of the underlying dynamics. The spatiotemporal dynamic distribution of dispersers greatly contributes to the realized connectivity in the landscape. It is my hope that this review will help drive the discussion of connectivity forward, helping to increase crosstalk across ecological disciplines while explorations on how the core components of connectivity impact our ability to measure and understand ecological processes continue.

Connectivity is a spatiotemporally dynamic phenomenon yet is rarely considered as such. Some research has begun to explore how the long-term shift in vegetation and hydrology can impact connectivity between habitat patches. Extending this to incorporate how connectivity dynamics emerge as a function of spatiotemporal population dynamics has rarely been done. In Chapter 2, I developed a spatiotemporal dynamic connectivity model and applied it to a mammalian metapopulation system in the Highlands of Scotland. This long-term study system provided a useful opportunity to explore how assumptions about spatiotemporal dynamism and inclusion of demographically-weighted connectivity improved inference. My work suggests that while the relaxation of both the static assumptions and demographic-weighting was most supported, it was the inclusion of spatiotemporal demographic-weighting, which is itself temporally varying, that was the most important driver of colonization-extinction dynamics. Also, the inclusion of parameters estimated in spatiotemporally dynamic models provide additional depth to calculations of important conservation metrics, such as metapopulation capacity (MC).

Using a novel approach to describe the variation that surrounds the point estimate of MC, I demonstrated the potential to mis-interpret the persistence capacity in a habitat network. By demonstrating the spatiotemporally dynamic nature of connectivity, I hope that this work will allow others to consider connectivity dynamics role more carefully in ecological processes.

In chapter 3, I considered the landscape's influence on connectivity. Using recent modeling advances, I explored how the landscape structure impacts colonization-extinction dynamics in the water vole metapopulation study area of Assynt. Historically, identifying the landscape's influence on dispersers often relied on defining resistance values using expert opinion. Such methods, while having their place, could introduce erroneous conclusions if resistance was defined poorly. As well, alternatives to expert opinion are often costly and data intensive. However, I present a model that uses relatively easy-to-obtain presence-absence data. I tested how elevation impacted connectivity in the Assynt system, finding it influenced movement and shaped colonization dynamics. My results indicated that elevation, which can correlate with topographic ruggedness and vegetation communities, shapes local colonization in the Assynt metapopulation by impacting the effective dispersal of a riparian-specialist, the water vole. Comparing results to similar models that do not include these resistance estimates suggests that simple, Euclidean distance-based models may over-estimate the spatial scale of dispersal and thus the connectedness of a landscape. As habitats continue to be assailed from many threats, fragmentation and loss is increasingly problematic for threatened species, such as the water vole. I demonstrated the ability to estimate resistance directly from data and show the impact this can have to ecological inference.

As I have argued, determining the distribution of a species is key to understanding the connectivity between populations in the landscape. In my fourth chapter, I present a test of emerging biomonitoring techniques. Environmental DNA (eDNA) has the potential to revolutionize our ability to monitor species across ecosystems, but it has been relatively untested against traditional survey methods. This is true, particularly for semi-aquatic and terrestrial animals. I presented a collaborative research on the emerging method of eDNA metabarcoding to assess the efficiency in detecting semi-aquatic and terrestrial mammals in Assynt riparian habitat. Using occupancy modeling, I was able to determine the comparative efficiency between eDNA methods and conventional survey techniques for the mammal community in Assynt. Results suggest that water-based eDNA was comparable for detection efficiency based on per unit effort compared to traditional methods. I examined three species of conservation concern in depth, using occupancy modeling to further compare camera trapping, water-based eDNA sampling, and traditional detection surveys. I provide evidence that each of these methods fills a role in a flexible toolbox for comparatively reasonable and successful detection of a wide range of mammalian species. eDNA methods could be used to generate libraries of distribution maps if samples were systematically taken at key locations through a watershed. Combining this biomonitoring scheme with connectivity modeling could prove useful in early detection of range shifts and spread of threatened or invasive species. My hope is this could help provide a reliable baseline of a landscape's biodiversity, allowing for optimized monitoring efforts in tandem with conventional survey and management methods.

Connectivity is a complicated, multi-faceted phenomenon. It is in part driving, and in part driven by the distribution of populations in the landscape. Combined with the resistance that landscape structure imposes on the success of dispersers, connectivity could be seen as an intractably complex process. Yet, by addressing core components and the spatiotemporal dynamism these components contribute, connectivity and its contribution to ecological processes is decipherable. I believe that this dissertation provides a meaningful contribution to understanding connectivity and the detection of organisms on the landscape. These two facets compliment each other, for without an understanding of the distribution of populations, understanding the realized connectivity among populations is unlikely. My research provides important contributions to ecological theory and applications of connectivity through this lens. First, my review provides a conceptual framework I call demographically-weighted connectivity that draws across ecological subdisciplines and synthesizes the core constituent components of connectivity. Identifying these provides a useful framework that illustrated an underappreciated component of connectivity. It also demonstrated the importance of using my framework using a simulation to illustrate bias that emerges when demographic components are abstracted away from reality. Second, I applied this framework to a real metapopulation to demonstrate how accounting for spatiotemporal dynamism and the distribution of populations impacts model performance and parameter estimates. Further, I investigated the contribution of landscape structure on connectivity estimates. The results suggest that each facet of connectivity can influence how connectivity emerges in a landscape, yet the role of the disperser is central. Due to the importance of the distribution of a study organism plays in understanding connectivity, advancing and

confirming the efficacy of monitoring methods is also key. Combining emerging and conventional monitoring methods will be key to advancing and confirming existing theory driven by ecological processes influenced by connectivity. As climate change and habitat fragmentation and loss continues, mitigating our impact on ecosystems will be increasingly necessary. By understanding the dynamic interplay between populations of organisms and the landscape they interact with, connectivity driven process may be sustained. I hope this research provides such a framework to enable conservation and research a springboard in which to increase and pursue connectivity applications across ecological disciplines.

APPENDICES

APPENDIX A

CHAPTER 1: SIMULATION CODE

Drake, J. C., Lambin, X., and Sutherland, C. 2021.The value of considering demographic contributions to connectivity - a review. Ecography.

Supplemental information including 1) Simulation code in R script 2) NIMBLE Bayesian metapopulation modeling code, and 3) R code needed to execute model recovery in parallel.

This file is an RMarkdown produced file.

Data Simulation code

Custom built R function for data simulation This needs to be saved in a separate R file to be able to be accessed by the implementation code

```
sim.spom <- function(n.patches = 100,              # number of patches to
include
                     spatial.extent = c(0,0,100,100), # size of the stu
dy area
                     patch.size.range = c(1,3), # range of patch sizes
                     n.years = 20,             # number of years to simul
ate
                     AreaEqualsInds = TRUE,  #TRUE = A:N maintained; FA
LSE= A:N disrupted
                     psi1 = 0.4,               #initial occupancy
                     lam_b0 = -1,              # intercept for the Poisso
n relationship of population to patch area
                     lam_b1 = 1,               # slope for the Poisson re
lationship of population to patch area
                     pr.ext = 0.4,             # probability of extenctio
n for simulated population
                     alpha = 5,                # mean dispersal distance
                     gamma = 0.2,              # per capita effective dis
persal rate
                     theta = 1,                # control dispersal kernel
1=neg exp 2=half-normal
                     plots=FALSE,              # generates visualization
of the simulated landscape
                     boxplots=FALSE){          # generates boxplots of si
mulated data

  library("actuar")
  library("AHMbook")
  library("raster")
  #make hetergeneous patches
  occ.mat <- matrix(NA,n.patches,n.years)
  n.mat <- matrix(NA,n.patches,n.years)
```

```
  if(is.null(alpha)){
    alpha <- max(diff(spatial.extent[c(1,3)]),
                 diff(spatial.extent[c(2,4)])) / 20 #approx 50 dispersa
l ranges
  }

  patches <- cbind(x=runif(n.patches,spatial.extent[1]+2*alpha,spatial.
extent[3]-2*alpha),
                   y=runif(n.patches,spatial.extent[2]+2*alpha,spatial.
extent[4]-2*alpha),
                   area = runif(n.patches,patch.size.range[1],patch.siz
e.range[2]))

  #make occupancy and populations
  occ.mat[,1] <- rbinom(n.patches,1,psi1)  # occupancy

  n.mat[,1] <- occ.mat[,1] * rztpois(n.patches,exp(lam_b0 + lam_b1*patc
hes[,3])) # abundance
  if(AreaEqualsInds==FALSE){   # disrupted relationship abundance
    n.mat[which(n.mat[,1] >= 1),1] <- sample(n.mat[which(n.mat[,1] >=1
),1],length(which(n.mat[,1]>=1)))
  }

  for(tt in 2:n.years){
    ee <- matrix(1,n.patches,1) %*% pr.ext
    con <- n.mat[,tt-1] * exp(-as.matrix(dist(patches[,1:2])^(theta)) /
(theta*alpha^(theta)))
    diag(con) <- 0
    cc <- 1-exp(-gamma * apply(con,2,sum))
    occ.mat[,tt] <- rbinom(n.patches,1,occ.mat[,tt-1] * (1-ee) + (1-occ
.mat[,tt-1]) * cc)

    n.mat[,tt] <- occ.mat[,tt] * rztpois(n.patches,exp(lam_b0 + lam_b1*
patches[,3]))
    if(AreaEqualsInds==FALSE){
      n.mat[which(n.mat[,tt] >= 1),tt] <- sample(n.mat[which(n.mat[,tt]
>=1 ),tt],length(which(n.mat[,tt]>=1)))
    }

    if(plots){
      yy <- expand.grid(x=spatial.extent[1]:spatial.extent[3],
                        y=spatial.extent[2]:spatial.extent[4])
      dd <- e2dist(patches[,1:2],yy)
      cc <- exp(-dd^theta / (theta*alpha^theta)) * n.mat[,tt]
      diag(cc) <- 0
      plot(rasterFromXYZ(cbind(yy,1-exp(-c(gamma*apply(cc,2,sum))))), a
xes=F,legend=F)
      points(patches[,c(1,2)],pch=21,bg=ifelse(occ.mat[,tt]==1,"blue","
white"))
    }
```

```
    if(boxplots){
      boxplot(cc[occ.mat[,tt-1]==0]~occ.mat[occ.mat[,tt-1]==0,tt], ylim
=c(0,1))
    }
  }
  if(plots) plot(apply(occ.mat,2,sum),type="o",pch=16,ylim=c(0,n.patche
s))

  return(list("occ" = occ.mat, "abund" = n.mat, "area"= patches[,3], "c
oords" = patches[,1:2],
              "dmat"=as.matrix(dist(patches[,1:2])), "alpha"=alpha, "co
l.mat"=cc, "con.mat"=con))
}
```

NIMBLE Metapopulation Model Code

This needs to be saved in a seperate R file in the working directory to be able to be accessed by the implementation code

```
metapop.fit <- nimbleCode({

#~~~~~~~Priors~~~~~~~~~~~~~~~~~~~~~~~~~~~~~~~~~~~~~~~~~~~~~~~~~~~~~~~~~~~~~#

  psi1 ~ dunif(0,1)               # Initial occupancy probability

  #alpha.link ~ dnorm(0,0.01)     # alpha
  #log(alpha) <- alpha.link       # -> reals scale
  alpha ~ dunif(0,10)             # alpha

  gamma.link ~ dnorm(0,0.1)     # logit(gamma) # dbeta(2,2)
  logit(gamma) <- gamma.link     # -> reals scale

  epsilon.link ~ dnorm(0,0.01)   # logit(epsilon)
  logit(epsilon) <- epsilon.link
#~~~~~~~Likelihood~~~~~~~~~~~~~~~~~~~~~~~~~~~~~~~~~~~~~~~~~~~~~~~~~~~~~~~~~~~#

  for(i in 1:n.patches){ #occupancy in yr 1
    z[i,1] ~ dbern(psi1)
  }

  for(k in 2:n.years){ #occupancy t2-T
    for(i in 1:n.patches){
      for(j in 1:n.patches){
        con.arr[i,j,k-1] <- exp(-(dmat[i,j]^(theta)) / (theta*(alpha^(t
heta)))) * #kernel...
                                                                      #
negative exponential: theta = 1
                                                                      #
half normal: theta = 2
                            (demog*n[j,k-1] + 1 - demog) *     #demogra
```

```
phy (N)
                              (nprox*Area[j]  + 1 - nprox) *    #area app
roximation (A)
                              ((1-struct)*z[j,k-1] + 1*struct) * #ALL: st
ruct=1, OCC: struct=0
                              (1 - equals(i,j))                  #remove
self
      }

      col.mat[i,k-1] <- 1 - exp(-gamma * sum(con.arr[i,1:n.patches,k-1]
))
      ext.mat[i,k-1] <- epsilon

      #occupancy
      psi.t[i,k-1] <- z[i,k-1]       * max(0.001, min((1-ext.mat[i,k-1]
), 0.999)) +
                      (1 - z[i,k-1]) * max(0.001, min(   col.mat[i,k-1]
,  0.999))
      z[i,k] ~ dbern(psi.t[i,k-1])
    }
  }

#~~~~~~~Derived parameters~~~~~~~~~~~~~~~~~~~~~~~~~~~~~~~~~~~~~~~~~~~~~~~#

  for(t in 1:n.years){
    m.occ[t] <- sum(z[1:n.patches,t])
  }
})
```

Code for implementation in parallel

```
library(nimble)
library(foreach)
library(doParallel)
library(actuar)
library(AHMbook)
library(ggplot2)

source("simcode.R")
source("metapop_jags.R")

file.path <- "NnotequalsA_HighN/" #where to dump files
AeN <- FALSE                      #set A:N relationship

###
###
# We wish to to make a note that this simulation is computationally int
ensive. It can take several days to weeks depending
# the number of cores you dedicate to the model and the number of patch
es, years, and iterations you explore.
```

```
# For example, we used 64 bit Windows operating system running a Dual I
ntel Xeon Processor 2.2 GHz with a dedicated 32 gb (4X8gb) DDR4 RAM
# It took us several days to run midrange combinations of parameters fo
r iter = 500
###
###

start_time <- Sys.time()

n.iterations <- 500  # how many ties to run
n.models     <- 5    # N, AZ, Z, A, U
n.params     <- 3    # number of parameters you are tracking (don't for
get that some params are longer than 1 item)
modelnames   <- c("N", "AZ", "Z", "A", "U")

n.patches <- c(30, 50, 100, 150)[3]
n.years   <- c( 5,  10,  20)[2]
int <- c(-1,-1)[2]        # refers to which intercept for the Poisson r
elationship of population to patch area used in simulation
slp <- c(1,2)[2]          # this refers to the slope of the Poisson rel
ationship of population to patch area used in simulation
gamm <- c(0.2, 0.03)[2]   # this is referring to which gamma you wish t
o use and should reflect the generated simulation data


#model 1: N (abundance weighted connectivity)
mod.N.consts <- list(n.years   = n.years,
                     n.patches = n.patches,
                     theta     = 1,          # 1 = neg exp; 2 = half no
rmal
                     demog     = 1,          # demographic = 1
                     nprox     = 0,          # approximate N with A = 1
(if demo=1, nprox MUST = 0)
                     struct    = 0)          # patches are populations
= 1 (if demo=1, struct MUST = 0)

#model 2: AZ (area-informed occupancy weighting connectivity)
mod.AZ.consts <- list(n.years   = n.years,
                      n.patches = n.patches,
                      theta     = 1,         # 1 = neg exp; 2 = half no
rmal
                      demog     = 0,         # demographic = 1
                      nprox     = 1,         # approximate N with A = 1
(if demo=1, nprox MUST = 0)
                      struct    = 0)         # patches are populations
= 1 (if demo=1, struct MUST = 0)

#model 3: Z (occupancy weighted connectivity)
mod.Z.consts <- list(n.years   = n.years,
                     n.patches = n.patches,
```

```
                      theta     = 1,          # 1 = neg exp; 2 = half no
rmal
                      demog     = 0,          # demographic = 1
                      nprox     = 0,          # approximate N with A = 1
(if demo=1, nprox MUST = 0)
                      struct    = 0)          # patches are populations
= 1 (if demo=1, struct MUST = 0)

#model 4: A (area weighted connectivity)
mod.A.consts <- list(n.years   = n.years,
                      n.patches = n.patches,
                      theta     = 1,          # 1 = neg exp; 2 = half no
rmal
                      demog     = 0,          # demographic = 1
                      nprox     = 1,          # approximate N with A = 1
(if demo=1, nprox MUST = 0)
                      struct    = 1)          # patches are populations
= 1 (if demo=1, struct MUST = 0)

#model 5: U (uninformed connectivity)
mod.U.consts <- list(n.years   = n.years,
                      n.patches = n.patches,
                      theta     = 1,          # 1 = neg exp; 2 = half no
rmal
                      demog     = 0,          # demographic = 1
                      nprox     = 0,          # approximate N with A = 1
(if demo=1, nprox MUST = 0)
                      struct    = 1)          # patches are populations
= 1 (if demo=1, struct MUST = 0)

consts.list <-list(mod.N.consts=mod.N.consts,
                   mod.AZ.consts=mod.AZ.consts,
                   mod.Z.consts=mod.Z.consts,
                   mod.A.consts=mod.A.consts,
                   mod.U.consts=mod.U.consts)

#parameters to track during the sim
params <- c("alpha", "gamma", "epsilon" ) # "m.occ"

out.ests <- data.frame(mean = double(),
                       median = double(),
                       SD = double(),
                       CI025 = double(),
                       CI975 = double(),
                       model = factor(),
                       parameter = factor(),
                       iteration = double())
if(1==2) load("") # here you can input iterations that were paused beca
use of the set seed implementation
```

```
for(i in 1:n.iterations){ # number of iterations of all simulations; ca
n start from last finished run

  set.seed(i)     # this helps allow for replicable results
  #  sim.spom simulates that data you will try to recover parameters fr
om
  simulated.pops <- sim.spom(n.patches = n.patches,
                             n.years = n.years,
                             AreaEqualsInds = AeN,
                             lam_b0 = int,
                             lam_b1 = slp,
                             gamma = gamm)
  data <- list(Area = simulated.pops$area,
               z    = simulated.pops$occ,
               n    = simulated.pops$abund,
               dmat = as.matrix(simulated.pops$dmat))

  #initial seeds for non-constants (anything with a prior)
  inits <- function(){
    list(psi1         = runif(1, 0.1,0.9),   #0.4,         #runif(1,0.1
,0.9),
         alpha        = runif(1, 1, 10),     #5,           #runif(1,-2,
2),
         gamma.link   = runif(1, 0.001, 10), #log(0.2),    #runif(1,-2,
2)
         epsilon.link = runif(1, 0.001, 10) )#qlogis(0.4)) #runif(1,-2,
2))
  }

  #loop through each model
  cl <- makeCluster(8)      # this defines the number of cores to dedic
ate to this simulation. more cores is faster,
                            # but not all machines have the same number
to use.
  registerDoParallel(cl)

  tmp.dat <- foreach(j = 1:n.models,  .combine='rbind', .packages='nimb
le')  %dopar% {

    mod <- nimbleMCMC(code = metapop.fit,
                      constants = consts.list[[j]],
                      data = data,
                      inits = inits,
                      monitors = params,
                      niter = 30000,
                      nburnin = 10000,
                      thin = 1,
                      nchains = 1,
                      summary = TRUE,
                      WAIC = FALSE,
```

```
                      check = FALSE,
                      samplesAsCodaMCMC = TRUE)

    # put the data in the frames
    # c("mean", "median", "SD", "CI025","CI975","model")
    # here we have hard coded the number of parameters (3), but you cou
ld replace these with n.params as well
    tmp <- data.frame(mean = mod$summary[1:3,1],
                      median = mod$summary[1:3,2],
                      SD = mod$summary[1:3,3],
                      CI025 = mod$summary[1:3,4],
                      CI975 = mod$summary[1:3,5],
                      model = rep(c("N", "AZ", "Z", "A", "U")[j],3),
                      parameter = rev(params),
                      iteration = rep(i,3))
    tmp
  }
  out.ests <- rbind(out.ests,tmp.dat)
  rownames(out.ests) <- NULL
  stopCluster(cl)
  #save(out.ests, file=paste0("disrupted_modelrun_",n.years,"years_",n.
patches,"patches.RData")) # initial settins, but A:N interrupted
  save(out.ests, file=paste0(file.path,"modelrun_",n.years,"years_",n.p
atches,"patches.RData")) # initial settings, and A:N preserved
}

end_time <- Sys.time()
end_time - start_time
```

APPENDIX B

CHAPTER 1. EXPANDED VISUALIZATIONS OF SIMULATION OUTPUT

INCLUDING COVERAGE AND BIAS FOR MODEL PARAMETERS SIGMA

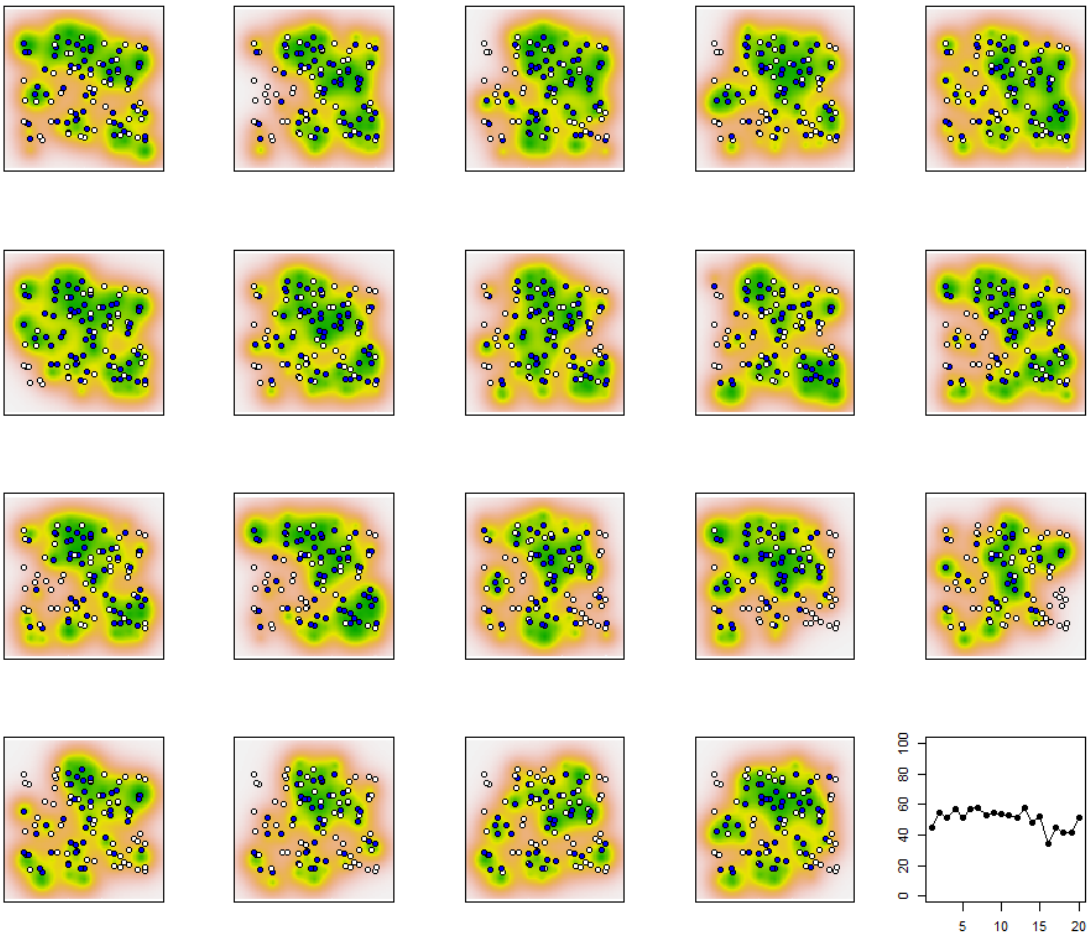

Appendix Figure 1: Example simulation of landscape, occupancy states (white= unoccupied, blue=occupied), and the demographically-weighted connected that emerges between patches for years 2:20 in a simulation run. Darker green is higher connectivity with orange/khaki being the lower connectivity with white being of the least or no connectivity. The bottom right panel represents the average number of occupied patches throughout the time period of this simulated iteration of the landscape and population. These plots may be made with the bespoke simulation function provided in Appendix 1 associated with this work.

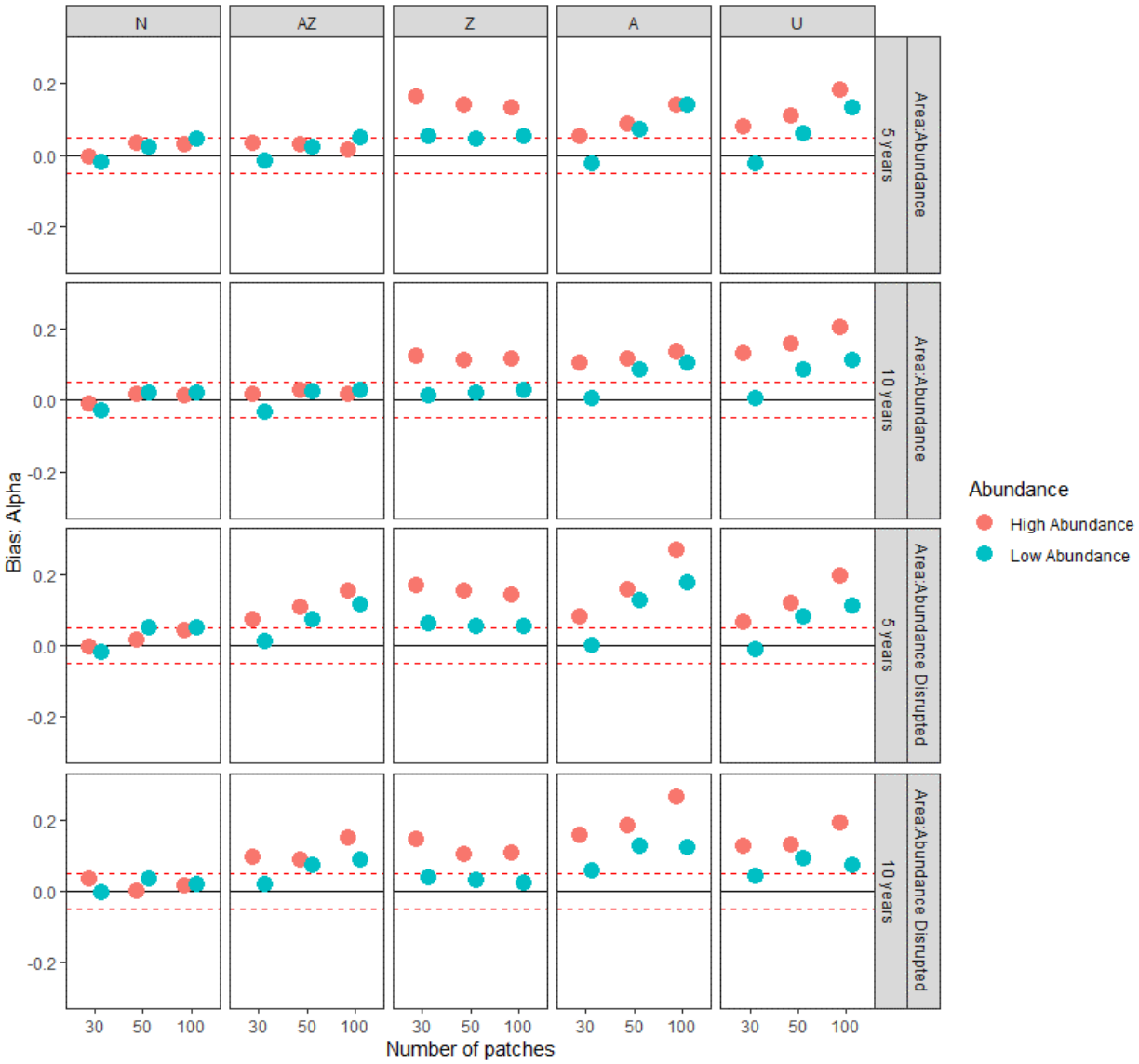

Appendix Figure 2A. Extended figure for bias in estimated metapopulation model mean dispersal parameter alpha (α). Notice that as the relationship to patch area and patch population is disrupted, i.e. made weaker, the accumulation of bias is generally more. As well, only scenarios that directly model population abundance do well across all combinations of years and patch network size.

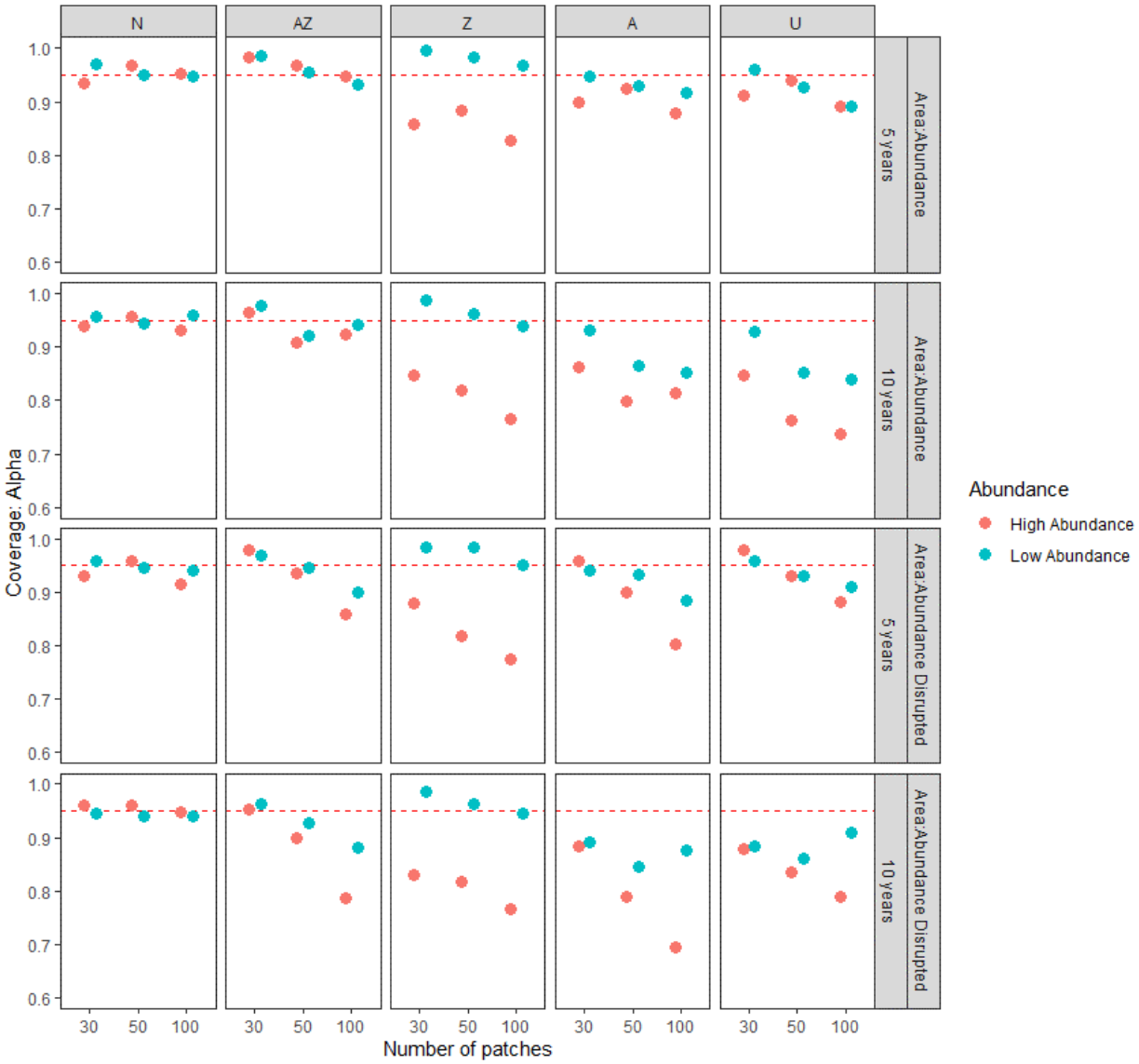

Appendix Figure 2B. The amount of coverage that accumulated across iterations when recovering the alpha (α) value representing mean dispersal. Again, using abundance to model connectivity and dispersal allows a reasonable coverage across all scenarios. However, coverage greatly reduces as the data accumulates, especially as the relationship between patch area and patch population size breaks down.

APPENDIX D

CHAPTER 2: CODE

Overview

Drake, J. C., Lambin, X., and Sutherland, C. 2021. Spatiotemporal connectivity dynamics in spatially structured populations. IN PREP 000: 000-000

Supplemental information referred to as Appendix S1 in text, including 1) NIMBLE code for dynamic metapopulation code with prior distribution details 2) R code for execution of model, and 3) GVS model selection script

Nimble Dynamic Metapopulation Model

Save this as a separate R script named "nimblecode.R" so that it can be sourced by execution script.

```
#####################################################################
#  A Dynamic Col-Ext metapopulation model SPOM
#  Data:
#    Area: a vector of patch sizes
#    dmat: npatch x npatch distance matrix
#    Y: npatch x nyears matrix of detection FREQUENCIES
#    K: npatch x t matrix of number of VISITS
#    z: npatch X nyear matrix of occupancy (1 or NA)
#    nsite: numnber of patches
#    nyear: numnber of years

flexispom <- nimbleCode({

  #~~~~~~~~PRIORS~~~~~~~~~~~~~~~~~~~~~~~~~~~~~~~~~~~~~~~~~~~~~~~~~~~~~~~~~~~#

  #PSI1 prior
  psi1 ~ dunif(0,1)

  # Detection prior

  p_mu ~ dnorm(0,0.001)
  p_sd ~ dunif(0,10)
  p_tau <- pow(p_sd, -2)
  for(t in 1:(nyear.obs)){
    P_t[t] ~ dnorm(p_mu, p_tau)
    logit(p_t[t]) <- P_t[t]
  }

  # Connectivity model priors
```

```
  b1_mu ~ dnorm(0, 0.01)
  b1_sd ~ dunif(0,10)
  b1_tau <- pow(b1_sd, -2)

  alpha_mu ~ dnorm(0, 0.01)
  alpha_sd ~ dunif(0, 10)
  alpha_tau <- pow(alpha_sd, -2)


  for(t in 1:(nyear.sim-1)){

    Alpha[t] ~ dnorm(0, alpha_tau)
    alpha[t] <- alpha_mu + c.dyn*Alpha[t]
    sigterm[t] <- 1/(exp(alpha[t]))  # sigterm is mean dispersal distan
ce

    B1_t[t] ~ dnorm(0, b1_tau)
    b1_t[t] <- exp(b1_mu + c.dyn*B1_t[t])

  }

  # Extinction model priors
  # logit(ext) = g0 + g1 * Area
  g0_mu ~ dnorm(0, 0.01)
  g0_sd ~ dunif(0,10)
  g0_tau <- pow(g0_sd, -2)
  g1_mu ~ dnorm(0, 0.01)
  g1_sd ~ dunif(0,10)
  g1_tau <- pow(g0_sd, -2)

  #time specific random transition parameters
  for(t in 1:(nyear.sim-1)){
    G0_t[t] ~ dnorm(0, g0_tau)
    G1_t[t] ~ dnorm(0, g1_tau)
    g0_t[t] <- g0_mu + e.dyn*G0_t[t]
    g1_t[t] <- g1_mu + e.dyn*G1_t[t]
  }


  #~~~~~~~Likelihood~~~~~~~~~~~~~~~~~~~~~~~~~~~~~~~~~~~~~~~~~~~~~~~~~~~~~~~~#

  for(i in 1:nsite){          #initial occupancy t0
    z[i,1] ~ dbern(psi1)
  }

  for(k in 2:nyear.sim){      #for occupancy t1 and after
    for(i in 1:nsite){
      for(j in 1:nsite){
        con[i,j,k-1] <- exp(-sigterm[k-1] * dmat[i,j]) * #kernel
```

```
                        (1 - equals(i,j)) *            #self
                        max(z[j,k-1], struct) *        #functional weig
ht
                        Area[j]                        #area weight con
trib
      }

      #transition probs
      conx[i,k-1] <- sum(con[i,1:nsite,k-1])

      col[i,k-1] <- 1-exp(-b1_t[k-1]*conx[i,k-1]) #  akin to Sutherland
et al. 2014 to help with model convergence
      logit(ext[i,k-1]) <- g0_mu + g1_mu * Area[i]

      #occupancy
      mu.z[i,k-1] <- z[i,k-1] * max(0.001, min((1-ext[i,k-1]), 0.999))
+
                     (1 - z[i,k-1]) * max(0.001, min(col[i,k-1],  0.999
)) # min-max trick to prevent calculation issues
      z[i,k] ~ dbern(mu.z[i,k-1])
    }
  }
  #### observation model
  for(i in 1:nsite){
    for (t in 1:nyear.obs){
      mu.p[i, t] <- z[i,t] * p_t[t]
      Y[i, t] ~ dbin(mu.p[i, t], K[i,t])
    }
  }
  #### Derived parameters
  for(t in 1:nyear.sim){
    m.occ[t] <- sum(z[1:nsite,t])
    }

})
```

R Script for Model Execution

```
library(nimble)

## the "Drake_etal_2020_ecology.RData object is available as a suppleme
nt
## download and place in your working directory, then load using:

load("Drake_etal_2020_ecology.RData")


#  Data:
#    Area: a vector of patch sizes
#    dmat: npatch x npatch distance matrix
```

```
#    Y: npatch x nyears matrix of detection FREQUENCIES
#    K: npatch x t matrix of number of VISITS
#    z: npatch X nyear matrix of occupancy (1 or NA)
#    nsite: numnber of patches
#    nyear: numnber of years



data <- list(Area=Area, #
             Y=Y,       #
             K=K,       #
             dmat=dmat, #
             z=z)       #

#1. struct. connectivity (nwork position only) + static effect (beta_t
= beta)  (model UI)
#2. struct. connectivity (nwork position only) + dynamic effect (beta_t
)        (model UV)
#3. funct. connectivity (z-weighted) + static effect (beta_t = beta)
(model DI)
#4. funct. connectivity (z-weighted) + dynamic effect (beta_t)
(model DV)

#1 and 2 are *non*-demographic or demographically naive
#3 and 4 are demographic connectivity

#model 1
sta.consts.struct <- list(nyear.obs=nyear.obs,
                  nyear.sim=nyear.sim,
                  nsite=nsite,
                  c.dyn=0,  #0=invariant, 1=time-varying
                  e.dyn=0,  #0=invariant, 1=time-varying
                  struct=1) #1=structural, 0=functional

#model 2
dyn.consts.struct <- list(nyear.obs=nyear.obs,
                  nyear.sim=nyear.sim,
                  nsite=nsite,
                  c.dyn=1,
                  e.dyn=0,
                  struct=1) #1=structural, 0=functional

#model 3
sta.consts <- list(nyear.obs=nyear.obs,
                  nyear.sim=nyear.sim,
                  nsite=nsite,
                  c.dyn=0,
                  e.dyn=0,
                  struct=0) #1=structural, 0=functional
```

```
#model 4
dyn.consts <- list(nyear.obs=nyear.obs,
                   nyear.sim=nyear.sim,
                   nsite=nsite,
                   c.dyn=1,
                   e.dyn=0,
                   struct=0) #1=structural, 0=functional


# Parameters to track
params <- c("alpha","b1_t","m.occ","sigterm", "Alpha", "alpha_mu", "b1_
mu", "B1_t")


inits <- function(){
    list( psi1=runif(1,0.1,0.9),
          p_mu=rnorm(1,0,0.1),
          p_sd=runif(1,0.1,1),
          P_t=rnorm(nyear.obs,0,0.1),

          alpha_mu=rnorm(1,0,0.1),
          alpha_sd=runif(1,0.1,1),
          b1_mu=rnorm(1,0,0.1),
          b1_sd=runif(1,0.1,1),
          B1_t=rnorm(nyear.sim-1,0,0.1),

          g0_mu=runif(1,-1,1),
          g1_mu=rnorm(1,-1,0.1),
          G0_t=rnorm(nyear.sim-1,0,0.1),
          G1_t=rnorm(nyear.sim-1,0,0.1))
}

source("nimblecode.R")


mp_DV <- nimbleMCMC(code=flexispom,
                        constants=dyn.consts,
                        data=data, inits=inits, monitors = params,
                        nchains=3, niter = 80000, nburnin = 30000,   #
80k run 30k burnin
                        thin = 1, summary = TRUE, WAIC =FALSE,
                        check= TRUE, samples = TRUE, samplesAsCodaMCMC
=TRUE)
save(mp_DV, file=paste("mp_DV",format(Sys.time(), "%Y%m%d"), ".RData",
sep=""))


mp_UV <- nimbleMCMC(code=flexispomv,
                        constants=dyn.consts.struct,
```

```
                          data=data, inits=inits, monitors = params,
                          nchains=3, niter = 80000, nburnin = 30000,
                          thin = 1, summary = TRUE, WAIC = FALSE,
                          check= TRUE, samples = TRUE, samplesAsCodaMCMC
=TRUE)
save(mp_UV, file=paste("mp_UV",format(Sys.time(), "%Y%m%d"), ".RData",
sep=""))


mp_DI  <- nimbleMCMC(code=flexispom,
                          constants=sta.consts,
                          data=data, inits=inits, monitors = params,
                          nchains=3, niter = 80000, nburnin = 30000,
                          thin = 1, summary = TRUE, WAIC = FALSE,
                          check= TRUE, samples = TRUE, samplesAsCodaMCMC
=TRUE)
save(mp_DI, file=paste("mp_DI",format(Sys.time(), "%Y%m%d"), ".RData",
sep=""))


mp_UI  <- nimbleMCMC(code=flexispom,
                          constants=sta.consts.struct,
                          data=data, inits=inits, monitors = params,
                          nchains=3, niter = 80000, nburnin = 30000,
                          thin = 1, summary = TRUE, WAIC = FALSE,
# Use params2 for WAIC=TRUE
                          check= TRUE, samples = TRUE, samplesAsCodaMCMC
=TRUE)
save(mp_UI, file=paste("mp_UI",format(Sys.time(), "%Y%m%d"), ".RData",
sep=""))
```

Nimble GVS model selection Script

Save this as a separate R script named “gvscode.R” so that it can be sourced by execution script.

```
modelselection <- nimbleCode({

  #~~~~~~~PRIORS~~~~~~~~~~~~~~~~~~~~~~~~~~~~~~~~~~~~~~~~~~~~~~~~~~~~~~~~#

  #PSI1 prior
  psi1 ~ dunif(0,1)

  pick ~ dcat(probs[1:4])

  mod <- equals(pick,1) * 1  +
         equals(pick,2) * 2  +
         equals(pick,3) * 3  +
         equals(pick,4) * 4
```

```
 structural <- mod.binary[mod,1] #
 c.dyn  <- mod.binary[mod,2]

 #detection prior
 p_mu ~ dnorm(0,0.001)
 p_sd ~ dunif(0,10)
 p_tau <- pow(p_sd, -2)
 for(t in 1:(nyear.obs)){
   P_t[t] ~ dnorm(p_mu, p_tau)
   logit(p_t[t]) <- P_t[t]
 }

 #####connectivity model priors
 b1_mu ~ dnorm(0, 0.01)
 b1_sd ~ dunif(0,10)
 b1_tau <- pow(b1_sd, -2)

 alpha_mu ~ dnorm(0, 0.01)
 alpha_sd ~ dunif(0, 10)
 alpha_tau <- pow(alpha_sd, -2)

for(t in 1:(nyear.sim-1)){

   Alpha[t] ~ dnorm(0, alpha_tau)
   alpha[t] <- alpha_mu + c.dyn*Alpha[t]
   sigterm[t] <- 1/(exp(alpha[t]))

   B1_t[t] ~ dnorm(0, b1_tau)
   b1_t[t] <- exp(b1_mu + c.dyn*B1_t[t])

 }

 # Extinction model priors
 g0_mu ~ dnorm(0, 0.01)
 g0_sd ~ dunif(0,10)
 g0_tau <- pow(g0_sd, -2)
 g1_mu ~ dnorm(0, 0.01)
 g1_sd ~ dunif(0,10)
 g1_tau <- pow(g0_sd, -2)

 #time specific random transition parameters
 for(t in 1:(nyear.sim-1)){
   G0_t[t] ~ dnorm(0, g0_tau)
   G1_t[t] ~ dnorm(0, g1_tau)
   g0_t[t] <- g0_mu + e.dyn*G0_t[t]
   g1_t[t] <- g1_mu + e.dyn*G1_t[t]
 }
```

```
  #~~~~~~~Likelihood~~~~~~~~~~~~~~~~~~~~~~~~~~~~~~~~~~~~~~~~~~~~~~~~~~~~~~~~~~~#

  for(i in 1:nsite){           #initial occupancy t0
    z[i,1] ~ dbern(psi1)
  }

  for(k in 2:nyear.sim){       #for occupancy t1 and after
    for(i in 1:nsite){
      for(j in 1:nsite){
        con[i,j,k-1] <- exp(-sigterm[k-1] * dmat[i,j]) * #kernel
          (1 - equals(i,j)) *                 #self
          max(z[j,k-1], structural) *         #functional weight
          Area[j]                             #area weight contrib
      }

      #transition probs
      conx[i,k-1] <- sum(con[i,1:nsite,k-1])
      col[i,k-1] <- 1-exp(-b1_t[k-1]*conx[i,k-1]) #  akin to Sutherland
et al. 2014 to help with model convergence
      logit(ext[i,k-1]) <- g0_mu + g1_mu * Area[i]

      #occupancy
      mu.z[i,k-1] <- z[i,k-1] * max(0.001, min((1-ext[i,k-1]), 0.999))
+
        (1 - z[i,k-1]) * max(0.001, min(col[i,k-1],  0.999))
      z[i,k] ~ dbern(mu.z[i,k-1])
    }
  }
  #### observation model
  for(i in 1:nsite){
    for (t in 1:nyear.obs){
      mu.p[i, t] <- z[i,t] * p_t[t]
      Y[i, t] ~ dbin(mu.p[i, t], K[i,t])
    }
  }
  #### Derived parameters
  for(t in 1:nyear.sim){
    m.occ[t] <- sum(z[1:nsite,t])
  }
})
```

GVS model selection R script

```
library(nimble)


#  Data:
#    Area: a vector of patch sizes
#    dmat: npatch x npatch distance matrix
```

```
#    Y: npatch x nyears matrix of detection FREQUENCIES
#    K: npatch x t matrix of number of VISITS
#    z: npatch X nyear matrix of occupancy (1 or NA)
#    nsite: numnber of patches
#    nyear: numnber of years

## Model selection matrix

# column 1 = func (0) vs. struc (1)
# column 2 = dynamic = 1, static =0
mod.binary <- matrix(c(1,0,               # struc static  (model UI)
                       1,1,               # struc dynamic (model UV)
                       0,0,               # func  static  (model DI)
                       0,1), 4,2, byrow=TRUE)  # func dynamic (model DV
)


#1. struct. connectivity (nwork position only) + static effect (beta_t
= beta)  (model UI)
#2. struct. connectivity (nwork position only) + dynamic effect (beta_t
)        (model UV)
#3. funct. connectivity (z-weighted) + static effect (beta_t = beta)
(model DI)
#4. funct. connectivity (z-weighted) + dynamic effect (beta_t)
(model DV)

#1 and 2 are *non*-demographic or demographically naive
#3 and 4 are demographic connectivity

data <- list(mod.binary=mod.binary,
             probs=c(0.25,0.25,0.25,0.25),
             Area=Area,
             Y=Y,
             K=K,
             dmat=dmat,
             z=z)



#constants

consts <- list(    mods=as.numeric(c(1,2,3,4)), # the list of models re
ferenced above
                   nyear.obs=nyear.obs, # number of years in data
                   nyear.sim=nyear.sim,
                   nsite=nsite,         # number of sites in data
                   e.dyn=0
                   )
```

```
params <- c("pick") # the parameter to track, which shows which model i
s selected by the GVS process



inits <- function(){
  list( psi1=runif(1,0.1,0.9),
        pick=1,
        p_mu=rnorm(1,0,0.1),
        p_sd=runif(1,0.1,1),
        P_t=rnorm(nyear.obs,0,0.1),

        alpha_mu=rnorm(1,0,0.1),
        alpha_sd=runif(1,0.1,1),
        b1_mu=rnorm(1,0,0.1),
        b1_sd=runif(1,0.1,1),
        B1_t=rnorm(nyear.sim-1,0,0.1),

        g0_mu=runif(1,-1,1),
        g1_mu=rnorm(1,-1,0.1),
        G0_t=rnorm(nyear.sim-1,0,0.1),
        G1_t=rnorm(nyear.sim-1,0,0.1))
}

source("gvs.R")


mp_modelselect <- nimbleMCMC(code=modelselection,
                         constants=consts,
                         data=data, inits=inits2, monitors = params,
                         nchains=3, niter = 110000, nburnin = 10000,
                         thin = 1, summary = TRUE, WAIC = FALSE,
                         check= TRUE, samples = TRUE, samplesAsCodaMCMC
=TRUE)
save(mp_modelselect, file=paste("mp_modselect",format(Sys.time(), "%Y%m
%d"), ".RData", sep=""))
```

APPENDIX D

CHAPTER 2: PARAMETER ESTIMATES

Appendix S2: This appendix contains supplemental information in support of results from Drake et al. (2020). These results are parameter and occupancy estimates for 4 different models assuming various degrees of realism for the connectivity process.

Table S2A. Parameter estimates for four dynamic and spatially-explicit stochastic patch occupancy models. Each model represents various amounts of abstraction for connectivity in the landscape: demographically-weighted and time-varying (DV), unweighted and time-varying (UV), demographically-weighted and time-invariant (DI), & unweighted and time-invariant (UI). Here α - μ represents the raw parameter estimate of the random effects mean of the dispersal scaling factor, while α – 1999 to α – 2011 represents year specific parameter estimate. Notice that time-invariant models do not change. The link function to bring this to kilometers would be $1/e^{\alpha}$ to represent mean dispersal distance. βt - μ represents the random effects mean of the connectivity parameter representing the per capita effective rate of dispersal. βt – 1999 to βt – 2011 represents the year specific value of the per capita rate of dispersal. Also note that time-invariant models do not vary across time. LCI and UCI stand for the lower confidence interval and upper confidence interval respectively.

Parameter	DV Posterior mean	(95% LCI)	(95% UCI)	UV Posterior mean	(95% LCI)	(95% UCI)	DI Posterior mean	(95% LCI)	(95% UCI)	UI Posterior mean	(95% LCI)	(95% UCI)
α - μ	0.638	-0.057	1.321	0.702	-0.144	1.773	0.993	0.458	1.632	4.04	0.249	18.917
α - 1999	0.630	-0.418	1.524	0.707	-0.403	1.946	-	-	-	-	-	-
α - 2000	0.532	-0.669	1.488	0.646	-0.573	1.905	-	-	-	-	-	-
α - 2001	0.779	-0.106	1.812	0.853	-0.239	2.338	-	-	-	-	-	-
α - 2002	0.457	-0.862	1.413	0.504	-0.816	1.758	-	-	-	-	-	-
α - 2003	0.600	-0.279	1.463	0.701	-0.285	1.949	-	-	-	-	-	-
α - 2004	0.520	-0.376	1.333	0.566	-0.489	1.678	-	-	-	-	-	-
α - 2005	0.739	0.176	1.432	0.766	-0.025	1.854	-	-	-	-	-	-
α - 2006	0.916	0.201	1.906	0.985	0.087	2.482	-	-	-	-	-	-
α - 2007	0.576	-0.460	1.447	0.666	-0.429	1.874	-	-	-	-	-	-
α - 2008	0.588	-0.495	1.510	0.596	-0.591	1.853	-	-	-	-	-	-
α - 2009	0.709	0.028	1.473	0.760	-0.041	1.900	-	-	-	-	-	-
α - 2010	0.762	-0.027	1.653	0.818	-0.165	2.141	-	-	-	-	-	-
α - 2011	0.541	-0.460	1.411	0.640	-0.466	1.871	-	-	-	-	-	-
βt - μ	0.124	0.044	0.346	-2.572	-3.846	-1.399	0.103	0.045	0.203	0.054	0.006	0.175
βt - 1999	0.124	0.013	0.363	0.087	0.009	0.281	-	-	-	-	-	-
βt - 2000	0.122	0.012	0.425	0.107	0.007	0.356	-	-	-	-	-	-
βt - 2001	0.233	0.042	0.790	0.147	0.018	0.523	-	-	-	-	-	-

βt - 2002	0.098	0.011	0.347	0.076	0.008	0.288	-	-	-	-	-	-
βt - 2003	0.155	0.030	0.470	0.082	0.013	0.262	-	-	-	-	-	-
βt - 2004	0.120	0.020	0.372	0.066	0.010	0.222	-	-	-	-	-	-
βt - 2005	0.179	0.051	0.441	0.099	0.021	0.266	-	-	-	-	-	-
βt - 2006	0.483	0.099	1.508	0.265	0.046	0.787	-	-	-	-	-	-
βt - 2007	0.123	0.015	0.391	0.088	0.008	0.311	-	-	-	-	-	-
βt - 2008	0.086	0.016	0.266	0.061	0.009	0.208	-	-	-	-	-	-
βt - 2009	0.181	0.056	0.449	0.108	0.024	0.284	-	-	-	-	-	-
βt - 2010	0.367	0.093	1.086	0.267	0.046	0.885	-	-	-	-	-	-
βt - 2011	0.128	0.021	0.413	0.100	0.013	0.352	-	-	-	-	-	-

Table S2B. Mean posterior estimates for occupancy as fraction of the 98 patches in the Assynt metapopulation system for four dynamic and spatially-explicit stochastic patch occupancy models. Each model represents various amounts of abstraction for connectivity in the landscape: demographically-weighted and time-varying (DV), unweighted and time-varying (UV), demographically-weighted and time-invariant (DI), & unweighted and time-invariant (UI). LCI and UCI stand for the lower confidence interval and upper confidence interval respectively.

Occupancy	DV Posterior mean	(95% LCI)	(95% UCI)	UV Posterior mean	(95% LCI)	(95% UCI)	DI Posterior mean	(95% LCI)	(95% UCI)	UI Posterior mean	(95% LCI)	(95% UCI)
1999	0.686	0.531	0.898	0.693	0.531	0.918	0.626	0.520	0.827	0.650	0.531	0.867
2000	0.630	0.531	0.745	0.637	0.531	0.755	0.619	0.531	0.724	0.629	0.531	0.735
2001	0.581	0.449	0.765	0.605	0.469	0.786	0.622	0.531	0.714	0.626	0.531	0.724
2002	0.646	0.561	0.765	0.648	0.561	0.786	0.608	0.551	0.684	0.619	0.561	0.694
2003	0.542	0.459	0.653	0.558	0.459	0.673	0.558	0.480	0.653	0.580	0.490	0.673
2004	0.540	0.469	0.633	0.551	0.480	0.643	0.538	0.469	0.622	0.564	0.490	0.653
2005	0.528	0.480	0.592	0.529	0.480	0.602	0.560	0.500	0.643	0.573	0.500	0.663
2006	0.649	0.592	0.714	0.648	0.592	0.714	0.681	0.622	0.745	0.685	0.622	0.755
2007	0.884	0.847	0.929	0.888	0.847	0.929	0.858	0.827	0.888	0.859	0.827	0.898
2008	0.608	0.561	0.673	0.607	0.551	0.673	0.586	0.551	0.633	0.590	0.551	0.643
2009	0.549	0.510	0.602	0.550	0.510	0.602	0.566	0.520	0.622	0.567	0.520	0.622
2010	0.631	0.602	0.663	0.630	0.602	0.663	0.636	0.612	0.673	0.636	0.602	0.673
2011	0.856	0.837	0.878	0.856	0.837	0.878	0.850	0.837	0.867	0.851	0.837	0.867
2012	0.633	0.571	0.704	0.633	0.571	0.704	0.637	0.582	0.704	0.637	0.582	0.704

APPENDIX E

CHAPTER 2: LANDSCAPE CONNECTIVITY

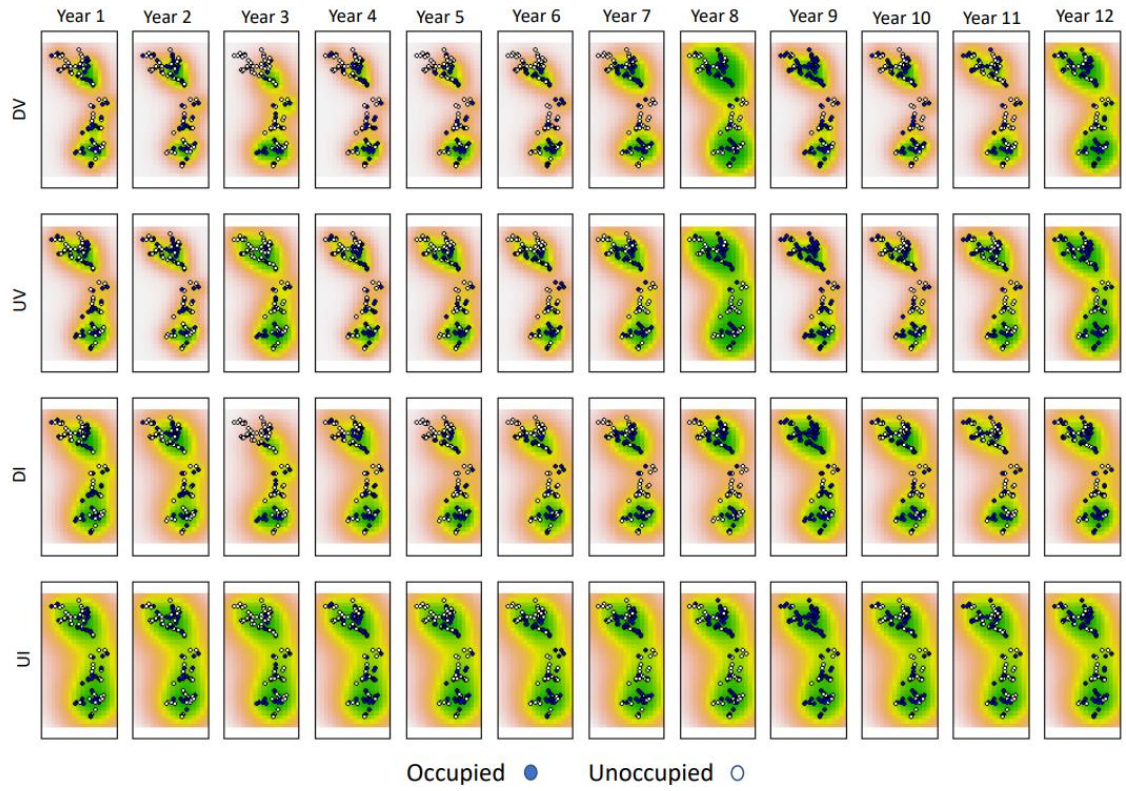

This figure represents the realized connectivity between habitat patches across all 12 scenario years. Demographically-weighted and time-varying connectivity (DV), unweighted and time-varying connectivity (UV), & demographically-weighted and time-invariant connectivity (DI) all contain varying levels of dynamism either accounted through model structure or through the inclusion of demographic data in the form of occupancy state-variables. Unweighted with time-invariant connectivity (UI) shows that no matter the observed occupancy in the landscape, the connectivity fails to shift, representing a structural view of the connectivity in the landscape. DV was the most supported connectivity model based on Bayesian model selection and the model UI was least supported.

APPENDIX F

CHAPTER 3: STUDY AREA

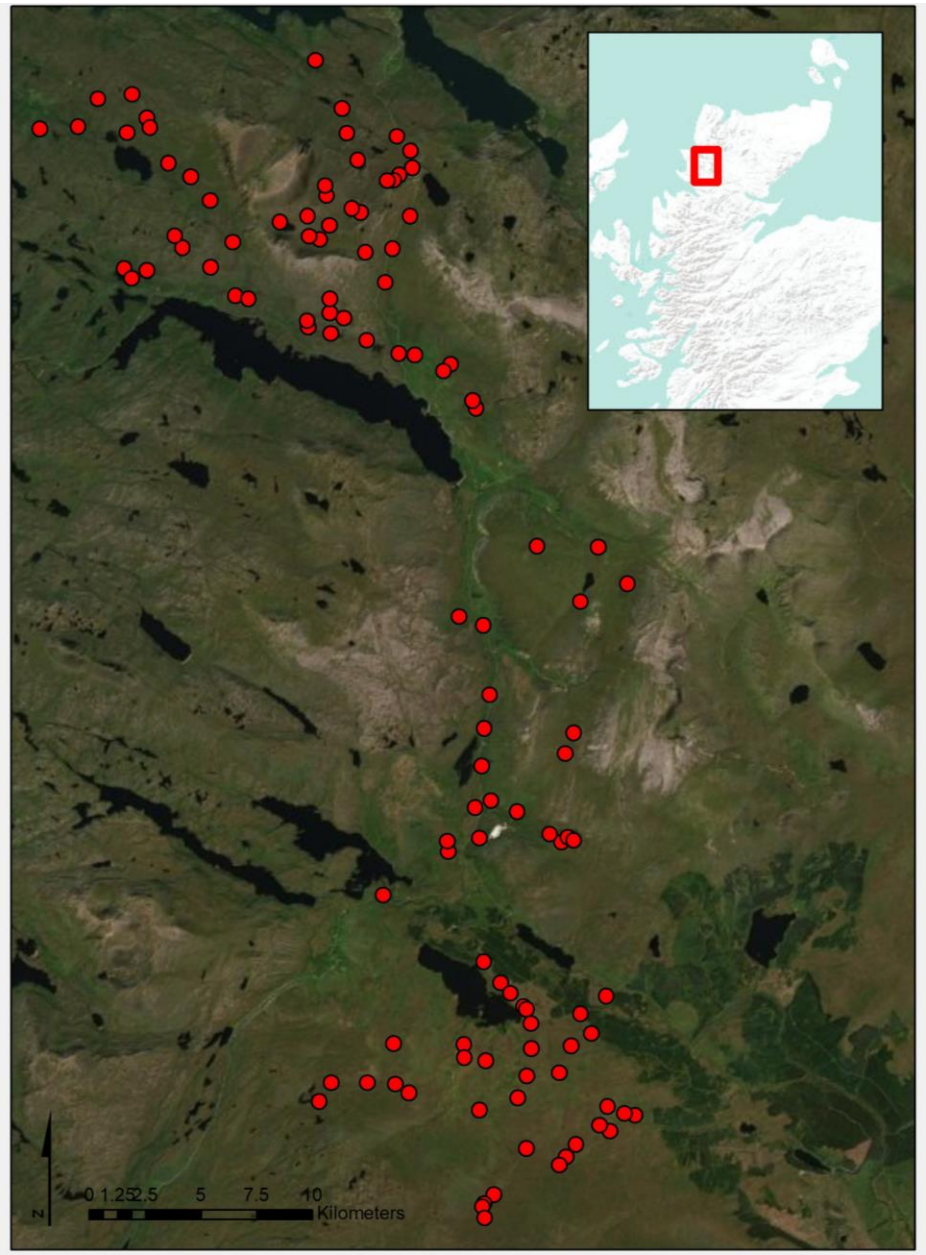

Figure A. Assynt study area in Northwest Scotland. Red dots represent approximate locations of patches in the landscape.

APPENDIX G

CHAPTER 3: TABLE OF NON-INFORMATIVE PRIORS

Prior distributions for parameters estimated in the spatially-explicit stochastic patch occupancy model.

Parameter	Description	Prior
$\boldsymbol{\alpha}$	scale parameter of colonization function	Gamma(0.001, 0.001)
$\boldsymbol{\beta}$	baseline colonization probability	Uniform(-∞,∞)
$\boldsymbol{\delta_0}$	intercept of extinction logit-linear model	Uniform(-10,10)
$\boldsymbol{\delta_1}$	slope of extinction logit-linear model	Uniform(-10,10)
$\boldsymbol{b_0}$	Detection model logit-linear intercept	Norm(0, 10)
$\boldsymbol{b_1}$	Detection model logit-linear slope	Norm(0, 10)
$\boldsymbol{\theta_1}$	linear effect of elevation on landscape resistance	Norm(0, 10)

APPENDIX H

CHAPTER 3: CHAIN CONVERGENCE DIAGNOSTICS

Trace plots and posterior density plots for elevation inclusive model. Models converged with r-hat scores <1.06 for all parameters and most parameters converging with r-hat scores <1.01. All years occupancy estimates converged well, but reduce length and increase clarity, their visualizations are excluded.

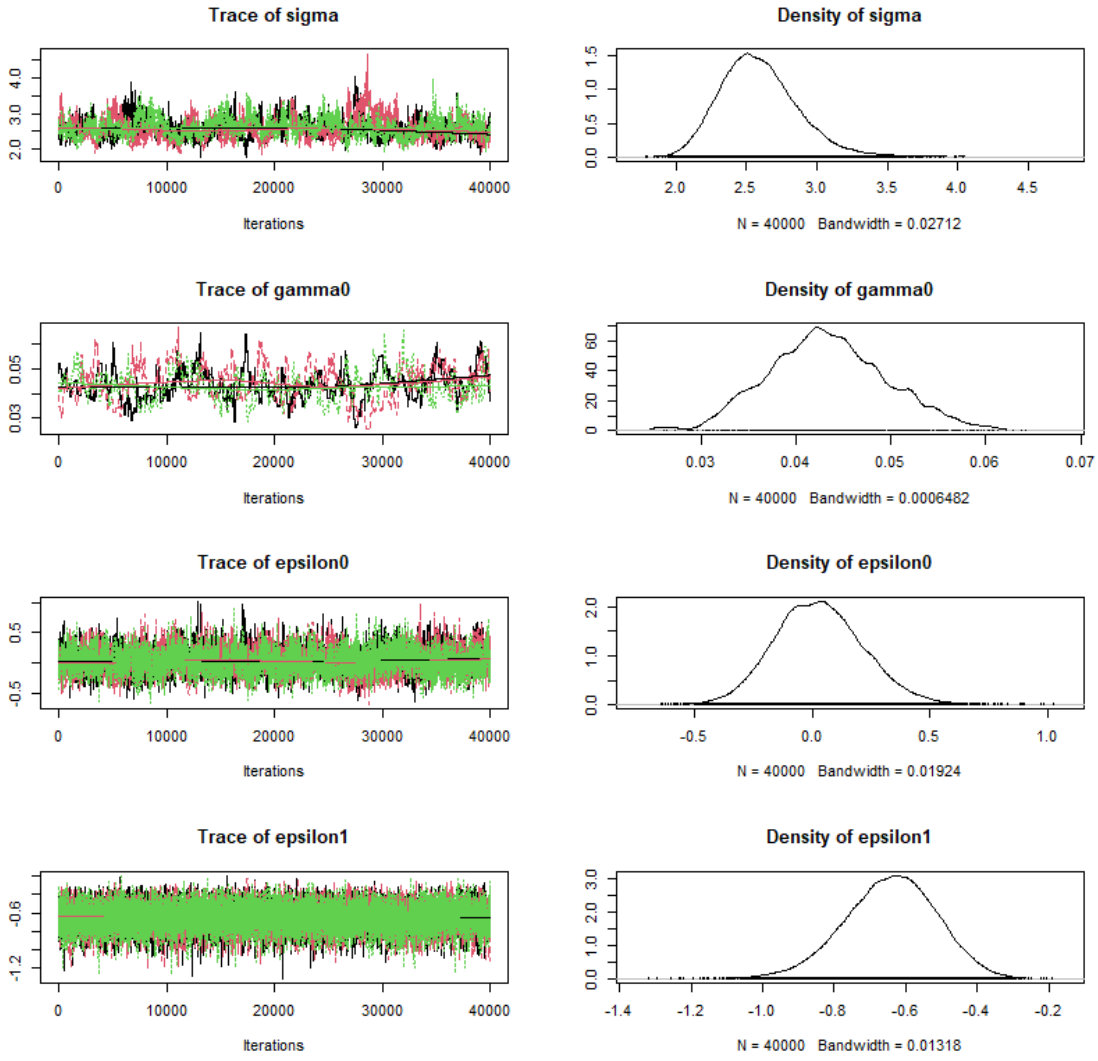

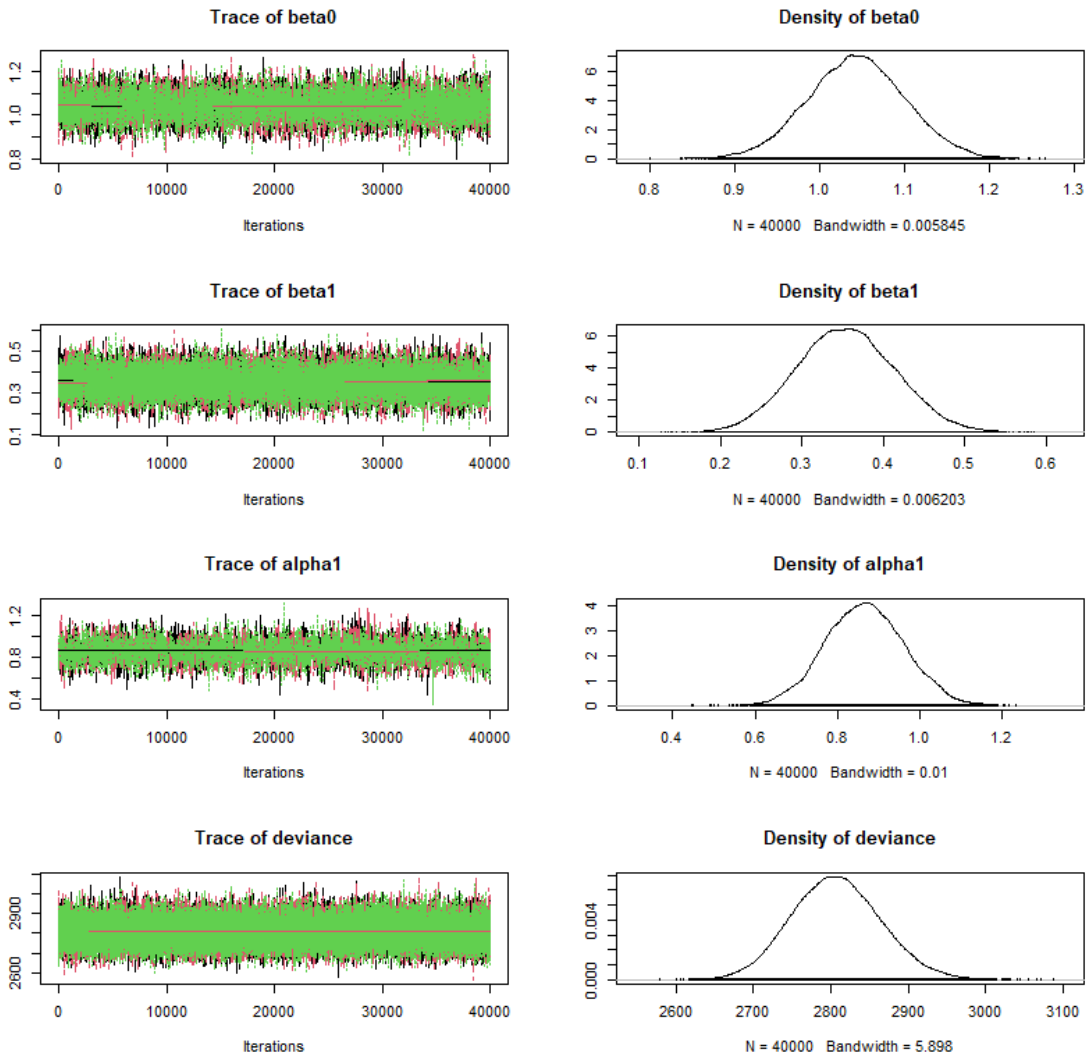
Trace of beta0
Density of beta0
Iterations
N = 40000 Bandwidth = 0.005845
Trace of beta1
Density of beta1
Iterations
N = 40000 Bandwidth = 0.006203
Trace of alpha1
Density of alpha1
Iterations
N = 40000 Bandwidth = 0.01
Trace of deviance
Density of deviance
Iterations
N = 40000 Bandwidth = 5.898

APPENDIX I

CHAPTER 3: R CODE OF THE MODEL

Drake, J. C. 2021. When does the matrix matter? Habitat specialists' potential for generalist dispersal. In: On Spatiotemporal Connectivity Dynamics: Perspectives from a Naturally Fragmented Metapopulation, PhD Dissertation..

Supplemental information of R code for the custom MCMC for spatially-explicit stochastic patch occupancy model that infers landscape resistance from turnover patterns.

Model Code

Save as seperate R file named "resistance_model.R" to use with run code below.

```
# Spatial Metapopulation Model with Landscape Resistance estimation
  # Adapted from code presented by Howell et al. 2018

#Author: Joseph Drake
#Date: 20210610
#

# necessary libraries
library(compiler)

##  Custom algorithm

ResistSPOM <- function( y,          # nSampled x nVisits X nYear array
of detection/non-detection
                        x,          # nSites x 2 matrix of site coordin
ates
                        r.cov1,     # resistance coveriate
                        r.cov2=NULL,
                        r.cov3=NULL,
                        r.cov4=NULL,
                        kernel=2,   # the shape of the kernel
                                      # 1= neg exp, 2 = gaussian/half-n
orm
                        e.cov,      # extinction covariates
                        p.cov1,     # detection covariate
                        nIter=10,   # MCMC iterations
                        tune,       # a vector of tuning parameters = p
roposal candidate distributions widths
                                    # the order ; the proposed values t
o run
                                         #1 sigma;    0.3
```

```
                                          #2 gamma0;   0.01
                                          #3 epsilon0; 0.1
                                          #4 epsilon1; 0.1
                                          #5 beta0;    0.9
                                          #6 beta1;    0.9
                                          #7 alpha[1]; 0.2
                                          #8 alpha[2]; 0.2
                                          #9 alpha[3]; 0.2
                                          #10 alpha[4];0.2
                                          #(10 in total)
                        estAlpha=TRUE,  # TRUE= estimate resistance coe
fficients
                        inits=NULL,     # initial values of candidates,
if null=preset in model
                        zProp=c("ind","vec"), # update z matrix by eith
er proposing z(i,k) or z(,k)
                        zProbs=NULL,    # marix of proposals probs to u
s if zProp="vec"
                        monitor.z=FALSE,# TRUE=store each iteration of
the z matrix
                        report=FALSE,   # only report on model progress
if >0 (TRUE)
                        save=FALSE,     # only save chain in progress i
f >0 (TRUE)
                        plot.z=FALSE,   # Plot the laten presence-absen
ce state (if report=TRUE)
                        tol=0           # Reject proposal of z(i,k=1) i
f mu(i,k-1) < tol
                        )

{

  zProp <- match.arg(zProp)

  ## Dimensions
  nSites <- nrow(x)   # number of all possible sites instead of only sa
mpled sites
  nReps <- ncol(y)
  nYears <- dim(y)[3] # number of slices in array y

  ## Specify sites sampled to calculate likelihoods more efficiently
  nSampled <- nrow(y)
  dataYears <- apply(!is.na(y),3, any) #if sites had any visits during
year, this is included

  anyDetections <- matrix(FALSE, nSites, nYears)
  anyDetections[1:nSampled,] <- apply(y, c(1,3), sum, na.rm=TRUE) > 0

  ## If a site is no longer sampled, because it is destroyed or lost
  known0 <- matrix(FALSE, nSites, nYears)
```

```
  notFailed <- 1 - known0

  if( any( anyDetections & known0 ))
    stop("detection at sampled sites and lost sites do not agree")

  ## containers for the  data
  y.wide <- matrix(y, nSampled)

  epsilon <- rep(NA, nSites) # container for epsilon
  gamma0 <- rep(NA, nSites) # container for gamma0

  # if only one landscape covariate, then these allow model to pass ext
ra resistance parameters
  rc2 <- is.null(r.cov2)
  if(rc2) {
    r.cov2 <- r.cov1
  }

  rc3 <- is.null(r.cov3)
  if(rc3) {
    r.cov3 <- r.cov1
  }

  rc4 <- is.null(r.cov4)
  if(rc4) {
    r.cov4 <- r.cov1
  }

  ## Define initial values (candidate means)
  gamma <- muz <- matrix(NA, nSites, nYears-1)
  if(is.null(inits)) {
    epsilon0 <- rnorm(1) # extinction intercept
    epsilon1 <- rnorm(1) # extinction covariate 1 slope
    epsilon <- plogis(epsilon0 + epsilon1*e.cov)

    sigma <- runif(1, 2, 3) # set initial sigma between 1 and 4
    gamma0 <- runif(1, 0.01,0.3) # set initial gamma0 between 0.01, 0.3

    beta0 <- rnorm(1) # detection intercept
    beta1 <- rnorm(1) # detection covariate 1 slope
    p <- plogis(beta0 + beta1*p.cov1)

    alpha<- c(0,0,0,0)

    z <- matrix(0, nSites, nYears)

    # we are assuming year one has perfectly known sites
    z[,1] <- rowSums(y.pre[,,1], na.rm = TRUE)
    z[,1] <- ifelse(z[,1] >= 1, 1, 0)
```

```
    ## resistance surface initial values
    # create surface
    cost <- exp(alpha[1]*r.cov1 + alpha[2]*r.cov2 + alpha[3]*r.cov3 + a
lpha[4]*r.cov4)
    # calculate conductances among neighbors
    tr1 <- transition(cost, transitionFunction = function(x) 1/mean(x),
directions=8)
    # adjust diag. conductances among neighbors
    tr1CorrC <- geoCorrection(tr1, type="c", multpl=FALSE,scl=FALSE)
    # if calculating LCP

    ## if you are not calculating LCPs/Resistances
    if(!estAlpha)
      alpha <- c(0,0,0,0) #Forcing alpha to be euclidean distances inst
ead of ecological distances

    D<-costDistance(tr1CorrC,x,x)/1000 #from meters to km for easier ca
lc
    G<-gamma0*exp(-D^kernel / (kernel*sigma^kernel) )

    for(k in 2:nYears) {
      PrNotColonizedByNeighbor <- 1 - gamma0*exp(-D^kernel/(kernel*sigm
a^kernel)) * t(z[,rep(k-1, nSites)])
      PrNotColonizedAtAll <- apply(PrNotColonizedByNeighbor, 1, prod)
      gamma[,k-1] <- 1 - PrNotColonizedAtAll
      muz[,k-1] <- z[,k-1]*(1-epsilon*(1-gamma[,k-1])) + (1-z[,k-1])*ga
mma[,k-1] #Rescue effect
      muz[,k-1] <- muz[,k-1]*notFailed[,k] # exclude destroyed sites

      z[,k] <- rbinom(nSites, 1, muz[,k-1])

      z[known0[,k],k] <- 0 # coding in destroyed sites
      z[which(anyDetections[,k]),k] <- 1
    }

  } else {

      gamma0 <- inits$samples["gamma0"]
      sigma <- inits$samples["sigma"]

      epsilon0 <- inits$samples["epsilon0"]
      epsilon1 <- inits$samples["epsilon1"]

      epsilon <- plogis(epsilon0 + epsilon1*e.cov)

      alpha<-c(inits$samples["alpha1"],inits$samples["alpha2"],inits$sa
mples["alpha3"],inits$samples["alpha4"])

      D <- inits$D
```

```
      beta0 <- inits$samples["beta0"]
      beta1 <- inits$samples["beta1"]
      p <- plogis(beta0 + beta1*p.cov1)

      z <- inits$z

      .Random.seed <- inits$seed ## use same random seed as before

    }

  # calculate likelihoods
  ll.z <- matrix(0,nSites,nYears) # container for occupancy
  ll.y <- array(0, c(nSampled, nReps, nYears)) # container for survey d
etection histories

  for(k in 2:nYears){
    PrNotColonizedByNeighbor <- 1 - gamma0*exp(-D^kernel/(kernel*sigma^
kernel  ))*t(z[,rep(k-1, nSites)])
    PrNotColonizedAtAll <- apply(PrNotColonizedByNeighbor, 1, prod)
    gamma[,k-1] <- 1 - PrNotColonizedAtAll
    muz[,k-1] <- z[,k-1]*(1-epsilon*(1-gamma[,k-1])) + (1-z[,k-1])*gamm
a[,k-1]
    muz[,k-1] <- muz[,k-1]*notFailed[,k]
    ll.z[,k-1] <- dbinom(z[,k], 1, muz[,k-1], log=TRUE)
    ll.y[,,k] <- dbinom(y[,,k], 1, z[1:nSampled,k]*p[,,k], log=TRUE)

    }

    ll.z.cand <- ll.z
    ll.z.sum <- sum(ll.z)
    ll.y.cand <- ll.y
    ll.y.sum <- sum(ll.y, na.rm=TRUE)
    gamma.cand <- gamma
    muz.cand <- muz

    nz1 <- z # for computing expected occ at each site
    zkup <- rep(0, nYears-1)

    ## Posterior samples

    nPar <- length(tune) + 1 + nYears + nSites # length of tune = # par
ams being estimated
                                        # +1 for deviance tracking and
then the # of years
                                        # + nSites for zp tracking

    samples <- array(NA, c(nIter, nPar))
    zK <- matrix(NA, nSites, nIter)
```

```
#Tracking the following parameters
colnames(samples) <- c("sigma",
                       "gamma0",
                       "epsilon0",
                       "epsilon1",
                       "beta0",
                       "beta1",
                       "alpha1",
                       "alpha2",
                       "alpha3",
                       "alpha4",
                       paste("zk", 1:nYears, sep=""),
                       "deviance",
                       paste("zp", 1:nSites, sep=""))

reportit <- report>0
saveit <- save>0

nzup <- rep(0, nYears-1)
zA <- NULL

if(monitor.z)
  zA <- array(NA_integer_, c(nSites,nYears,nIter))

if(reportit) {
  cat("iter 1\n")

  cat("    theta =", round(c(sigma,
                             gamma0,
                             epsilon0,
                             epsilon1,
                             beta0,
                             beta1,
                             alpha
                                  ), 5), "\n")


  cat("    z[k] =", round(colSums(z), 2), "\n")
  cat("    ll.z =", round(sum(ll.z), 2), "\n")
  cat("    deviance =", round(-2*ll.y.sum, 2), "\n")
  cat("    time =", format(Sys.time()), "\n")

  cat("    z[k] =", round(colSums(z), 2), "\n")
  cat("    ll.z =", round(sum(ll.z), 2), "\n")
  cat("    deviance =", round(-2*ll.y.sum, 2), "\n")
  cat("    time =", format(Sys.time()), "\n")

  if(plot.z) {
    library(lattice)
    zd <- data.frame(z=as.integer(z), year=factor(rep(1999:2019, ea
```

```
ch=nSites)),
                          x=as.numeric(x[,1])/1000, y=as.numeric(x[,2])/
1000)
        print(xyplot(y~x|year, zd,groups=z,aspect="iso",pch=c(1,16),as.
table=TRUE))
      }
    }

    ## Sample from posteriors
    for(s in 1:nIter) {

      ll.z.sum <- sum(ll.z)

      if(reportit) {
        if(s %in% c(2:100) || s %% report == 0) {
          cat("iter", s, "\n")
          cat("    theta =", round(samples[s-1,1:length(tune)], 5), "\n
")
          cat("    z[k] =", zk, "\n")
          cat("    accepted", round(zkup/(nSites)*100, 1), "percent of
z[k] proposals \n")
          cat("    sum(ll.z) =", ll.z.sum, "\n")
          cat("    deviance =", round(samples[s-1,"deviance"], 2), "\n"
)
          cat("    time =", format(Sys.time()), "\n")
          if(plot.z) {
            library(lattice)
            zd$z <- as.integer(z)
            print(xyplot(y ~ x | year, zd, groups=z, aspect="iso", pch=
c(1,16), as.table=TRUE))
          }
        }
      }


####### Estimating Alpha ########
      if(estAlpha){

        library(gdistance)

        ## resistance covariate 1

        # Metropolis update for alpha
        alpha1.cand <- rnorm(1, alpha[1], tune[7])
        # create resistance surface
        cost <- exp(alpha1.cand*r.cov1 + alpha[2]*r.cov2 + alpha[3]*r.c
ov3 + alpha[4]*r.cov4)
        ## calculate conductances among neighbors
        tr1 <- transition(cost, transitionFunction=function(x) 1/mean(x
), directions=8)
```

```
        tr1CorrC <- geoCorrection(tr1, type="c", multpl=FALSE,scl=FALSE
) #adjust diag.conductances
        ## calculate least cost distance between all pairs of sites.
        D.cand <- costDistance(tr1CorrC,x,x)/1000
        G.cand <- gamma0*exp(-D.cand^kernel / (kernel*sigma^kernel) )

        for(k in 2:nYears){
          zkt <- matrix(z[,k-1], nSites, nSites, byrow=TRUE)
          gamma.cand[,k-1] <- 1 - exp(rowSums(log(1-G.cand*zkt)))
          muz.cand[,k-1] <- (z[,k-1]*(1-epsilon*(1-gamma.cand[,k-1])) +
(1-z[,k-1])*gamma.cand[,k-1])*notFailed[,k]
          ll.z.cand[,k-1] <- dbinom(z[,k], 1, muz.cand[,k-1], log=TRUE)
        }

        prior.alpha.cand <- dnorm(alpha1.cand, 0, 10, log=TRUE)
        prior.alpha <- dnorm(alpha[1], 0, 10, log=TRUE)

        ll.z.sum.cand <- sum(ll.z.cand)
        # accept or reject candidate update
        if(runif(1) < exp((ll.z.sum.cand + prior.alpha.cand) -
                          (ll.z.sum + prior.alpha))) {

          alpha[1] <- alpha1.cand
          D <- D.cand
          G <- G.cand
          gamma <- gamma.cand
          muz <- muz.cand
          ll.z <- ll.z.cand
          ll.z.sum <- ll.z.sum.cand
        }

        ## resistance covariate 2
        if(!rc2) {
        alpha2.cand <- rnorm(1, alpha[2], tune[8])
        cost <- exp(alpha[1]*r.cov1 + alpha2.cand*r.cov2 + alpha[3]*r.c
ov3 + alpha[4]*r.cov4)
        tr1 <- transition(cost, transitionFunction=function(x) 1/mean(x
), directions=8)
        tr1CorrC <- geoCorrection(tr1, type="c", multpl=FALSE,scl=FALSE
)
        D.cand <- costDistance(tr1CorrC,x,x)/1000
        G.cand <- gamma0*exp(-D.cand^kernel/ (kernel*sigma^kernel) )

        for(k in 2:nYears) {
          zkt <- matrix(z[,k-1], nSites, nSites, byrow=TRUE)
          gamma.cand[,k-1] <- 1 - exp(rowSums(log(1-G.cand*zkt)))
          muz.cand[,k-1] <- (z[,k-1]*(1-epsilon*(1-gamma.cand[,k-1])) +
(1-z[,k-1])*gamma.cand[,k-1])*notFailed[,k]
          ll.z.cand[,k-1] <- dbinom(z[,k], 1, muz.cand[,k-1], log=TRUE)
        }
```

```
        prior.alpha.cand <- dnorm(alpha2.cand, 0, 10, log=TRUE)
        prior.alpha <- dnorm(alpha[2], 0, 10, log=TRUE)

        ll.z.sum.cand <- sum(ll.z.cand)
        if(runif(1) < exp((ll.z.sum.cand + prior.alpha.cand) -
                          (ll.z.sum + prior.alpha))) {
          alpha[2] <- alpha2.cand
          D <- D.cand
          G <- G.cand
          gamma <- gamma.cand
          muz <- muz.cand
          ll.z <- ll.z.cand
          ll.z.sum <- ll.z.sum.cand
        }
      }

      ## resistance covariate 3
      if(!rc3) {
        alpha3.cand <- rnorm(1, alpha[3], tune[9])
        cost <- exp(alpha[1]*r.cov1 + alpha[2]*r.cov2 + alpha3.cand*r.c
ov3 + alpha[4]*r.cov4)
        tr1 <- transition(cost, transitionFunction=function(x) 1/mean(x
), directions=8)
        tr1CorrC <- geoCorrection(tr1, type="c", multpl=FALSE,scl=FALSE
)
        D.cand <- costDistance(tr1CorrC,x,x)/1000
        G.cand <- gamma0*exp(-D.cand^kernel/ (kernel*sigma^kernel) )

        for(k in 2:nYears) {
          zkt <- matrix(z[,k-1], nSites, nSites, byrow=TRUE)
          gamma.cand[,k-1] <- 1 - exp(rowSums(log(1-G.cand*zkt)))
          muz.cand[,k-1] <- (z[,k-1]*(1-epsilon*(1-gamma.cand[,k-1])) +
(1-z[,k-1])*gamma.cand[,k-1])*notFailed[,k]
          ll.z.cand[,k-1] <- dbinom(z[,k], 1, muz.cand[,k-1], log=TRUE)
        }

        prior.alpha.cand <- dnorm(alpha3.cand, 0, 10, log=TRUE)
        prior.alpha <- dnorm(alpha[3], 0, 10, log=TRUE)

        ll.z.sum.cand <- sum(ll.z.cand)
        if(runif(1) < exp((ll.z.sum.cand + prior.alpha.cand) -
                          (ll.z.sum + prior.alpha))) {
          alpha[3] <- alpha3.cand
          D <- D.cand
          G <- G.cand
          gamma <- gamma.cand
          muz <- muz.cand
          ll.z <- ll.z.cand
          ll.z.sum <- ll.z.sum.cand
```

```
        }
      }

      ## resistance covariate 4

      if(!rc4) {
        alpha4.cand <- rnorm(1, alpha[4], tune[10])
        cost <- exp(alpha[1]*r.cov1 + alpha[2]*r.cov2 + alpha[3]*r.cov3
+ alpha4.cand*r.cov4)
        tr1 <- transition(cost, transitionFunction=function(x) 1/mean(x
), directions=8)
        tr1CorrC <- geoCorrection(tr1, type="c", multpl=FALSE,scl=FALSE
)
        D.cand <- costDistance(tr1CorrC,x,x)/1000
        G.cand <- gamma0*exp(-D.cand^kernel/ (kernel*sigma^kernel) )

        for(k in 2:nYears) {
          zkt <- matrix(z[,k-1], nSites, nSites, byrow=TRUE)
          gamma.cand[,k-1] <- 1 - exp(rowSums(log(1-G.cand*zkt)))
          muz.cand[,k-1] <- (z[,k-1]*(1-epsilon*(1-gamma.cand[,k-1])) +
(1-z[,k-1])*gamma.cand[,k-1])*notFailed[,k]
          ll.z.cand[,k-1] <- dbinom(z[,k], 1, muz.cand[,k-1], log=TRUE)
        }

        prior.alpha.cand <- dnorm(alpha4.cand, 0, 10, log=TRUE)
        prior.alpha <- dnorm(alpha[4], 0, 10, log=TRUE)

        ll.z.sum.cand <- sum(ll.z.cand)
        if(runif(1) < exp((ll.z.sum.cand + prior.alpha.cand) -
                          (ll.z.sum + prior.alpha))) {
          alpha[4] <- alpha4.cand
          D <- D.cand
          G <- G.cand
          gamma <- gamma.cand
          muz <- muz.cand
          ll.z <- ll.z.cand
          ll.z.sum <- ll.z.sum.cand
        }
      }
    }

####### Metropolis updates for other model parameters ########

    ## Metropolis update for sigma
    sigma.cand <- rnorm(1, sigma, tune[1])
    if(sigma.cand > 0) {
      G.cand <- gamma0*exp(-D^kernel/ (kernel*sigma.cand^kernel) )
      for(k in 2:nYears){
        zkt<-matrix(z[,k-1], nSites, nSites, byrow = TRUE)
        gamma.cand[,k-1] <- 1 - exp(rowSums(log(1-G.cand*zkt)))
```

```
        muz.cand[,k-1] <- (z[,k-1]*(1-epsilon*(1-gamma.cand[,k-1])) + (
1-z[,k-1])*gamma.cand[,k-1])* notFailed[,k-1]
        ll.z.cand[,k-1] <- dbinom(z[,k], 1, muz.cand[,k-1], log=TRUE)
      }
      prior.sigma.cand <- dgamma(sigma.cand, 0.001, 0.001)
      prior.sigma <- dgamma(sigma, 0.001, 0.001)


      ll.z.sum.cand <- sum(ll.z.cand)
      if(runif(1) < exp((ll.z.sum.cand + prior.sigma.cand) -
                        (ll.z.sum + prior.sigma))) {
        sigma <- sigma.cand
        gamma <- gamma.cand
        ll.z <- ll.z.cand
        ll.z.sum <- ll.z.sum.cand
        muz <- muz.cand
        G <- G.cand
      }
    }

  ## Metropolis update for gamma0

  prior.gamma0.cand <- prior.gamma0 <- 0

  gamma0.cand <- rnorm(1, gamma0, tune[2])
  if(gamma0.cand > 0 & gamma0.cand < 1 ) {
    G.cand <- gamma0.cand* exp(-D^kernel/ (kernel*sigma^kernel) )
    for( k in 2:nYears) {
      zkt <- matrix(z[,k-1], nSites, nSites, byrow=TRUE)
      gamma.cand[,k-1] <- 1 - exp(rowSums(log(1-G.cand*zkt)))
      muz.cand[,k-1] <-(z[,k-1]*(1-epsilon*(1-gamma.cand[,k-1])) + (1-z
[,k-1])*gamma.cand[,k-1])*notFailed[,k]
      ll.z.cand[,k-1] <- dbinom(z[,k], 1, muz.cand[,k-1], log=TRUE)
    }
    # Alternative priors for gamma0
    # prior.gamma0.cand <-  dunif(gamma0.cand, 0, 1)#, log=TRUE)  # lik
e Sutherland et al. 2012 but constrained
    # prior.gamma0 <- dunif(gamma0.cand, 0, 1)#, log=TRUE)  # like Suth
erland et al. 2012

    ll.z.sum.cand <- sum(ll.z.cand)
    if(runif(1) < exp((ll.z.sum.cand + prior.gamma0.cand) -
                      (ll.z.sum + prior.gamma0))) {

      gamma0 <- gamma0.cand
      gamma <- gamma.cand
      muz <- muz.cand
      ll.z <- ll.z.cand
      ll.z.sum <- ll.z.sum.cand
      G <- G.cand
```

```
    }
  }

  ## Metropolis update for epsilon0
  epsilon0.cand <- rnorm(1, epsilon0,tune[3])
  e.cand <- plogis(epsilon0.cand + epsilon1*e.cov)

  for(k in 2:nYears){
    muz.cand[,k-1] <- z[,k-1]*(1-e.cand*(1-gamma[,k-1])) + (1-z[,k-1])*
gamma[,k-1]
    muz.cand[,k-1] <- muz.cand[,k-1]*notFailed[,k]
    ll.z.cand[,k-1] <- dbinom(z[,k], 1, muz.cand[,k-1], log=TRUE)
  }
  prior.epsilon0.cand <- dunif(epsilon0.cand, -10, 10, log=TRUE) # chan
ged dbeta to dunif following Sutherland et al. 2012
  prior.epsilon0 <- dunif(epsilon0, -10, 10, log=TRUE)
  if(runif(1) < exp((sum(ll.z.cand) + prior.epsilon0.cand) -
                    (sum(ll.z) + prior.epsilon0))) {
    epsilon0 <- epsilon0.cand
    epsilon <- e.cand
    muz <- muz.cand
    ll.z <- ll.z.cand
  }

  ## Metropolis update for epsilon1
  epsilon1.cand <- rnorm(1, epsilon1, tune[4])
  e.cand <- plogis(epsilon0 + epsilon1.cand*e.cov)
  for(k in 2:nYears) {
    muz.cand[,k-1] <- z[,k-1]*(1-e.cand*(1-gamma[,k-1])) + (1-z[,k-1])*
gamma[,k-1]
    muz.cand[,k-1] <- muz.cand[,k-1]*notFailed[,k]
    ll.z.cand[,k-1] <- dbinom(z[,k], 1, muz.cand[,k-1], log=TRUE)
  }
  prior.epsilon1.cand <- dunif(epsilon1.cand, -10, 10, log=TRUE) # chan
ged dbeta to dunif following Sutherland et al. 2012
  prior.epsilon1 <- dunif(epsilon1, -10, 10, log=TRUE)
  if(runif(1) < exp((sum(ll.z.cand) + prior.epsilon1.cand) -
                    (sum(ll.z) + prior.epsilon1))) {
    epsilon1 <- epsilon1.cand
    epsilon <- e.cand
    muz<- muz.cand
    ll.z <- ll.z.cand
  }

###### Update Z #######



  zkup <- rep(0, nYears-1)
  for(k in 2:nYears) {
```

```
    anyDet <- anyDetections[,k]==1
    zknown <- anyDet | !notFailed[,k]

    prop.back <- prop.cand <- 0
    for(i in 1:nSites) {
      if(zknown[i])
        next

      if(z[i,k]<1 & muz[i,k-1]<tol)
        next
      zk.wide <- matrix(z[,k], nSites, nReps)
      zk.cand <- z[,k]
      zk.cand[i] <- 1-z[i,k]
      zk.cand.wide <- matrix(zk.cand, nSites, nReps)

      ll.y.tmp <- 0
      ll.y.cand.tmp <- 0
      if((k > 0) & (i <= nSampled)) {

        ll.y.cand.tmp <- dbinom(y[i,,k], 1, zk.cand[i]*p[i,,k], log=TRU
E)
        ll.y.tmp <- sum(ll.y[i,,k], na.rm=TRUE)
      }
      ## Calc for time t and t +1 as both effect z
      ll.z.cand[i,k-1] <- dbinom(zk.cand[i], 1, muz[i,k-1], log=TRUE)
      ll.z2 <- ll.z2.cand <- 0
      if(k < nYears) {
        zkt.cand <- matrix(zk.cand, nSites, nSites, byrow=TRUE)
        gamma.cand[,k] <- 1 - exp(rowSums(log(1-G*zkt.cand)))
        muz.cand[,k] <- (zk.cand*(1-epsilon*(1-gamma.cand[,k])) + (1-zk
.cand)*gamma.cand[,k])*notFailed[,k+1]
        ll.z.cand[,k] <- dbinom(z[,k+1], 1, muz.cand[,k], log=TRUE)
        ll.z2 <- sum(ll.z[,k])
        ll.z2.cand <- sum(ll.z.cand[,k])
      }
      if(runif(1) < exp((sum(ll.y.cand.tmp, na.rm=TRUE) + ll.z.cand[i,k
-1] +
                         ll.z2.cand + prop.back) -
                        (ll.y.tmp + ll.z[i,k-1] +
                         ll.z2 + prop.cand))) {
        z[,k] <- zk.cand
        ll.z[i,k-1] <- ll.z.cand[i,k-1]
        if(k < nYears) {

          gamma[,k] <- gamma.cand[,k]
          muz[,k] <- muz.cand[,k]
          ll.z[,k] <- ll.z.cand[,k]
        }
        if((i <= nSampled) & (k>0)) {
          ll.y[i,,k] <- ll.y.cand.tmp
```

```
        }
        zkup[k-1] <- zkup[k-1] + 1

    }
  }

}

 nz1 <- nz1+z

 ######## Observation model ######

 ## Metropolis update beta0
 beta0.cand <- rnorm(1, beta0, tune[5])
 p.cand <- plogis(beta0.cand + beta1*p.cov1)
 z.wide <- z[,rep(1:nYears, each=nReps)]
 z.a <- array(z.wide, c(nSites, nReps, nYears))

 ll.y[,,dataYears] <- dbinom(y[,,dataYears], 1, z.a[1:nSampled,,dataYea
rs]*p[,,dataYears], log=TRUE)
 ll.y.cand[,,dataYears] <- dbinom(y[,,dataYears], 1, z.a[1:nSampled,,da
taYears]*p.cand[,,dataYears], log=TRUE)

 prior.beta0.cand <- dnorm(beta0.cand, 0,10, log=TRUE)
 prior.beta0 <- dnorm(beta0, 0, 10, log=TRUE)

 ll.y.sum <- sum(ll.y, na.rm=TRUE)
 ll.y.sum.cand <- sum(ll.y.cand, na.rm=TRUE)

 if(runif(1) < exp((ll.y.sum.cand + prior.beta0.cand) -
                   (ll.y.sum + prior.beta0))) {
   beta0 <- beta0.cand
   p <- p.cand
   ll.y <- ll.y.cand
   ll.y.sum <- ll.y.sum.cand
 }

 ## Metropolis update beta1
 beta1.cand <- rnorm(1, beta1, tune[6])
 p.cand <- plogis(beta0 + beta1.cand*p.cov1)
 z.wide <- z[,rep(1:nYears, each=nReps)]
 z.a <- array(z.wide, c(nSites, nReps, nYears))

 ll.y.cand[,,dataYears] <- dbinom(y[,,dataYears], 1, z.a[1:nSampled,,da
taYears]*p.cand[,,dataYears], log=TRUE)
 prior.beta1.cand <- dnorm(beta1.cand, 0, 10, log=TRUE)
 prior.beta1 <-dnorm(beta1, 0, 10, log=TRUE)

 ll.y.sum.cand <- sum(ll.y.cand, na.rm=TRUE)
 if(runif(1) < exp((ll.y.sum.cand + prior.beta1.cand) -
```

```
                    (ll.y.sum + prior.beta1))) {
   beta1 <- beta1.cand
   p <- p.cand
   ll.y <- ll.y.cand
   ll.y.sum <- ll.y.sum.cand
 }

 ##### Save your samples #####

 zk <- colSums(z)

 zp <- rowSums(z)/nYears

 samples[s,] <- c(sigma,
                  gamma0,
                  epsilon0,
                  epsilon1,
                  beta0,
                  beta1,
                  alpha,
                  zk=zk,
                  deviance=-2*ll.y.sum,
                  zp=zp)
 zK[,s] <- z[,nYears]
 if(monitor.z)
   zA[,,s] <- z

 # can help with problem solving if function throughs an error
 if(saveit) {
   if( s %in% seq(100, nIter, 100)){
     save(samples, file="chains.RData")
   }
 }

} # end of s in 1:nIter

final.state <- list(z=z, D=D, samples=samples[s,])
library(coda)
return(list(samples=samples,
            final.state=final.state,
            zK=zK,
            zA=zA,
            Ez=nz1/nIter,
            seed=.Random.seed))

} # function end


ResistSPOM <- cmpfun(ResistSPOM)
```

Simple Implementation Code

```
# Spatial Metapopulation Model Implementation Code
  # Adapted from code presented by Howell et al. 2018

#Author: Joseph Drake
#Date: 20210610
#


#load libraries
library(raster)
library(gdistance)
library(coda)

##### Load and scale data ######

#site coordinates
  # xy coordinates, nrow=#sites, ncol=2
coords <- read.table("")

#site data
  # vector # sites long
patch.size <- read.table("")

# detection covariate
  # rows=site, cols=detect, slice=year
p.cov1 <- read.table("")


# extinction data
  # here a vector nsites long
e.cov <- read.table("")

# occupancy data
  # rows=site, cols=survey, slice=year
y.pre <- read.table("")

#landscape covariates
  # raster file

r.cov1 <- raster("")
r.cov2 <- raster("")
r.cov3 <- raster("")
r.cov4 <- raster("")

##### Run Code for 3 chains ####

#load mcmc sampler
```

```
source("resistance_model.R")

pre.time.total <- Sys.time()
pre.time <- Sys.time()
# individual chain code, replicate for additional chains and run serial
Chain1 <- ResistSPOM(y=y.pre,    #occupancy data
                x=coords,        # coordinates of patches
                kernel=2,        # shape of dispersal kernal
                                      # 1 = neg exp, 2=half norm
                r.cov1=r.cov1,   # resistance covariates
                #r.cov2=r.cov2,   # NULL if not included
                #r.cov3=r.cov3,   # NULL if not included
                #r.cov4=r.cov4,   # NULL if not included

                e.cov=e.cov,   # extinction covariates

                p.cov1=p.cov1, # detection covariate

                nIter=45000,   #
                inits=NULL,
                monitor.z=FALSE,
                # tune = the width of the proposal distribution
                tune=c(0.5,   #1 sigma
                       0.1,  #2 gamma0
                       0.2,   #3 epsilon0
                       0.2,   #4 epsilon1
                       0.3,   #5 beta0
                       0.2,   #6 beta1
                       0.4,   #7 alpha[1]
                       0.5,   #8 alpha[2]
                       0.5,   #9 alpha[3]
                       0.5    #10 alpha[4]
                          ),
                estAlpha=TRUE,  # TRUE = est landscape resistance
##                zProp="vec", zProbs=Ez,             ## This results in
slooow mixing
                report=10,
                save=TRUE,
                plot.z=FALSE, tol=1e-3)
post.time<-Sys.time()
time.elapsed <- post.time - pre.time
time.elapsed
#save(Chain1, file=paste0("Chain1_",Sys.Date(),".gzip"))


### view output

library(MCMCvis)
```

```
mc1 <- mcmc(Chain1$samples)
mc.list <- mcmc.list(mc1)
MCMCsummary(mc.list,round=2)
```

APPENDIX J

CHAPTER 3: ESTIMATED OCCUPANCY DATA

Table A. Posterior estimate means and 95% credible intervals (CI) for occupancy estimates for both resistance-based and Euclidean-based distances in a novel spatially explicit stochastic patch occupancy model.

Model	Year	Mean	2.5% CI	97.5% CI
Euclidean-Based	2000	0.5029	0.4464	0.5625
	2001	0.5233	0.4554	0.5982
	2002	0.6166	0.5536	0.6875
	2003	0.5837	0.5089	0.6518
	2004	0.5888	0.5179	0.6607
	2005	0.6285	0.5625	0.6964
	2006	0.7291	0.6607	0.7946
	2007	0.8259	0.7768	0.8750
	2008	0.6158	0.5625	0.6696
	2009	0.4796	0.4375	0.5268
	2010	0.6419	0.6071	0.6786
	2011	0.8327	0.8036	0.8571
	2012	0.5909	0.5536	0.6339
	2013	0.6868	0.6339	0.7411
	2014	0.8925	0.8661	0.9196
	2015	0.7372	0.6964	0.7768
	2016	0.7206	0.6786	0.7679
	2017	0.7165	0.6786	0.7589
	2018	0.6958	0.6696	0.7232
	2019	0.4509	0.4196	0.4911
	-			
Resistance-Based	2000	0.5076	0.4464	0.5714
	2001	0.5299	0.4554	0.6071
	2002	0.6255	0.5625	0.6964
	2003	0.5886	0.5179	0.6607
	2004	0.5940	0.5268	0.6607
	2005	0.6313	0.5625	0.6964
	2006	0.7325	0.6696	0.7946
	2007	0.8328	0.7857	0.8750
	2008	0.6155	0.5625	0.6696
	2009	0.4787	0.4375	0.5179
	2010	0.6420	0.6071	0.6786
	2011	0.8339	0.8125	0.8571

	2012	0.5891	0.5536	0.6339
	2013	0.6824	0.6250	0.7411
	2014	0.8923	0.8661	0.9196
	2015	0.7352	0.6964	0.7768
	2016	0.7217	0.6786	0.7679
	2017	0.7181	0.6786	0.7589
	2018	0.6955	0.6696	0.7232
	2019	0.4530	0.4196	0.4911
	-			

APPENDIX K

CHAPTER 4: LINKS TO PUBLISHED APPENDICES

Please see the following links for appendices and supplemental materials hosted on the journal's website: https://besjournals.onlinelibrary.wiley.com/doi/abs/10.1111/1365-2664.13592

Supplemental Material 1:

- https://besjournals.onlinelibrary.wiley.com/action/downloadSupplement?doi=10.1111%2F1365-2664.13592&file=jpe13592-sup-0001-Supinfo.docx
- Containing:
    - Appendix 1
        - eDNA sample-collection information
        - Reference database information
        - eDNA laboratory methods information
    - Table S1
        - Detection non-detection data for species in study areas
    - Table S4
        - Number of reads information
    - Table S5
        - Camera trap detection information
    - Table S6
        - Tissue sample list for mammal local reference database
    - Table S7
        - Reads subtracted for contamination protocols
    - Figure S1
        - Presence and absence of water voles based on survey method
    - Figure S2
        - Water vole latrine example
    - Figure S3
        - Examples of camera trap photos
    - Figure S4
        - Sample site examples
    - Figure S5
        - Bubble graph representing presence-absence in the Peak District Study area

Supplemental Material 2

- https://besjournals.onlinelibrary.wiley.com/action/downloadSupplement?doi=10.1111%2F1365-2664.13592&file=jpe13592-sup-0002-TableS2.xlsx
- Table S2
    - Species identified in water based eDNA samples

Supplemental Material 3

- https://besjournals.onlinelibrary.wiley.com/action/downloadSupplement?doi=10.1111%2F1365-2664.13592&file=jpe13592-sup-0003-TableS3.xlsx
- Table S3
    - Species identified in sedimentary eDNA samples

BIBLIOGRAPHY

Aars, J., J. F. Dallas, S. B. Piertney, F. Marshall, J. L. Gow, S. Telfer, and X. Lambin. 2006. Widespread gene flow and high genetic variability in populations of water voles Arvicola terrestris in patchy habitats. Molecular Ecology 15:1455–1466.

Abrams, J. F., L. A. Hörig, R. Brozovic, J. Axtner, A. Crampton-Platt, A. Mohamed, S. T. Wong, R. Sollmann, D. W. Yu, and A. Wilting. 2019. Shifting up a gear with iDNA: From mammal detection events to standardised surveys. Journal of Applied Ecology 56:1637–1648.

Acevedo, P., J. Ferreres, M. A. Escudero, J. Jimenez, M. Boadella, and J. Marco. 2017. Population dynamics affect the capacity of species distribution models to predict species abundance on a local scale. Diversity and Distributions 23:1008–1017.

Adriaensen, F., J. P. Chardon, G. De Blust, E. Swinnen, S. Villalba, H. Gulinck, and E. Matthysen. 2003. The application of 'least-cost' modelling as a functional landscape model. Landscape and Urban Planning 64:233–247.

Alston, D., D. P. Mallon, and D. Whitely. 2012. The mammals of derbyshire. Page England: Derbyshire Mammal Group and Sorby Natural History Society.

Amarasekare, P. 1998. Allee effects in metapopulation dynamics. The American Naturalist 152:298–302.

Auffret, A. G., Y. Rico, J. M. Bullock, D. A. P. Hooftman, R. J. Pakeman, M. B. Soons, A. Suárez-Esteban, A. Traveset, H. H. Wagner, and S. A. O. Cousins. 2017. Plant functional connectivity – integrating landscape structure and effective dispersal. Journal of Ecology 105:1648–1656.

Baguette, M. 2004. The classical metapopulation theory and the real, natural world: A critical appraisal. Basic and Applied Ecology 5:213–224.

Baguette, M., S. Blanchet, D. Legrand, V. M. Stevens, and C. Turlure. 2013. Individual dispersal, landscape connectivity and ecological networks. Biological Reviews 88:310–326.

Bani, R., M. J. Fortin, R. M. Daigle, and F. Guichard. 2019. Dispersal traits interact with dynamic connectivity to affect metapopulation growth and stability. Theoretical Ecology 12:111–127.

Banks, S. C., D. B. Lindenmayer, S. J. Ward, and A. C. Taylor. 2005. The effects of habitat fragmentation via forestry plantation establishment on spatial genotypic structure in the small marsupial carnivore, Antechinus agilis. Molecular Ecology 14:1667–1680.

Barthold, J. A., A. J. Loveridge, D. W. Macdonald, C. Packer, and F. Colchero. 2016. Bayesian estimates of male and female African lion mortality for future use in population management. Journal of Applied Ecology 53:295–304.

BBC News. 2018. Mystery of pine marten found dead '100 miles from home'. BBC News.

Beier, P., M. L. Hunter, and M. Anderson. 2015. Conserving Natures Stage: Introduction. Conservation Biology 29:613–617.

Beier, P., and R. F. Noss. 2008. Do Habitat Corridors Provide Connectivity? Conservation Biology 12:1241–1252.

Bender, D. J., T. A. Contreras, and L. Fahrig. 1998. Habitat Loss and Population Decline:

A Meta-Analysis of the Patch Size Effect. Ecology 79:517.
Benson, J. F., P. J. Mahoney, J. A. Sikich, L. E. K. Serieys, J. P. Pollinger, H. B. Ernest, and S. P. D. Riley. 2016. Interactions between demography , genetics , and landscape connectivity increase extinction probability for a small population of large carnivores in a major metropolitan area. Proceedings of the Royal Society B: Biological Sciences 283:20160957.
Bertassello, L. E., E. Bertuzzo, G. Botter, J. W. Jawitz, A. F. Aubeneau, J. T. Hoverman, A. Rinaldo, and P. S. C. Rao. 2021. Dynamic spatio-temporal patterns of metapopulation occupancy in patchy habitats. Royal Society Open Science 8:201309.
Berthier, K., M. Galan, J. C. Foltête, N. Charbonnel, and J. F. Cosson. 2005. Genetic structure of the cyclic fossorial water vole (Arvicola terrestris): Landscape and demographic influences. Molecular Ecology 14:2861–2871.
Best, A. S., K. Johst, T. Münkemüller, and J. M. J. Travis. 2007. Which species will succesfully track climate change? The influence of intraspecific competition and density dependent dispersal on range shifting dynamics. Oikos 116:1531–1539.
Betts, M. G., N. L. Rodenhouse, T. Scott Sillett, P. J. Doran, and R. T. Holmes. 2008. Dynamic occupancy models reveal within-breeding season movement up a habitat quality gradient by a migratory songbird. Ecography 31:592–600.
Bishop-Taylor, R., M. G. Tulbure, and M. Broich. 2017. Surface-water dynamics and land use influence landscape connectivity across a major dryland region. Ecological Applications 27:1124–1137.
Bishop-Taylor, R., M. G. Tulbure, and M. Broich. 2018. Evaluating static and dynamic landscape connectivity modelling using a 25-year remote sensing time series. Landscape Ecology 33:625–640.
Blazquez-Cabrera, S., Ö. Bodin, and S. Saura. 2014. Indicators of the impacts of habitat loss on connectivity and related conservation priorities: Do they change when habitat patches are defined at different scales? Ecological Indicators 45:704–716.
Blowes, S. A., and S. R. Connolly. 2012. Risk spreading, connectivity, and optimal reserve spacing. Ecological Applications 22:311–321.
Bonte, D., H. Van Dyck, J. M. Bullock, A. Coulon, M. Delgado, M. Gibbs, V. Lehouck, E. Matthysen, K. Mustin, M. Saastamoinen, N. Schtickzelle, V. M. Stevens, S. Vandewoestijne, M. Baguette, K. Barton, T. G. Benton, A. Chaput-Bardy, J. Clobert, C. Dytham, T. Hovestadt, C. M. Meier, S. C. F. Palmer, C. Turlure, and J. M. J. Travis. 2012. Costs of dispersal. Biological reviews of the Cambridge Philosophical Society 87:290–312.
Bonte, D., S. Masier, and F. Mortier. 2018. Eco-evolutionary feedbacks following changes in spatial connectedness. Current Opinion in Insect Science 29:64–70.
Boulanger, E., A. Dalongeville, M. Andrello, D. Mouillot, and S. Manel. 2020. Spatial graphs highlight how multi-generational dispersal shapes landscape genetic patterns. Ecography:1–13.
Bowler, D. E., and T. G. Benton. 2005. Causes and consequences of animal dispersal strategies: relating individual behaviour to spatial dynamics. Biological Reviews 80:205–225.
Boyer, F., C. Mercier, A. Bonin, Y. Le Bras, P. Taberlet, and E. Coissac. 2016. obitools: A unix-inspired software package for DNA metabarcoding. Molecular Ecology

Resources 16:176–182.
Bradbury, I. R., L. C. Hamilton, M. J. Robertson, C. E. Bourgeois, A. Mansour, and J. B. Dempson. 2014. Landscape structure and climatic variation determine Atlantic salmon genetic connectivity in the Northwest Atlantic. Canadian Journal of Fisheries and Aquatic Sciences 71:246–258.
Brady, M. J., C. A. McAlpine, C. J. Miller, H. P. Possingham, and G. S. Baxter. 2009. Habitat attributes of landscape mosaics along a gradient of matrix development intensity: matrix management matters. Landscape Ecology 24:879–891.
Brennan, A., P. Beytell, O. Aschenborn, P. Du Preez, P. J. Funston, L. Hanssen, J. W. Kilian, G. Stuart-Hill, R. D. Taylor, and R. Naidoo. 2020. Characterizing multispecies connectivity across a transfrontier conservation landscape. Journal of Applied Ecology:1700–1710.
Brost, B. M., B. A. Mosher, and K. A. Davenport. 2018. A model-based solution for observational errors in laboratory studies. Molecular Ecology Resources 18:580–589.
Brown, J. H., and A. Kodric-Brown. 1977. Turnover Rates in Insular Biogeography: Effect of Immigration on Extinction. Ecology 58:445–449.
Brown, L. M., R. K. Fuda, N. Schtickzelle, H. Coffman, A. Jost, A. Kazberouk, E. Kemper, E. Sass, and E. E. Crone. 2017. Using animal movement behavior to categorize land cover and predict consequences for connectivity and patch residence times. Landscape Ecology 32:1657–1670.
Brzeziński, M., P. Ignatiuk, M. Żmihorski, and A. Zalewski. 2018. An invasive predator affects habitat use by native prey: American mink and water vole co-existence in riparian habitats. Journal of Zoology 304:109–116.
Burgess, S. C., K. J. Nickols, C. D. Griesemer, L. A. K. Barnett, A. G. Dedrick, E. V. Satterthwaite, L. Yamane, S. G. Morgan, J. W. White, and L. W. Botsford. 2014. Beyond connectivity: How empirical methods can quantify population persistence to improve marine protected-area design. Ecological Applications 24:257–270.
Cabeza, M., and A. Moilanen. 2001. Design of reserve networks and the persistence of biodiversity. Trends in Ecology and Evolution 16:242–248.
Calabrese, J. M., and W. F. Fagan. 2004. A comparison-shopper's guide to connectivity metrics. Frontiers in Ecology and the Environment 2:529–536.
Carroll, E. L., A. Hall, M. T. Olsen, A. B. Onoufriou, O. E. Gaggiotti, and D. J. Russell. 2020. Perturbation drives changing metapopulation dynamics in a top marine predator. Proceedings. Biological sciences 287:20200318.
Casagrandi, R., and M. Gatto. 1999. A mesoscale approach to extinction risk in fragmented habitats. Nature 400:560–562.
Casagrandi, R., and M. Gatto. 2002. Habitat Destruction, Environmental Catastrophes, and Metapopulation Extinction. Theoretical Population Biology 61:127–140.
Castorani, M. C. N., D. C. Reed, F. Alberto, T. W. Bell, R. D. Simons, K. C. Cavanaugh, D. A. Siegel, and P. T. Raimondi. 2015. Connectivity structures local population dynamics: A long-term empirical test in a large metapopulation system. Ecology 96:3141–3152.
Castorani, M. C. N., D. C. Reed, P. T. Raimondi, F. Alberto, T. W. Bell, K. C. Cavanaugh, D. A. Siegel, and R. D. Simons. 2017. Fluctuations in population fecundity drive variation in demographic connectivity and metapopulation

dynamics. Proceedings of the Royal Society B: Biological Sciences 284:20162086.
Cavanaugh, K. C., D. A. Siegel, P. T. Raimondi, and F. Alberto. 2014. Patch definition in metapopulation analysis: A graph theory approach to solve the mega-patch problem. Ecology 95:316–328.
Ceballos, G., P. R. Ehrlich, A. D. Barnosky, A. García, R. M. Pringle, and T. M. Palmer. 2015. Accelerated modern human-induced species losses: Entering the sixth mass extinction. Science Advances 1:9–13.
Centeno-Cuadros, A., J. Román, M. Delibes, and J. A. Godoy. 2011. Prisoners in their habitat? generalist dispersal by habitat specialists: A case study in Southern water vole (Arvicola sapidus). PLoS ONE 6.
Chandler, R. B., E. Muths, B. H. Sigafus, C. R. Schwalbe, C. J. Jarchow, and B. R. Hossack. 2015a. Spatial occupancy models for predicting metapopulation dynamics and viability following reintroduction. Journal of Applied Ecology 52:1325–1333.
Chandler, R. B., E. Muths, B. H. Sigafus, C. R. Schwalbe, C. J. Jarchow, and B. R. Hossack. 2015b. Spatial occupancy models for predicting metapopulation dynamics and viability following reintroduction. Journal of Applied Ecology 52:1325–1333.
Cilleros, K., A. Valentini, L. Allard, T. Dejean, R. Etienne, G. Grenouillet, A. Iribar, P. Taberlet, R. Vigouroux, and S. Brosse. 2019. Unlocking biodiversity and conservation studies in high-diversity environments using environmental DNA (eDNA): A test with Guianese freshwater fishes. Molecular Ecology Resources 19:27–46.
Clinchy, M., D. T. Haydon, and A. T. Smith. 2002. Pattern does not equal process: what does patch occupancy really tell us about metapopulation dynamics? The American Naturalist 159:351–362.
Clobert, J., M. Baguette, T. G. Benton, J.-F. Le Galliard, J. Cote, T. G. Benton, and J. Bullock. 2012. Dispersal Ecology and Evolution. Page Dispersal Ecology and Evolution. University of Oxford Press, Oxford.
Clobert, J., J. F. Le Galliard, J. Cote, S. Meylan, and M. Massot. 2009a. Informed dispersal, heterogeneity in animal dispersal syndromes and the dynamics of spatially structured populations. Ecology Letters 12:197–209.
Clobert, J., J. F. Le Galliard, J. Cote, S. Meylan, and M. Massot. 2009b. Informed dispersal, heterogeneity in animal dispersal syndromes and the dynamics of spatially structured populations. Ecology Letters 12:197–209.
Compton, B. W., K. McGarigal, S. a. Cushman, and L. R. Gamble. 2007. A resistant-kernel model of connectivity for amphibians that breed in vernal pools. Conservation Biology 21:788–799.
Cote, J., E. Bestion, S. Jacob, J. Travis, D. Legrand, and M. Baguette. 2017. Evolution of dispersal strategies and dispersal syndromes in fragmented landscapes. Ecography 40:56–73.
Cote, J., and J. Clobert. 2007. Social personalities influence natal dispersal in a lizard. Proceedings of the Royal Society B: Biological Sciences 274:383–390.
Cote, J., and J. Clobert. 2010. Risky dispersal: Avoiding kin competition despite uncertainty. Ecology 91:1485–1493.
Cowen, R. K., and S. Sponaugle. 2009. Larval dispersal and marine population connectivity. Annual Review of Marine Science 1:443–466.
Cozzi, G., N. Maag, L. Börger, T. H. Clutton-Brock, and A. Ozgul. 2018. Socially

informed dispersal in a territorial cooperative breeder. Journal of Animal Ecology:1–12.
Crooks, K., and M. Sanjayan. 2006. Connectivity conservation: maintaining connections for nature. Pages 1–19 *in* K. Crooks and M. Sanjayan, editors. Connectivity Conservation. 1st edition. Cambridge University Press, Cambridge.
Cushman, S. A., and E. L. Landguth. 2012. Multi-taxa population connectivity in the Northern Rocky Mountains. Ecological Modelling 231:101–112.
Cushman, S. A., B. Mcrae, F. Adriaensen, P. Beier, M. Shirley, and K. Zeller. 2013. Biological corridors and connectivity. Pages 384–404 Key Topics in Conservation Biology 2.
Cushman, S. A., A. J. Shirk, G. T. Howe, M. A. Murphy, R. J. Dyer, and S. Joost. 2018. Editorial: The Least Cost Path From Landscape Genetics to Landscape Genomics: Challenges and Opportunities to Explore NGS Data in a Spatially Explicit Context. Frontiers in Genetics 9:e.2018.00215.
Daigle, R. M., A. Metaxas, A. C. Balbar, J. Mcgowan, E. A. Treml, C. D. Kuempel, H. P. Possingham, and M. Beger. 2020. Operationalizing ecological connectivity in spatial conservation planning with Marxan Connect. Methods in Ecology and Evolution 11:570–579.
Deiner, K., H. M. Bik, E. Mächler, M. Seymour, A. Lacoursière-Roussel, F. Altermatt, S. Creer, I. Bista, D. M. Lodge, N. de Vere, M. E. Pfrender, and L. Bernatchez. 2017. Environmental DNA metabarcoding: Transforming how we survey animal and plant communities. Molecular Ecology 26:5872–5895.
Deza, A. A., and T. W. Anderson. 2010. Habitat fragmentation, patch size, and the recruitment and abundance of kelp forest fishes. Marine Ecology Progress Series 416:229–240.
Dickson, B. G., C. M. Albano, R. Anantharaman, P. Beier, J. Fargione, T. A. Graves, M. E. Gray, K. R. Hall, J. J. Lawler, P. B. Leonard, C. E. Littlefield, M. L. McClure, J. Novembre, C. A. Schloss, N. H. Schumaker, V. B. Shah, and D. M. Theobald. 2019. Circuit-theory applications to connectivity science and conservation.
Dilts, T. E., P. J. Weisberg, P. Leitner, M. D. Matocq, R. D. Inman, K. E. Nussear, and T. C. Esque. 2016. Multiscale connectivity and graph theory highlight critical areas for conservation under climate change. Ecological Applications 26:1223–1237.
Diniz, M. F., S. A. Cushman, R. B. Machado, and P. De Marco Júnior. 2020. Landscape connectivity modeling from the perspective of animal dispersal. Landscape Ecology 35:41–58.
Dixon, J. D., M. K. Oli, M. C. Wooten, T. H. Eason, J. W. McCown, and D. Paetkau. 2006. Effectiveness of a regional corridor in connecting two Florida black bear populations. Conservation biology : the journal of the Society for Conservation Biology 20:155–62.
Drake, J., K. L. Griffis-Kyle, and N. E. McIntyre. 2017a. Graph theory as an invasive species management tool: case study in the Sonoran Desert. Landscape Ecology 32:1739–1752.
Drake, J., K. Griffis-Kyle, and N. McIntyre. 2017b. Using nested connectivity models to resolve management conflicts of isolated water networks in the Sonoran Desert. Ecosphere 8:e01652.
Drake, J., X. Lambin, and C. Sutherland. 2021a. Spatiotemporal connectivity dynamics in

spatially structured populations. In Review.
Drake, J., X. Lambin, and C. Sutherland. 2021b. The value of considering demographic contributions to connectivity - a review. Ecography Accepted.
Driscoll, D. A., S. C. Banks, P. S. Barton, K. Ikin, P. Lentini, D. B. Lindenmayer, A. L. Smith, L. E. Berry, E. L. Burns, A. Edworthy, M. J. Evans, R. Gibson, R. Heinsohn, B. Howland, G. Kay, N. Munro, B. C. Scheele, I. Stirnemann, D. Stojanovic, N. Sweaney, N. R. Villaseñor, and M. J. Westgate. 2014. The Trajectory of Dispersal Research in Conservation Biology. Systematic Review. PLoS ONE 9:e95053.
Driscoll, D. A., and C. M. Hardy. 2005. Dispersal and phylogeography of the agamid lizard Amphibolurus nobbi in fragmented and continuous habitat. Molecular Ecology 14:1613–1629.
Dunning, J. B., B. J. Danielson, H. R. Pulliam, and I. Ecology. 1992. Ecological Processes That Affect Populations in Complex Landscapes. Oikos 65:169–175.
Van Dyck, H., and M. Baguette. 2005. Dispersal behaviour in fragmented landscapes: Routine or special movements? Basic and Applied Ecology 6:535–545.
Dytham, C., J. M. J. Travis, K. Mustin, and T. G. Benton. 2014. Changes in species' distributions during and after environmental change: Which eco-evolutionary processes matter more? Ecography 37:1210–1217.
Edelsparre, A. H., A. Shahid, and M. J. Fitzpatrick. 2018. Habitat connectivity is determined by the scale of habitat loss and dispersal strategy. Ecology and Evolution 8:5508–5514.
Elliot, N. B., S. A. Cushman, A. J. Loveridge, G. Mtare, and D. W. Macdonald. 2014a. Movements vary according to dispersal stage, group size, and rainfall: The case of the African lion. Ecology 95:2860–2869.
Elliot, N. B., S. A. Cushman, D. W. Macdonald, and A. J. Loveridge. 2014b. The devil is in the dispersers: Predictions of landscape connectivity change with demography. Journal of Applied Ecology 51:1169–1178.
Epps, C. W., J. D. Wehausen, V. C. Bleich, S. G. Torres, and J. S. Brashares. 2007. Optimizing dispersal and corridor models using landscape genetics. Journal of Applied Ecology 44:714–724.
Eriksson, A., F. Elis-Wolff, B. Mehlig, A. Manica, A. Eriksson, F. Elı, and A. Manica. 2014. The emergence of the rescue effect from explicit within- and between-patch dynamics in a metapopulation. Proceedings of The Royal Society Biological Sciences 281:1–8.
van Etten, J. 2017. R package gdistance: Distances and routes on geographical grids. Journal of Statistical Software 76.
Fedriani, J. M., M. Delibes, P. Ferreras, and J. Roman. 2002. Local and landscape habitat determinants of water vole distribution in a patchy Mediterranean environment. Ecoscience 9:11–20.
Ficetola, G. F., J. Pansu, A. Bonin, E. Coissac, C. Giguet-Covex, M. De Barba, L. Gielly, C. M. Lopes, F. Boyer, F. Pompanon, G. Rayé, and P. Taberlet. 2015. Replication levels, false presences and the estimation of the presence/absence from eDNA metabarcoding data. Molecular Ecology Resources 15:543–556.
Fisher, D. O., X. Lambin, and S. M. Yletyinen. 2009. Experimental translocation of juvenile water voles in a Scottish lowland metapopulation. Population Ecology 51:289–295.

Fiske, I., and R. B. Chandler. 2011. unmarked: An R Package for Fitting Hierarchical Models of Wildlife Occurrence and Abundance. Journal of Statistical Software 43.
Fletcher, R. J., M. A. Acevedo, B. E. Reichert, K. E. Pias, and W. M. Kitchens. 2011. Social network models predict movement and connectivity in ecological landscapes. Proceedings of the National Academy of Sciences 108:19282–19287.
Fletcher, R. J., N. S. Burrell, B. E. Reichert, D. Vasudev, and J. D. Austin. 2016. Divergent Perspectives on Landscape Connectivity Reveal Consistent Effects from Genes to Communities. Current Landscape Ecology Reports 1:67–79.
Fletcher, R. J., J. A. Sefair, C. Wang, C. L. Poli, T. A. H. H. Smith, E. M. Bruna, R. D. Holt, M. Barfield, A. J. Marx, and M. A. Acevedo. 2019. Towards a unified framework for connectivity that disentangles movement and mortality in space and time. Ecology Letters 22:1680–1689.
Fobert, E. K., E. A. Treml, and S. E. Swearer. 2019. Dispersal and population connectivity are phenotype dependent in a marine metapopulation. Proceedings of the Royal Society B: Biological Sciences 286:20191104.
Fronhofer, E. A., and F. Altermatt. 2017. Classical metapopulation dynamics and eco-evolutionary feedbacks in dendritic networks. Ecography 40:1455–1466.
Le Galliard, J. F., A. Rémy, R. A. Ims, and X. Lambin. 2012. Patterns and processes of dispersal behaviour in arvicoline rodents. Molecular Ecology 21:505–523.
Gelman, A. 2006. Prior distributions for variance parameters in hierarchical models:515–533.
Gelman, A., J. B. Carlin, H. S. Stern, D. B. Dunson, A. Vehtari, and D. B. Rubin. 2003. Bayesian Data Analysis. Chapman and Hall/CRC.
Gelman, A., D. Simpson, and M. Betancourt. 2017. The prior can often only be understood in the context of the likelihood. Entropy 19:1–13.
Graves, T., R. B. Chandler, J. A. Royle, P. Beier, and K. C. Kendall. 2014. Estimating landscape resistance to dispersal. Landscape Ecology 29:1201–1211.
Greenwood, P. J., and P. Harvey. 1982. The Natal and Breeding Dispersal of Birds. Annual Review of Ecology and Systematics 13:1–21.
Griffen, B. D., and J. M. Drake. 2008. A review of extinction in experimental populations. Journal of Animal Ecology 77:1274–1287.
Guillera-Arroita, G. 2017. Modelling of species distributions, range dynamics and communities under imperfect detection: advances, challenges and opportunities. Ecography 40:281–295.
Guillera-Arroita, G., and J. J. Lahoz-Monfort. 2012. Designing studies to detect differences in species occupancy: Power analysis under imperfect detection. Methods in Ecology and Evolution 3:860–869.
Gupta, A., B. Dilkina, D. J. Morin, A. K. Fuller, J. A. Royle, C. Sutherland, and C. P. Gomes. 2019. Reserve design to optimize functional connectivity and animal density. Conservation Biology 33:1023–1034.
Haddad, N. M., L. A. Brudvig, J. Clobert, K. F. Davies, A. Gonzalez, R. D. Holt, T. E. Lovejoy, J. O. Sexton, M. P. Austin, C. D. Collins, W. M. Cook, E. I. Damschen, R. M. Ewers, B. L. Foster, C. N. Jenkins, A. J. King, W. F. Laurance, D. J. Levey, C. R. Margules, B. A. Melbourne, A. O. Nicholls, J. L. Orrock, D. X. Song, and J. R. Townshend. 2015. Habitat fragmentation and its lasting impact on Earth's ecosystems. Science Advances 1:1–10.

Haddad, N. M., R. D. Holt, R. J. Fletcher, M. Loreau, and J. Clobert. 2016. Connecting models, data, and concepts to understand fragmentation's ecosystem-wide effects. Ecography 40:336–342.
Hänfling, B., L. L. Handley, D. S. Read, C. Hahn, J. Li, P. Nichols, R. C. Blackman, A. Oliver, and I. J. Winfield. 2016. Environmental DNA metabarcoding of lake fish communities reflects long-term data from established survey methods. Molecular Ecology 25:3101–3119.
Hanski, I. 1994. A practical model of metapopulation dynamics. Journal of Animal Ecology 63:151–162.
Hanski, I. 1998. Metapopulation dynamics. Nature 396:41–49.
Hanski, I. 1999. Metapoplution Ecology. Oxford University Press, Oxford.
Hanski, I. 2004. Metapopulation theory, its use and misuse. Basic and Applied Ecology 5:225–229.
Hanski, I., and M. Gilpin. 1991. Metapopulation dynamics: brief history and conceptual domain. Biological Journal of the Linnean Society 42:3–16.
Hanski, I., and M. Gilpin, editors. 1997. Metapopulation Biology: ecology, genetics, and evolution. Academic Press, Inc., San Diego.
Hanski, I., and T. Mononen. 2011. Eco-evolutionary dynamics of dispersal in spatially heterogeneous environments. Ecology Letters 14:1025–1034.
Hanski, I., and O. Ovaskainen. 2000. The metapopulation capacity of a fragmented landscape. Nature 404:755–758.
Hanski, I., and O. Ovaskainen. 2003. Metapopulation theory for fragmented landscapes. Theoretical Population Biology 64:119–127.
Harman, R. R., J. Goddard, R. Shivaji, and J. T. Cronin. 2020. Frequency of occurrence and population-dynamic consequences of different forms of density-dependent emigration. American Naturalist 195:851–867.
Harper, L. R., L. Lawson Handley, A. I. Carpenter, M. Ghazali, C. Di Muri, C. J. Macgregor, T. W. Logan, A. Law, T. Breithaupt, D. S. Read, A. D. McDevitt, and B. Hänfling. 2019. Environmental DNA (eDNA) metabarcoding of pond water as a tool to survey conservation and management priority mammals. Biological Conservation 238.
Hartfelder, J., C. Reynolds, R. A. Stanton, M. Sibiya, A. Monadjem, R. A. McCleery, and R. J. Fletcher. 2020. The allometry of movement predicts the connectivity of communities. Proceedings of the National Academy of Sciences:202001614.
Heinrichs, J. A., J. J. Lawler, and N. H. Schumaker. 2016. Intrinsic and extrinsic drivers of source-sink dynamics. Ecology and Evolution 6:892–904.
Higgins, K., and M. Lynch. 2001. Metapopulation extinction caused by mutation accumulation. Proceedings of the National Academy of Sciences of the United States of America 98:2928–2933.
Hilderbrand, R. H., A. C. Watts, and A. M. Randle. 2005. The myths of restoration ecology. Ecology and Society 10.
Hilty, J., G. L. Worboys, A. Keeley, S. Woodley, B. J. Lausche, H. Locke, M. Carr, I. Pulsford, J. Pittock, J. W. White, D. M. Theobald, J. Levine, M. Reuling, J. E. M. Watson, R. Ament, and G. M. Tabor. 2020. Guidelines for conserving connectivity through ecological networks and corridors. Page (C. Groves, Ed.) Best Practice Protected Area Guidelines Series. IUCN, International Union for Conservation of

Nature.
Hobbs, N. T., and M. B. Hooten. 2015. Bayesian Models: A Statistical Primer for Ecologists:320.
Hofmeester, T. R., J. P. G. M. Cromsigt, J. Odden, H. Andrén, J. Kindberg, and J. D. C. Linnell. 2019. Framing pictures: A conceptual framework to identify and correct for biases in detection probability of camera traps enabling multi-species comparison. Ecology and Evolution 9:2320–2336.
Holman, L. E., M. de Bruyn, S. Creer, G. Carvalho, J. Robidart, and M. Rius. 2019. Detection of introduced and resident marine species using environmental DNA metabarcoding of sediment and water. Scientific Reports 9:1–10.
Holt, R. D. 1992. A Neglected Face of Island Biogeography: The Role of Internal Spatial Dynamics in Area Effects. Theoretical Population Biology 41:354–371.
Hooten, M. B., N. T. Hobbs, and A. M. Ellison. 2015. A guide to Bayesian model selection for ecologists. Ecological Monographs.
Horváth, Z., R. Ptacnik, C. F. Vad, and J. M. Chase. 2019. Habitat loss over six decades accelerates regional and local biodiversity loss via changing landscape connectance. Ecology Letters 22:1019–1027.
Hovel, K. A., and R. N. Lipcius. 2001. Habitat fragmentation in a seagrass landscape: Patch size and complexity control blue crab survival. Ecology 82:1814–1829.
Howell, P. E., B. R. Hossack, E. Muths, B. H. Sigafus, and R. B. Chandler. 2020a. Informing Amphibian Conservation Efforts with Abundance-based Metapopulation Models. Herpetologica 76:240–250.
Howell, P. E., B. R. Hossack, E. Muths, B. H. Sigafus, A. Chenevert-Steffler, and R. B. Chandler. 2020b. A statistical forecasting approach to metapopulation viability analysis. Ecological Applications 30:1–10.
Howell, P. E., E. Muths, B. R. Hossack, B. H. Sigafus, and R. B. Chandler. 2018. Increasing connectivity between metapopulation ecology and landscape ecology. Ecology 99:1119–1128.
Hui, C., N. Roura-Pascual, L. Brotons, R. A. Robinson, and K. L. Evans. 2012. Flexible dispersal strategies in native and non-native ranges: Environmental quality and the "good-stay, bad-disperse" rule. Ecography 35:1024–1032.
Ims, R. A., and N. G. Yoccoz. 1997. Studying Transfer Processes in Metapopulations. Pages 247–265 Metapopulation Biology.
Jangjoo, M., S. F. Matter, J. Roland, and N. Keyghobadi. 2016. Connectivity rescues genetic diversity after a demographic bottleneck in a butterfly population network. Proceedings of the National Academy of Sciences of the United States of America 113:10914–10919.
Janin, A., J.-P. Léna, N. Ray, C. Delacourt, P. Allemand, and P. Joly. 2009. Assessing landscape connectivity with calibrated cost-distance modelling: predicting common toad distribution in a context of spreading agriculture. Journal of Applied Ecology 46:833–841.
Jones, N. T., R. M. Germain, T. N. Grainger, A. M. Hall, L. Baldwin, and B. Gilbert. 2015. Dispersal mode mediates the effect of patch size and patch connectivity on metacommunity diversity. Journal of Ecology 103:935–944.
Keeley, A. T. H., P. Beier, B. W. Keeley, and M. E. Fagan. 2017. Habitat suitability is a poor proxy for landscape connectivity during dispersal and mating movements.

Landscape and Urban Planning 161:90–102.
Kery, M., and J. A. Royle. 2016. Applied Hierarchical Modeling in Ecology. Page Applied Hierarchical Modeling in Ecology. Academic Press.
Kimmig, S. E., J. Beninde, M. Brandt, A. Schleimer, S. Kramer-Schadt, H. Hofer, K. Börner, C. Schulze, U. Wittstatt, M. Heddergott, T. Halczok, C. Staubach, and A. C. Frantz. 2020. Beyond the landscape: Resistance modelling infers physical and behavioural gene flow barriers to a mobile carnivore across a metropolitan area. Molecular Ecology 29:466–484.
Kimura, M., T. Maruyama, and J. F. Crow. 1963. The mutation load in small populations. Genetics 48:1303–12.
Kindlmann, P., and F. Burel. 2008. Connectivity measures: A review. Landscape Ecology 23:879–890.
Kinnison, M. T., and N. G. Hairston. 2007. Eco-evolutionary conservation biology: Contemporary evolution and the dynamics of persistence. Functional Ecology 21:444–454.
Koen, E. L., J. Bowman, and A. a Walpole. 2012. The effect of cost surface parameterization on landscape resistance estimates. Molecular Ecology Resources 12:686–96.
Koen, E. L., C. J. Garroway, P. J. Wilson, and J. Bowman. 2010. The effect of map boundary on estimates of landscape resistance to animal movement. PLoS ONE 5:e11785.
Komonen, A., and J. Müller. 2018. Dispersal ecology of deadwood organisms and connectivity conservation. Conservation Biology 32:535–545.
Kool, J. T., A. Moilanen, and E. a. Treml. 2013. Population connectivity: recent advances and new perspectives. Landscape Ecology 28:165–185.
Lahoz-Monfort, J. J., G. Guillera-Arroita, and R. Tingley. 2016. Statistical approaches to account for false-positive errors in environmental DNA samples. Molecular Ecology Resources 16:673–685.
Laliberté, J., and M. H. St-Laurent. 2020. Validation of functional connectivity modeling: The Achilles' heel of landscape connectivity mapping. Landscape and Urban Planning 202:103878.
Lambin, X., J. Aars, and S. B. Piertney. 2001. Dispersal, intraspecific competition, kin competition, and kin facilitation: A review of the empirical evidence. Page *in* J. Clobert, E. Danchin, A. Dhondt, and J. D. Nichols, editors. Dispersal. Oxford University Press, Oxford.
Lambin, X., J. Aars, S. B. Piertney, and S. Telfer. 2004. Inferring pattern and process in small mammal metapopulations: insights from ecological and genetic data. Page Ecology, Genetics and Evolution of Metapopulations. Elsevier Inc.
Lambin, X., D. Le Bouille, M. K. Oliver, C. Sutherland, E. Tedesco, and A. Douglas. 2012. High connectivity despite high fragmentation: iterated dispersal in a vertebrate metapopulation. Pages 405–412 Dispersal Ecology and Evolution. Oxford University Press.
Landguth, E. L., S. A. Cushman, M. K. Schwartz, K. S. McKelvey, M. Murphy, and G. Luikart. 2010. Quantifying the lag time to detect barriers in landscape genetics. Molecular Ecology 19:4179–4191.
Larkin, J. L., D. S. Maehr, T. S. Hoctor, M. A. Orlando, and K. Whitney. 2004.

Landscape linkages and conservation planning for the black bear in west-central Florida. Animal Conservation 7:23–34.
Lawton, J. H., G. L. Woodroffe, T. Journal, and N. Feb. 1991. Habitat and the Distribution of Water Voles: Why are there Gaps in a Species' Range? The Journal of Animal Ecology 60:79.
Leempoel, K., T. Hebert, and E. A. Hadly. 2020. A comparison of eDNA to camera trapping for assessment of terrestrial mammal diversity. Proceedings of the Royal Society B: Biological Sciences 287.
Legrand, D., J. Cote, E. A. Fronhofer, R. D. Holt, O. Ronce, N. Schtickzelle, J. M. J. J. Travis, and J. Clobert. 2017. Eco-evolutionary dynamics in fragmented landscapes. Ecography 40:9–25.
Littlefield, C. E., M. Krosby, J. L. Michalak, and J. J. Lawler. 2019. Connectivity for species on the move: supporting climate-driven range shifts. Frontiers in Ecology and the Environment 17:270–278.
Littlefield, C. E., B. H. McRae, J. L. Michalak, J. J. Lawler, and C. Carroll. 2017. Connecting today's climates to future climate analogs to facilitate movement of species under climate change. Conservation Biology 31:1397–1408.
Long, R. A., T. M. DONOVAN, P. MACKAY, W. J. ZIELINSKI, and J. S. BUZAS. 2007. Comparing Scat Detection Dogs, Cameras, and Hair Snares for Surveying Carnivores. Journal of Wildlife Management 71:2018–2025.
Lookingbill, T. R., R. H. Gardner, J. R. Ferrari, and C. E. Keller. 2010. Combining a dispersal model with network theory to assess habitat connectivity. Ecological Applications 20:427–441.
Lowe, W. H., R. P. Kovach, and F. W. Allendorf. 2017. Population Genetics and Demography Unite Ecology and Evolution. Trends in Ecology and Evolution 32:141–152.
Lugg, W. H., J. Griffiths, A. R. van Rooyen, A. R. Weeks, and R. Tingley. 2018. Optimal survey designs for environmental DNA sampling. Methods in Ecology and Evolution 9:1049–1059.
MacKenzie, D. I., J. D. Nichols, J. E. Hines, M. G. Knutson, and A. B. Franklin. 2003. Estimating site occupancy, colonization, and local extinction when a species is detected imperfectly. Ecology 84:2200–2207.
Mackenzie, D. I., J. D. Nichols, G. B. Lachman, S. Droege, J. Andrew, C. A. Langtimm, A. A. Royle, and C. A. Langtimm. 2002. Estimating site occupancy rates when detection probabilities are less than one. Ecology 83:2248–2255.
Mackenzie, D. I., and J. A. Royle. 2005. Designing occupancy studies: general advice and allocating survey effort. Journal of Applied Ecology 42:1105–1114.
MacKenzie, D., J. Nichols, J. Royle, K. Pollock, L. Bailey, and J. Hines. 2018. Occupancy estimation and modeling: inferring patterns and dynamics of species occurrence. 2nd edition. Academic Press, Inc., London.
MacPherson, J. L., and P. W. Bright. 2011. Metapopulation dynamics and a landscape approach to conservation of lowland water voles (Arvicola amphibius). Landscape Ecology 26:1395–1404.
Maher, S. P., T. L. Morelli, M. Hershey, A. L. Flint, L. E. Flint, C. Moritz, and S. R. Beissinger. 2017. Erosion of refugia in the Sierra Nevada meadows network with climate change. Ecosphere 8:e01673.

Margosian, M. L., K. A. Garrett, J. M. S. Hutchinson, and K. A. With. 2009. Connectivity of the American agricultural landscape: Assessing the national risk of crop pest and disease spread. BioScience 59:141–151.
Marrotte, R. R., J. Bowman, M. G. C. Brown, C. Cordes, K. Y. Morris, M. B. Prentice, and P. J. Wilson. 2017. Multi-species genetic connectivity in a terrestrial habitat network. Movement Ecology 5:1–11.
Marshall, D. J., K. Monro, M. Bode, M. J. Keough, and S. Swearer. 2010. Phenotype-environment mismatches reduce connectivity in the sea. Ecology Letters 13:128–140.
Martensen, A. C., S. Saura, and M. J. Fortin. 2017. Spatio-temporal connectivity: Assessing the amount of reachable habitat in dynamic landscapes. Methods in Ecology and Evolution 8:1253–1264.
Mathews, F., L. M. Kubasiewicz, J. Gurnell, C. A. Harrower, R. A. McDonald, and R. F. Shore. 2018. A Review of the Population and Conservation Status of British Mammals: Technical Summary. Peterborough, UK.
Matter, S. F., J. Goff, N. Keyghobadi, and J. Roland. 2020. Direct estimates of metapopulation capacity from dispersal show high interannual variability, but little effect of recent forest encroachment on network persistence. Landscape Ecology 35:675–688.
Matthysen, E. 2005. Density-dependent dispersal in birds and mammals. Ecography 28:403–416.
Matthysen, E. 2012. Multicausality of dispersal : a review. Pages 3–17 Dispersal ecology and evolution. Oxford University Press.
Matthysen, E., F. Adriaensen, A. A. Dhondt, and A. A. Dhondt. 1995. Dispersal Distances of Nuthatches, Sitta europaea, in a Highly Fragmented Forest Habitat. Oikos 72:375.
McCallum, M. 2007. Amphibian decline or extinction? Current declines dwarf background extinction rate. Journal of Herpetology 41:483–491.
McIntyre, N. E., S. D. Collins, L. J. Heintzman, S. M. Starr, and N. van Gestel. 2018. The challenge of assaying landscape connectivity in a changing world: A 27-year case study in the southern Great Plains (USA) playa network. Ecological Indicators 91:607–616.
McRae, B. 2006. Isolation by resistance. Evolution 60:1551–1561.
McRae, B., B. Dickson, T. Keitt, and V. Shah. 2008. Using circuit theory to model connectivity in ecology, evolution, and conservation. Ecology 89:2712–2724.
Meyer, N. F. V., R. Moreno, C. Sutherland, J. A. de la Torre, H. J. Esser, C. A. Jordan, M. Olmos, J. Ortega, R. Reyna-Hurtado, S. Valdes, and P. A. Jansen. 2020. Effectiveness of Panama as an intercontinental land bridge for large mammals. Conservation Biology 34:207–219.
Miguet, P., H. B. Jackson, N. D. Jackson, A. E. Martin, and L. Fahrig. 2016. What determines the spatial extent of landscape effects on species? Landscape Ecology 31:1177–1194.
Miller, D. A., J. D. Nichols, B. T. McClintock, E. H. C. Grant, L. L. Bailey, and L. A. Weir. 2011. Improving occupancy estimation when two types of observational error occur: Non-detection and species misidentification. Ecology 92:1422–1428.
Mills, L. S., and F. W. Allendorf. 1996. The One-Migrant-per-Generation Rule in

Conservation and Management. Conservation Biology 10:1509–1518.
Moilanen, A. 1999. Patch occupancy models of metapopulation dynamics: Efficient parameter estimation using implicit statistical inference. Ecology 80:1031–1043.
Moilanen, A. 2002. Implications of empirical data quality to metapopulation model parameter estimation and application. Oikos 96:516–530.
Moilanen, A. 2004. SPOMSIM: Software for stochastic patch occupancy models of metapopulation dynamics. Ecological Modelling 179:533–550.
Moilanen, A., and I. Hanski. 1998. Metapopulation dynamics: Effects of habitat quality and landscape structure. Ecology 79:2503–2515.
Moilanen, A., and I. Hanski. 2001. On the use of connectivity measures in spatial ecology. Oikos 95:147–151.
Moilanen, A., and M. Nieminen. 2002. Simple connectivity measures in spatial ecology. Ecology 83:1131–1145.
Van Moorter, B., I. Kivimäki, M. Panzacchi, and M. Saerens. 2021. Defining and quantifying effective connectivity of landscapes for species' movements. Ecography:ecog.05351.
Morgan, W. H., T. Cornulier, and X. Lambin. 2019. Colonisation dynamics during range expansion is poorly predicted by dispersal in the core range. Ecography 42:1142–1151.
Morin, D. J., A. K. Fuller, J. A. Royle, and C. Sutherland. 2017. Model-based estimators of density and connectivity to inform conservation of spatially structured populations. Ecosphere 8:1–16.
Munoz, J. 2004. Wind as a Long-Distance Dispersal Vehicle in the Southern Hemisphere. Science 304:1144–1147.
Nathan, R., E. K. Klein, J. J. Robledo-Arnuncio, and E. Revilla. 2012. Dispersal kernels: review. Pages 186–210 Dispersal Ecology and Evolution.
Nelson, M. C., H. G. Morrison, J. Benjamino, S. L. Grim, and J. Graf. 2014. Analysis, optimization and verification of illumina-generated 16s rRNA gene amplicon surveys. PLoS ONE 9.
Nichols, J. D., L. L. Bailey, F. Allan, O. C. Jr, N. W. Talancy, E. H. C. Grant, A. T. Gilbert, E. M. Annand, and P. Thomas. 2008. Multi-scale occupancy estimation and modelling using multiple detection methods:1321–1329.
Niedballa, J., R. Sollmann, A. Courtiol, and A. Wilting. 2016. camtrapR: an R package for efficient camera trap data management. Methods in Ecology and Evolution.
O'Hara, R. B., E. Arjas, H. Toivonen, and I. Hanski. 2002. Bayesian analysis of metapopulation data. Ecology 83:2408–2415.
O'Hara, R. B., and M. J. Sillanpaa. 2009. A Review of Bayesian Variable Selection Methods: What , How and Which. Bayesian Analysis:85–118.
Ofori, B. Y., A. J. Stow, J. B. Baumgartner, and L. J. Beaumont. 2017. Combining dispersal, landscape connectivity and habitat suitability to assess climate-induced changes in the distribution of Cunningham's skink, Egernia cunninghami. PLOS ONE 12:e0184193.
Ordnance Survey. 2017. OS Terrain 50. Ordnance Survey.
Ovaskainen, O. 2002. The Effective Size of a Metapopulation Living in a Heterogeneous Patch Network. The American Naturalist 160:612–628.
Ovaskainen, O., and I. Hanski. 2001. Spatially structured metapopulation models: Global

and local assessment of metapopulation capacity. Theoretical Population Biology 60:281–302.
Ovaskainen, O., and I. Hanski. 2004. From Individual Behavior to Metapopulation Dynamics: Unifying the Patchy Population and Classic Metapopulation Models. The American Naturalist 164:364–377.
Ovaskainen, O., D. B. Roy, R. Fox, and B. J. Anderson. 2016. Uncovering hidden spatial structure in species communities with spatially explicit joint species distribution models. Methods in Ecology and Evolution 7:428–436.
Ozgul, A., M. K. Oli, K. B. Armitage, D. T. Blumstein, and D. H. Van Vuren. 2009. Influence of local demography on asymptotic and transient dynamics of a yellow-bellied marmot metapopulation. American Naturalist 173:517–530.
Palstra, F. P., and D. E. Ruzzante. 2008. Genetic estimates of contemporary effective population size: What can they tell us about the importance of genetic stochasticity for wild population persistence? Molecular Ecology 17:3428–3447.
Parmesan, C. 2006. Ecological and evolutionary responses to recent climate change. Annual Review of Ecology and Systematics 37:637–669.
Parsons, A. W., C. Goforth, R. Costello, and R. Kays. 2018. The value of citizen science for ecological monitoring of mammals. PeerJ 2018:1–21.
Pellet, J., E. Fleishman, D. S. Dobkin, A. Gander, and D. D. Murphy. 2007. An empirical evaluation of the area and isolation paradigm of metapopulation dynamics. Biological Conservation 136:483–495.
Peterman, W. E., and N. S. Pope. 2020. The use and misuse of regression models in landscape genetic analyses. Molecular Ecology:1–11.
Peterman, W. E., K. J. Winiarski, C. E. Moore, C. da S. Carvalho, A. L. Gilbert, and S. F. Spear. 2019. A comparison of popular approaches to optimize landscape resistance surfaces. Landscape Ecology 34:2197–2208.
Pinto, S. M., and A. S. MacDougall. 2010. Dispersal limitation and environmental structure interact to restrict the occupation of optimal habitat. American Naturalist 175:675–686.
Plummer, M., N. Best, K. Cowles, and V. Karen. 2006. CODA: Convergence Diagnosis and Output Analysis for MCMC. R News 6:7–11.
Poli, C., J. Hightower, and R. J. Fletcher. 2020. Validating network connectivity with observed movement in experimental landscapes undergoing habitat destruction. Journal of Applied Ecology 57:1426–1437.
Prugh, L. R. 2009. An evaluation of patch connectivity measures. Ecological Applications 19:1300–1310.
Prugh, L. R., K. E. Hodges, A. R. E. Sinclair, and J. S. Brashares. 2008. Effect of habitat area and isolation on fragmented animal populations. Proceedings of the National Academy of Sciences 105:20770–20775.
Pulliam, H. R. 1988. Sources , Sinks , and Population Regulation. Regulation 132:652–661.
R Core Team. 2017. R: A Language and Environment for Statistical Computing. R Foundation, Vienna, Austria.
R Core Team. 2019. R: A Language and Environment for Statistical Computing.
Rapacciuolo, G., and J. L. Blois. 2019. Understanding ecological change across large spatial, temporal and taxonomic scales: integrating data and methods in light of

theory. Ecography 42:1247–1266.
Rayfield, B., M. J. Fortin, and A. Fall. 2011. Connectivity for conservation: A framework to classify network measures. Ecology 92:847–858.
Revilla, E., T. Wiegand, F. Palomares, P. Ferreras, and M. Delibes. 2004. Effects of matrix heterogeneity on animal dispersal: from individual behavior to metapopulation-level parameters. The American Naturalist 164:E130–E153.
Ricketts, T. H. 2001. The matrix matters: effective isolation in fragmented landscapes. The American naturalist 158:87–99.
Riotte-Lambert, L., and F. Laroche. 2021. Dispersers' habitat detection and settling abilities modulate the effect of habitat amount on metapopulation resilience. Landscape Ecology en révisio.
Risk, B. B., P. De Valpine, and S. R. Beissinger. 2011. A robust-design formulation of the incidence function model of metapopulation dynamics applied to two species of rails. Ecology 92:462–474.
Robertson, E. P., R. J. Fletcher, and J. D. Austin. 2019. The number of breeders explains genetic connectivity in an endangered bird. Molecular Ecology Early View:2746–2756.
Robertson, E. P., R. J. Fletcher, C. E. Cattau, B. J. Udell, B. E. Reichert, J. D. Austin, and D. Valle. 2018. Isolating the roles of movement and reproduction on effective connectivity alters conservation priorities for an endangered bird. Proceedings of the National Academy of Sciences 115:8591–8596.
Ronce, O. 2007. How does it feel to be like a rolling stone? Ten questions about dispersal evolution. Annual Review of Ecology, Evolution, and Systematics 38:231–253.
Royle, J. A., R. B. Chandler, C. C. Sun, and A. K. Fuller. 2013. Integrating resource selection information with spatial capture-recapture. Methods in Ecology and Evolution 4:520–530.
Royle, J. A., and M. Kery. 2007. A Bayesian State-Space Formulation of Dynamic Occupancy Models. Ecology 88:1813–1823.
Royle, J. A., and W. A. Link. 2006. Generalized site occupancy models allowing for false positive and false negative errors. Ecology 87:835–841.
Royle, J., and R. Dorazio. 2009. Hierarchical Modeling and Inference in Ecology. Page Hierarchical Modeling and Inference in Ecology.
Ruffell, J., M. N. Clout, and R. K. Didham. 2017. The matrix matters, but how should we manage it? Estimating the amount of high-quality matrix required to maintain biodiversity in fragmented landscapes. Ecography 40:171–178.
Ruiz, L., N. Parikh, L. J. Heintzman, S. D. Collins, S. M. Starr, C. K. Wright, G. M. Henebry, N. van Gestel, and N. E. McIntyre. 2014a. Dynamic connectivity of temporary wetlands in the southern Great Plains. Landscape Ecology 29:507–516.
Ruiz, L., N. Parikh, L. J. Heintzman, S. D. Collins, S. M. Starr, C. K. Wright, G. M. Henebry, N. van Gestel, and N. E. McIntyre. 2014b. Dynamic connectivity of temporary wetlands in the southern Great Plains. Landscape Ecology 29:507–516.
Rushton, S. P., G. W. Barreto, R. M. Cormack, D. W. Macdonald, and R. Fuller. 2000. Modelling the effects of mink and habitat fragmentation on the water vole. Journal of Applied Ecology 37:475–490.
Russo, I. M. R. M., C. L. Sole, M. Barbato, U. Von Bramann, M. W. Bruford, Isa-Rita M. Russo, Catherine L. Sole, Mario Barbato, Ullrich von Bramann, MichaelW. Bruford,

I. M. R. M. Russo, C. L. Sole, M. Barbato, U. Von Bramann, and W. Michael. 2016. Landscape determinants of fine-scale genetic structure of a small rodent in a heterogeneous landscape (Hluhluwe-iMfolozi Park, South Africa). Scientific Reports 6:1–14.
Sainsbury, K. A., R. F. Shore, H. Schofield, E. Croose, R. D. Campbell, and R. A. Mcdonald. 2019. Recent history, current status, conservation and management of native mammalian carnivore species in Great Britain. Mammal Review 49:171–188.
Sales, N. G., M. da C. Kaizer, I. Coscia, J. C. Perkins, A. Highlands, J. P. Boubli, W. E. Magnusson, M. N. F. Da Silva, C. Benvenuto, and A. D. Mcdevitt. 2020a. Assessing the potential of environmental DNA metabarcoding for monitoring Neotropical mammals: a case study in the Amazon and Atlantic Forest, Brazil. Mammal Review 50:221–225.
Sales, N. G., M. B. McKenzie, J. Drake, L. R. Harper, S. S. Browett, I. Coscia, O. S. Wangensteen, C. Baillie, E. Bryce, D. A. Dawson, E. Ochu, B. Hänfling, L. Lawson Handley, S. Mariani, X. Lambin, C. Sutherland, and A. D. McDevitt. 2020b. Fishing for mammals: Landscape-level monitoring of terrestrial and semi-aquatic communities using eDNA from riverine systems. Journal of Applied Ecology 57:707–716.
Sánchez-Bayo, F., and K. A. G. Wyckhuys. 2019. Worldwide decline of the entomofauna: A review of its drivers. Biological Conservation 232:8–27.
Saura, S., Ö. Bodin, and M.-J. Fortin. 2014. EDITOR'S CHOICE: Stepping stones are crucial for species' long-distance dispersal and range expansion through habitat networks. Journal of Applied Ecology 51:171–182.
Saura, S., and L. Pascual-Hortal. 2007. A new habitat availability index to integrate connectivity in landscape conservation planning: Comparison with existing indices and application to a case study. Landscape and Urban Planning 83:91–103.
Schnell, I. B., K. Bohmann, and M. T. P. Gilbert. 2015. Tag jumps illuminated - reducing sequence-to-sample misidentifications in metabarcoding studies. Molecular Ecology Resources 15:1289–1303.
Schnell, J. K., G. M. Harris, S. L. Pimm, and G. J. Russell. 2013. Estimating Extinction Risk with Metapopulation Models of Large-Scale Fragmentation. Conservation Biology 27:520–530.
Senner, N. R., M. Stager, and Z. A. Cheviron. 2018. Spatial and temporal heterogeneity in climate change limits species' dispersal capabilities and adaptive potential. Ecography 41:1428–1440.
Shakespeare, W. 1623. Mr. William Shakespeares Comedies, Histories & Tragedies. First Foli. London.
Shima, J. S., and S. E. Swearer. 2009. Larval quality is shaped by matrix effects: Implications for connectivity in a marine metapopulation. Ecology 90:1255–1267.
Shine, R., G. P. Brown, and B. L. Phillips. 2011. An evolutionary process that assembles phenotypes through space rather than through time. Proceedings of the National Academy of Sciences of the United States of America 108:5708–5711.
Sibly, R. M., D. Collett, D. E. L. Promislow, D. J. Peacock, and P. H. Harvey. 1997. Mortality rates of mammals. Journal of Zoology 243:1–12.
Soulé, M. E. 1987. Viable populations for conservation. Cambridge University Press.
Space Intelligence. 2021. Habitat Maps of Scotland 2019 and 2020. https://www.space-

intelligence.com/2021/04/01/weve-just-published-the-first-ever-scotland-wide-high-resolution-habitat-maps-for-free/.
Spanowicz, A. G., and J. A. G. Jaeger. 2019. Measuring landscape connectivity: On the importance of within-patch connectivity. Landscape Ecology 0.
Spear, S. F., N. Balkenhol, M. J. Fortin, B. H. McRae, and K. Scribner. 2010. Use of resistance surfaces for landscape genetic studies: Considerations for parameterization and analysis. Molecular Ecology 19:3576–3591.
Stoddart, D. M. 1970a. Individual Range, Dispersion and Dispersal in a Population of Water Voles. Journal of Animal Ecology 39:403–425.
Stoddart, D. M. 1970b. Individual range, dispersion and dispersal in a population of Water Voles (Arvicola terrestris (L.)). Journal of Animal Ecology 39:403–425.
Strachan, R. 2004. Conserving water voles: Britain's fastest declining mammal. Water and Environment Journal 18:1–4.
Strimas-Mackey, M., and J. F. Brodie. 2018a. Reserve design to optimize the long-term persistence of multiple species. Ecological Applications 28:1354–1361.
Strimas-Mackey, M., and J. F. Brodie. 2018b. metacapa: Metapopulation Capacity-based Conservation Prioritization.
Sutherland, C. 2013. A quantitative investigation of metapopulation dynamics in a naturally fragmented population of water voles arvicola amphibius. University of Aberdeen.
Sutherland, C., D. A. Elston, and X. Lambin. 2012. Multi-scale processes in metapopulations: Contributions of stage structure, rescue effect, and correlated extinctions. Ecology 93:2465–2473.
Sutherland, C., D. A. Elston, and X. Lambin. 2013. Accounting for false positive detection error induced by transient individuals. Wildlife Research 40:490–498.
Sutherland, C., D. A. Elston, and X. Lambin. 2014. A demographic, spatially explicit patch occupancy model of metapopulation dynamics and persistence. Ecology 95:3149–3160.
Sutherland, C., A. K. Fuller, and J. A. Royle. 2015. Modelling non-Euclidean movement and landscape connectivity in highly structured ecological networks. Methods in Ecology and Evolution 6:169–177.
Sutherland, G. D., A. S. Harestad, K. Price, and K. P. Lertzman. 2000. Scaling of natal dispersal distances in terrestrial birds and mammals. Ecology and Society 4.
Taylor, P. D., L. Fahrig, and K. A. With. 2010. Landscape connectivity: a return to the basics. Connectivity Conservation:29–43.
Taylor, P. P. D., L. Fahrig, K. Henein, and G. Merriam. 1993. Connectivity is a vital element of landscape structure. Oikos 68:571–573.
Telfer, S., A. Holt, R. Donaldson, and X. Lambin. 2001. Metapopulation processes and persistence in remnant water vole populations. Oikos 95:31–42.
Telfer, S., S. B. Piertney, J. F. Dallas, W. A. Stewart, F. Marshall, J. L. Gow, and X. Lambin. 2003a. Parentage assignment detects frequent and large-scale dispersal in water voles. Molecular Ecology 12:1939–1949.
Telfer, S., S. B. Piertney, J. F. Dallas, W. A. Stewart, F. Marshall, J. L. Gow, X. Lambin, T. Avenue, and T. Avenue. 2003b. Parentage assignment detects frequent and large-scale dispersal in water voles. Molecular Ecology 12:1939–1949.
Tenan, S., R. B. O'Hara, I. Hendriks, and G. Tavecchia. 2014. Bayesian model selection:

The steepest mountain to climb. Elsevier B.V.
Thomas, C. D. 2000. Dispersal and extinction in fragmented landscapes. Proceedings of the Royal Society of London. Series B: Biological Sciences 267:139–145.
Thomas, C. D., and W. E. Kunin. 1999. The spatial structure of populations. Journal of Animal Ecology Anim Ecology 68:647–657.
Thomsen, P. F., J. Kielgast, L. L. Iversen, C. Wiuf, M. Rasmussen, M. T. P. Gilbert, L. Orlando, and E. Willerslev. 2012. Monitoring endangered freshwater biodiversity using environmental DNA. Molecular Ecology 21:2565–2573.
Tingley, R., M. Greenlees, S. Oertel, A. R. van Rooyen, and A. R. Weeks. 2019. Environmental DNA sampling as a surveillance tool for cane toad Rhinella marina introductions on offshore islands. Biological Invasions 21:1–6.
Tischendorf, L., and L. Fahrig. 2000. On the usage and measurement of landscape connectivity. Oikos 90:7–19.
Tischendorf, L., and L. Fahrig. 2001. On the use of connectivity measures in spatial ecology. A reply. Oikos 95:152–155.
Trochet, A., E. A. Courtois, V. M. Stevens, M. Baguette, A. Chaine, D. S. Schmeller, J. Clobert, D. J. Irschick, and J. J. Wiens. 2016. Evolution of Sex-Biased Dispersal. The Quarterly Review of Biology 91:297–320.
Tucker, J. M., F. W. Allendorf, R. L. Truex, and M. K. Schwartz. 2017. Sex-biased dispersal and spatial heterogeneity affect landscape resistance to gene flow in fisher. Ecosphere 8:e01839.
Turner, C. R., K. L. Uy, and R. C. Everhart. 2015. Fish environmental DNA is more concentrated in aquatic sediments than surface water. Biological Conservation 183:93–102.
Turner, M. G. 2005. Landscape ecology: What is the state of the science? Annual Review of Ecology, Evolution, and Systematics 36:319–344.
Urban, D., and T. Keitt. 2001. Landscape connectivity: a graph-theoretic perspective. Ecology 82:1205–1218.
Ushio, M., H. Fukuda, T. Inoue, K. Makoto, O. Kishida, K. Sato, K. Murata, M. Nikaido, T. Sado, Y. Sato, M. Takeshita, W. Iwasaki, H. Yamanaka, M. Kondoh, and M. Miya. 2017. Environmental DNA enables detection of terrestrial mammals from forest pond water. Molecular Ecology Resources 17:e63–e75.
Valentini, A., P. Taberlet, C. Miaud, R. Civade, J. Herder, P. F. Thomsen, E. Bellemain, A. Besnard, E. Coissac, F. Boyer, C. Gaboriaud, P. Jean, N. Poulet, N. Roset, G. H. Copp, P. Geniez, D. Pont, C. Argillier, J. M. Baudoin, T. Peroux, A. J. Crivelli, A. Olivier, M. Acqueberge, M. Le Brun, P. R. Møller, E. Willerslev, and T. Dejean. 2016. Next-generation monitoring of aquatic biodiversity using environmental DNA metabarcoding. Molecular Ecology 25:929–942.
de Valpine, P., D. Turek, C. J. Paciorek, C. Anderson-Bergman, D. T. Lang, and R. Bodik. 2017. Programming With Models: Writing Statistical Algorithms for General Model Structures With NIMBLE. Journal of Computational and Graphical Statistics 26:403–413.
Vandermeer, and Carvajal. 2001. Metapopulation Dynamics and the Quality of the Matrix. The American Naturalist.
Vasudev, D., and R. J. Fletcher. 2016. Mate choice interacts with movement limitations to influence effective dispersal. Ecological Modelling 327:65–73.

Vasudev, D., R. J. Fletcher, V. R. Goswami, and M. Krishnadas. 2015. From dispersal constraints to landscape connectivity: Lessons from species distribution modeling. Ecography 38:967–978.
Visconti, P., and C. Elkin. 2009. Using connectivity metrics in conservation planning – when does habitat quality. Diversity and Distributions 15:602–612.
Visconti, P., R. L. Pressey, D. Giorgini, L. Maiorano, M. Bakkenes, L. Boitani, R. Alkemade, A. Falcucci, F. Chiozza, and C. Rondinini. 2011. Future hotspots of terrestrial mammal loss. Philosophical Transactions of the Royal Society B: Biological Sciences 366:2693–2702.
Wan, H., S. Cushman, and J. Ganey. 2018. Habitat Fragmentation Reduces Genetic Diversity and Connectivity of the Mexican Spotted Owl: A Simulation Study Using Empirical Resistance Models. Genes 9:403.
Wang, J., and M. C. Whitlock. 2003. Estimating effective population size and migration rates from genetic samples over space and time. Genetics 163:429–446.
Wang, S., and F. Altermatt. 2019. Metapopulations revisited: the area-dependence of dispersal matters. Ecology 100:1–11.
Ward, M., S. Saura, B. Williams, J. P. Ramírez-Delgado, N. Arafeh-Dalmau, J. R. Allan, O. Venter, G. Dubois, and J. E. M. Watson. 2020. Just ten percent of the global terrestrial protected area network is structurally connected via intact land. Nature Communications 11:1–10.
Wasserman, T. N., S. A. Cushman, a. S. Shirk, E. L. Landguth, and J. S. Littell. 2012. Simulating the effects of climate change on population connectivity of American marten (Martes americana) in the northern Rocky Mountains, USA. Landscape Ecology 27:211–225.
Wickham, H. 2016. ggplot2: Elegant Graphics for Data Analysis. Springer-Verlag, New York.
Wiens, J. J. 2001. The landscape context of dispersal. Pages 96–109 *in* J. Clobert, E. Danchin, A. A. Dhondt, and J. D. Nichols, editors. Dispersal. Oxford University Press, Oxford, UK.
Williams, K. E., K. P. Huyvaert, K. C. Vercauteren, A. J. Davis, and A. J. Piaggio. 2018. Detection and persistence of environmental DNA from an invasive, terrestrial mammal. Ecology and Evolution 8:688–695.
With, K. A. 2004. Metapopulation Dynamics. Perspectives from Landscape Ecology. Pages 23–44 Ecology, Genetics and Evolution of Metapopulations.
Zeigler, S. L., and W. F. Fagan. 2014. Transient windows for connectivity in a changing world. Movement Ecology 2:1.
Zeller, K. A., M. K. Jennings, T. W. Vickers, H. B. Ernest, S. A. Cushman, and W. M. Boyce. 2018. Are all data types and connectivity models created equal? Validating common connectivity approaches with dispersal data. Diversity and Distributions 24:868–879.
Zeller, K. A., R. Lewsion, R. J. Fletcher, M. G. Tulbure, and M. K. Jennings. 2020. Understanding the Importance of Dynamic Landscape Connectivity. Land 9:303.
Zeller, K. A., K. McGarigal, and A. R. Whiteley. 2012. Estimating landscape resistance to movement: a review. Landscape Ecology 27:777–797.
Ziółkowska, E., K. Ostapowicz, T. Kuemmerle, K. Perzanowski, V. C. Radeloff, and J. Kozak. 2012. Potential habitat connectivity of European bison (Bison bonasus) in

the Carpathians. Biological Conservation 146:188–196.